
An Augmented Coupling Interface Method for Elliptic Interface Problems

I-Liang Chern

National Taiwan University

Goal

- Propose a coupling interface method to solve the above elliptic interface problems.
 - Three applications:
 - Computing electrostatic potential for Macromolecule in solvent
 - Simulation of Tumor growth
 - Computing surface plasmon mode at nano scale
-

Collaborators

- Chieh-Cheng Chang: Inst. of Applied Mechanics, National Taiwan Univ.
 - Ruey-Lin Chern, Inst. Of Applied Mechanics, National Taiwan Univ.
 - Yu-Chen Shu: Center for Research on Applied Sciences, Academia Sinica
 - How-Chih Lee, Math, National Taiwan Univ.
 - Xian-Wen Dong, Math, National Taiwan Univ.
- Ref. Chern and Shu, J. Comp. Phys. 2007
Chang, Shu and Chern, Phys. Rev. B 2008
-

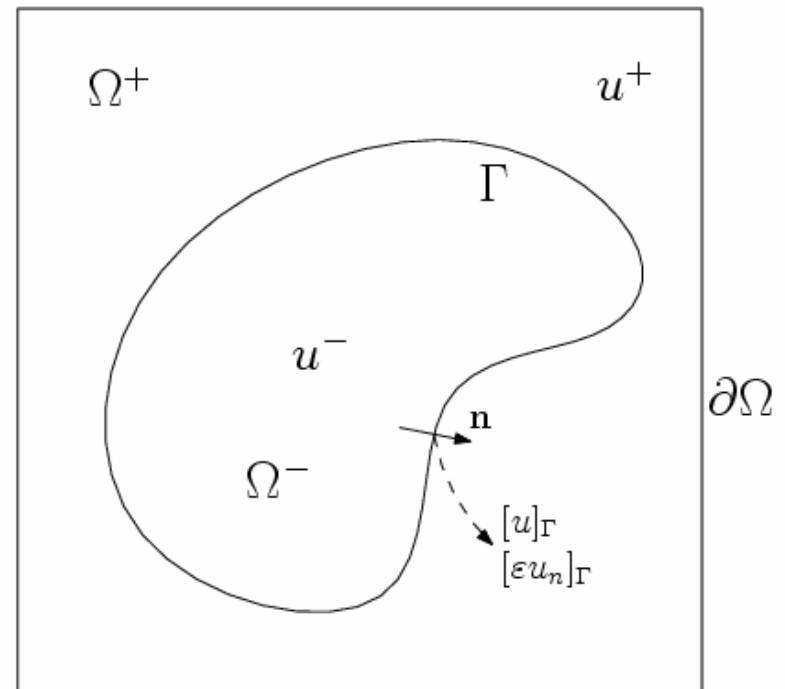
Elliptic Interface Problems

$$-\nabla \cdot (\varepsilon(\mathbf{x}) \nabla u(\mathbf{x})) = f(\mathbf{x}), \quad \mathbf{x} \in \Omega \setminus \Gamma,$$

$$[u] = \tau, \quad [\varepsilon u_n] = \sigma \quad \text{on } \Gamma,$$

$$u = g \quad \text{on } \partial\Omega.$$

ε and u are discontinuous,
 f is singular across Γ



Dielectric coefficients ϵ

- Vacuum: 1
 - Air :1-2
 - Silicon: 12-13
 - Water: 80
 - Metal: $\sim 10^6$
-

Elliptic irregular domain problems

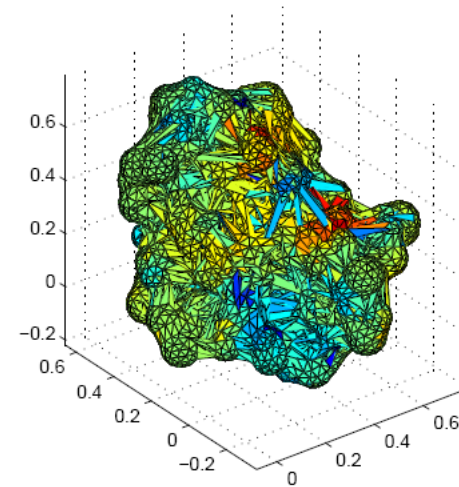
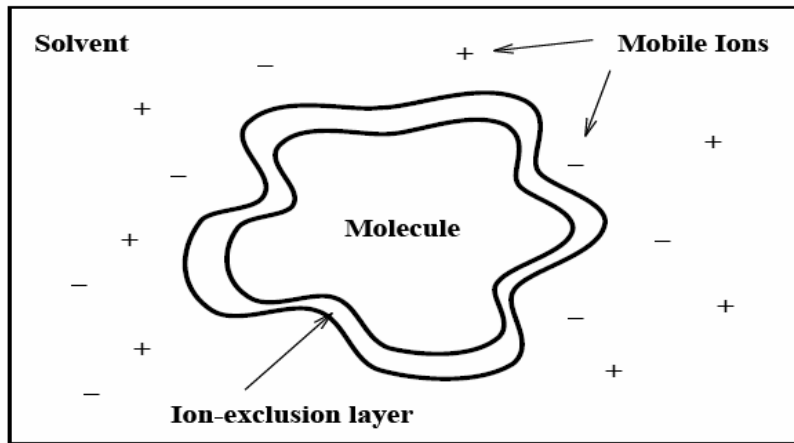
- Poisson equation

$$\Delta u = f \text{ in } \Omega$$

- Dirichlet or Neumann boundary condition
 - Ω can be quite general and complex.
-

Biomolecule in solvent: Poisson-Boltzmann Equation

$$-\nabla \cdot (\epsilon(x)\nabla u(x)) + \bar{\kappa}^2(x) \sinh(u(x)) = \frac{4\pi e_c^2}{k_B T} \sum_{i=1}^{N_m} z_i \delta(x - \bar{x}_i)$$

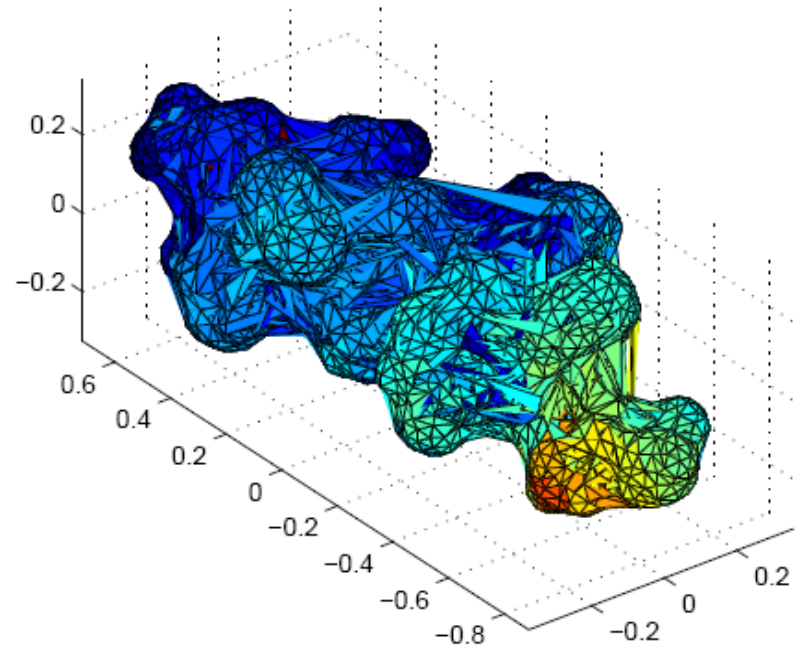


N. Baker, M. Holst, and F. Wang, [Adaptive multilevel finite element solution of the Poisson-Boltzmann equation II: refinement at solvent accessible surfaces in biomolecular systems](#). J. Comput. Chem., 21 (2000), pp. 1343-1352. (Paper at Wiley)

Biomolecule in solvent

Poisson-Boltzmann model

- Macromolecule: 50 Å
- Hydrogen layer: 1.5 – 3Å
- Molecule surface: thin
- Dielectric constants:
 - 2 inside molecule
 - 80 in water



a hydrophilic protein (PDB ID:1DNG)

Tumor growth simulation (free boundary) (Lowengrub et al)

$$\nabla^2 \bar{\Gamma} = \bar{\Gamma} \text{ in } \Omega(\bar{t}), \quad \bar{\Gamma}|_{\partial\Omega(\bar{t})} = 1$$

Γ : nutrient

p : pressure

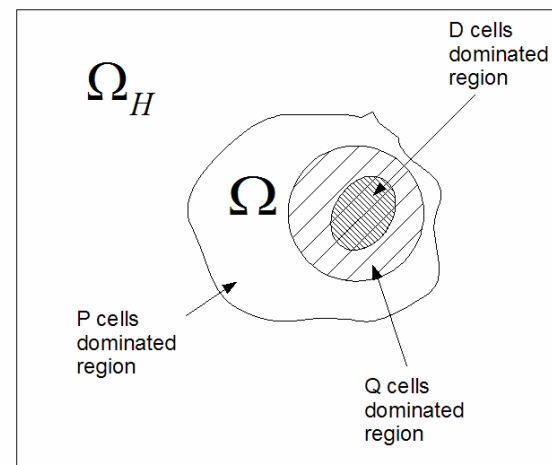
$$\nabla^2 \bar{p} = -G(\bar{\Gamma} - A) \text{ in } \Omega(\bar{t}), \quad \bar{p}|_{\partial\Omega(\bar{t})} = \kappa$$

$$V_n = -\frac{\partial p}{\partial n} \text{ on } \partial\Omega(t)$$

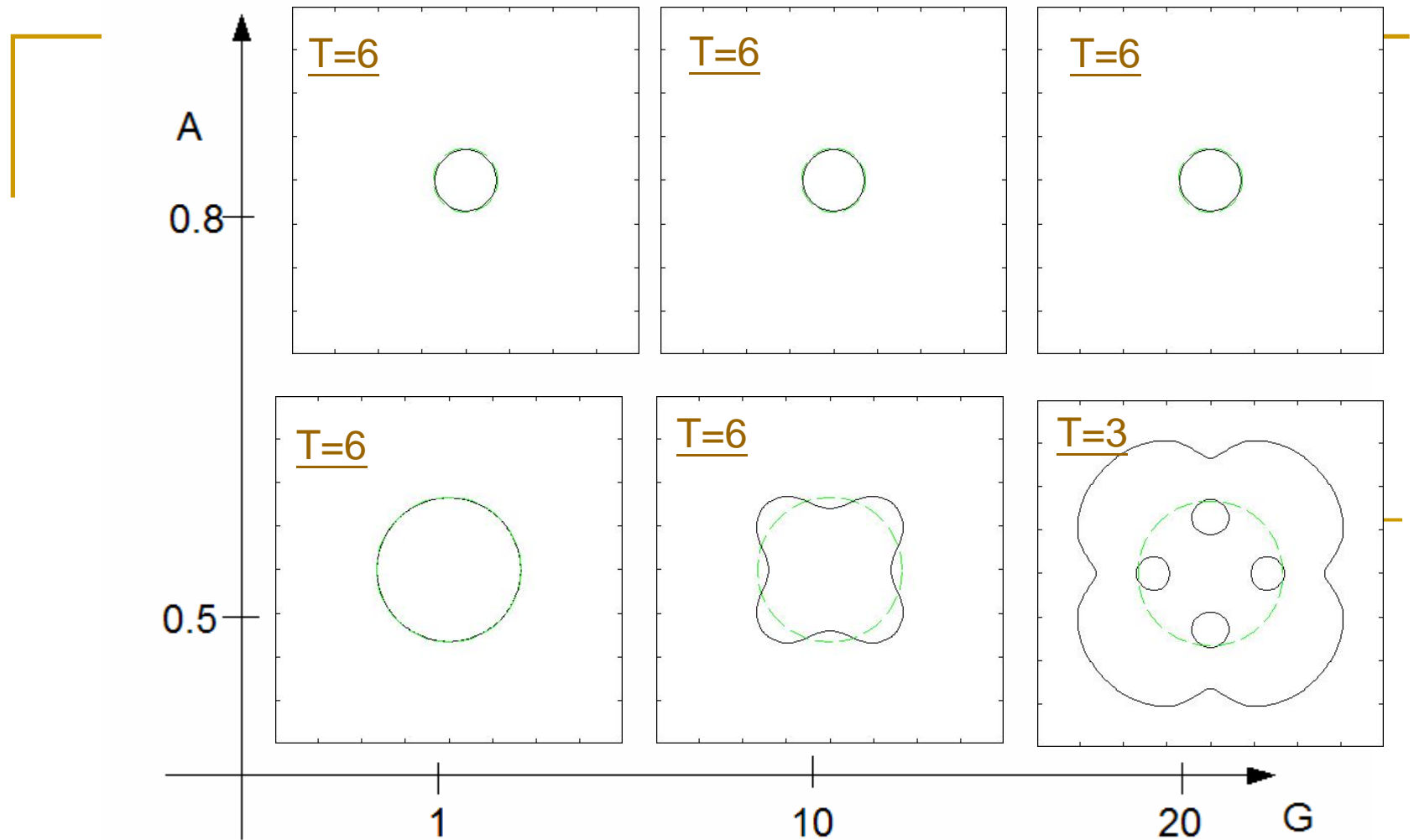
$$G = \frac{(k_a + k_b)\sigma^\infty}{\lambda_R} (1 - B)$$

$$A = \frac{k_a / (k_a + k_b) - B}{1 - B}$$

$$B = \frac{\sigma_B}{\sigma^\infty} \frac{\lambda_B}{\lambda_B + \lambda}$$



Bifurcation of tumor growth

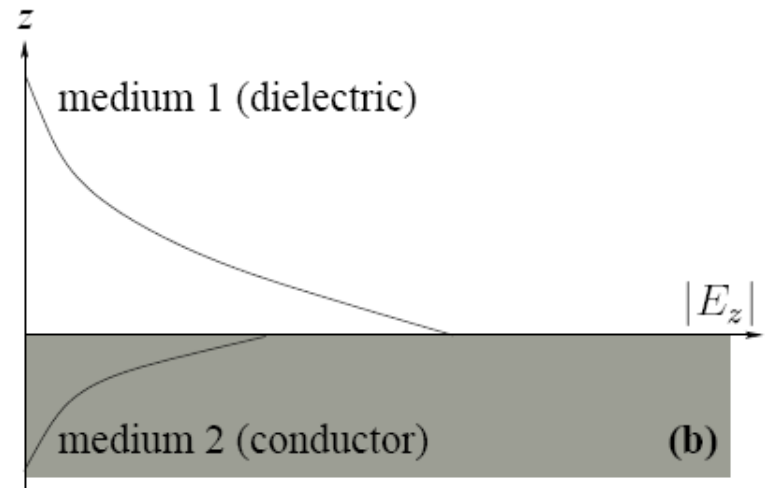
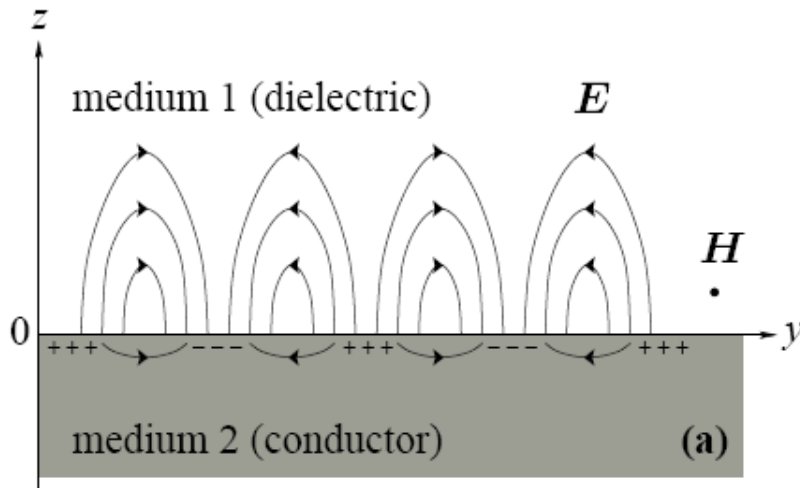


G (growth rate/adhesive force), A (apoptosis)

Initial condition: $R=2$.

Surface plasmons

- Surface plasmons are surface electromagnetic waves that propagate parallel along a metal/dielectric (or metal/vacuum) interface.
- E field excites electron motion on metal surface
- Fields decay exponentially from the interface: surface evanescent waves.



Surface plasmon

- Macroscopic Maxwell Equation

$$\left\{ \begin{array}{l} \nabla \cdot D = 0 \\ \nabla \cdot B = 0 \\ \nabla \times E = -\dot{B}_t \\ \nabla \times H = \dot{D}_t \end{array} \right.$$

$$\begin{array}{l} D = \varepsilon E \\ B = \mu H \end{array}$$

$$\begin{array}{l} \varepsilon(\omega) = \varepsilon_0 \left(1 - \frac{\omega_p^2}{\omega(\omega + i\omega_\tau)} \right) \\ \mu = \mu_0 \end{array}$$

Interface condition

$$[E] \cdot t = 0$$

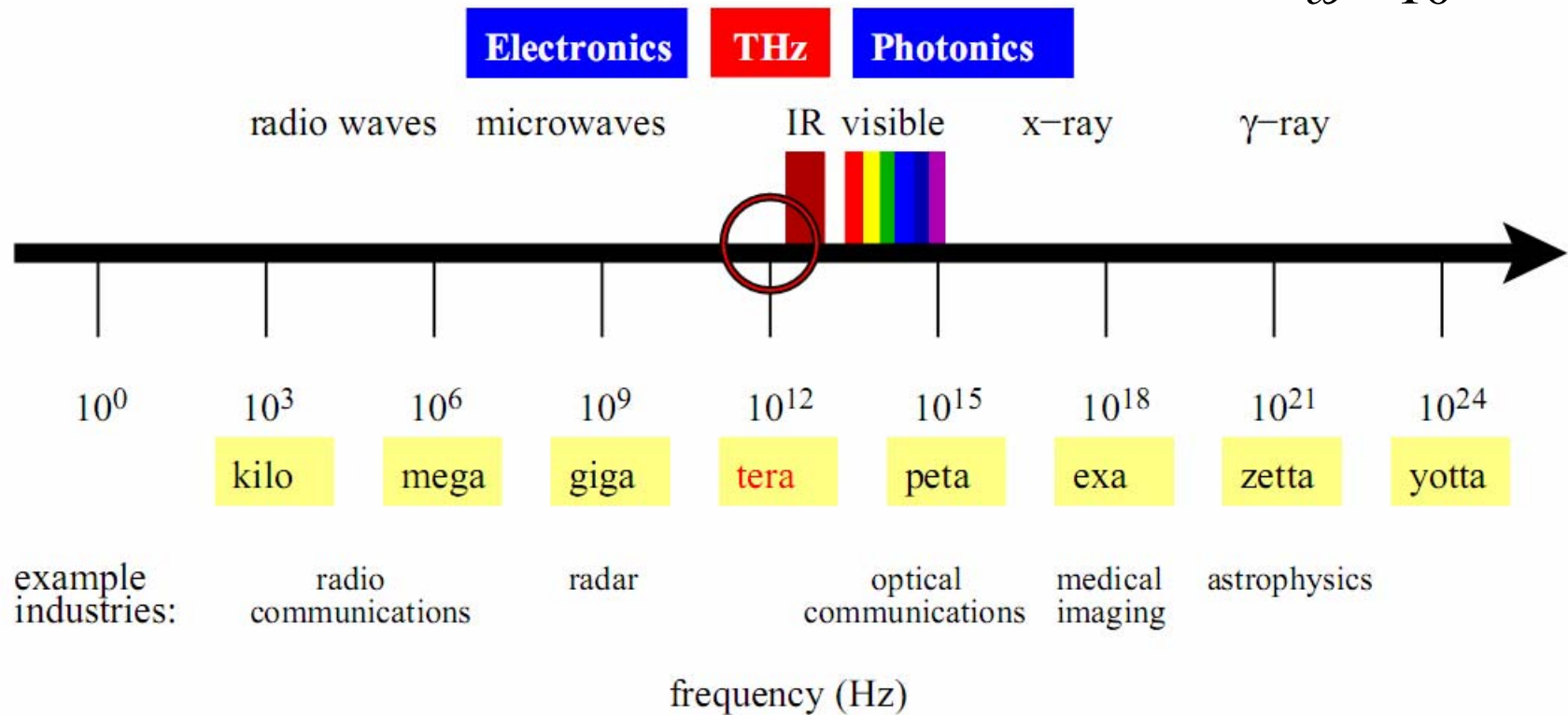
$$[H] \cdot t = 0$$

Plasma frequency

| | $\omega_p \text{ (s}^{-1}\text{)}$ | $\omega_T \text{ (s}^{-1}\text{)}$ |
|----|------------------------------------|------------------------------------|
| Au | 1.37×10^{16} | 4.05×10^{13} |
| Ag | 1.37×10^{16} | 2.73×10^{13} |
| Pt | 7.82×10^{15} | 1.05×10^{14} |

Optical communication frequency

$$\varepsilon_m(\omega) = -10^6,$$
$$\omega = 10^{13}$$



A goal of nanotechnology: fabrication of nanoscale photonic circuits operating at optical frequencies. Faster and Smaller devices.

Quoted from Jorg Saxler 2003

Quadratic Eigenvalue problem for k:

Interior:

$$\begin{cases} \nabla^2 E_z + \Lambda E_z = 0 \\ \nabla^2 H_z + \Lambda H_z = 0 \end{cases}$$

$$\Lambda = \omega^2 \varepsilon \mu - k^2$$

Boundary conditions:

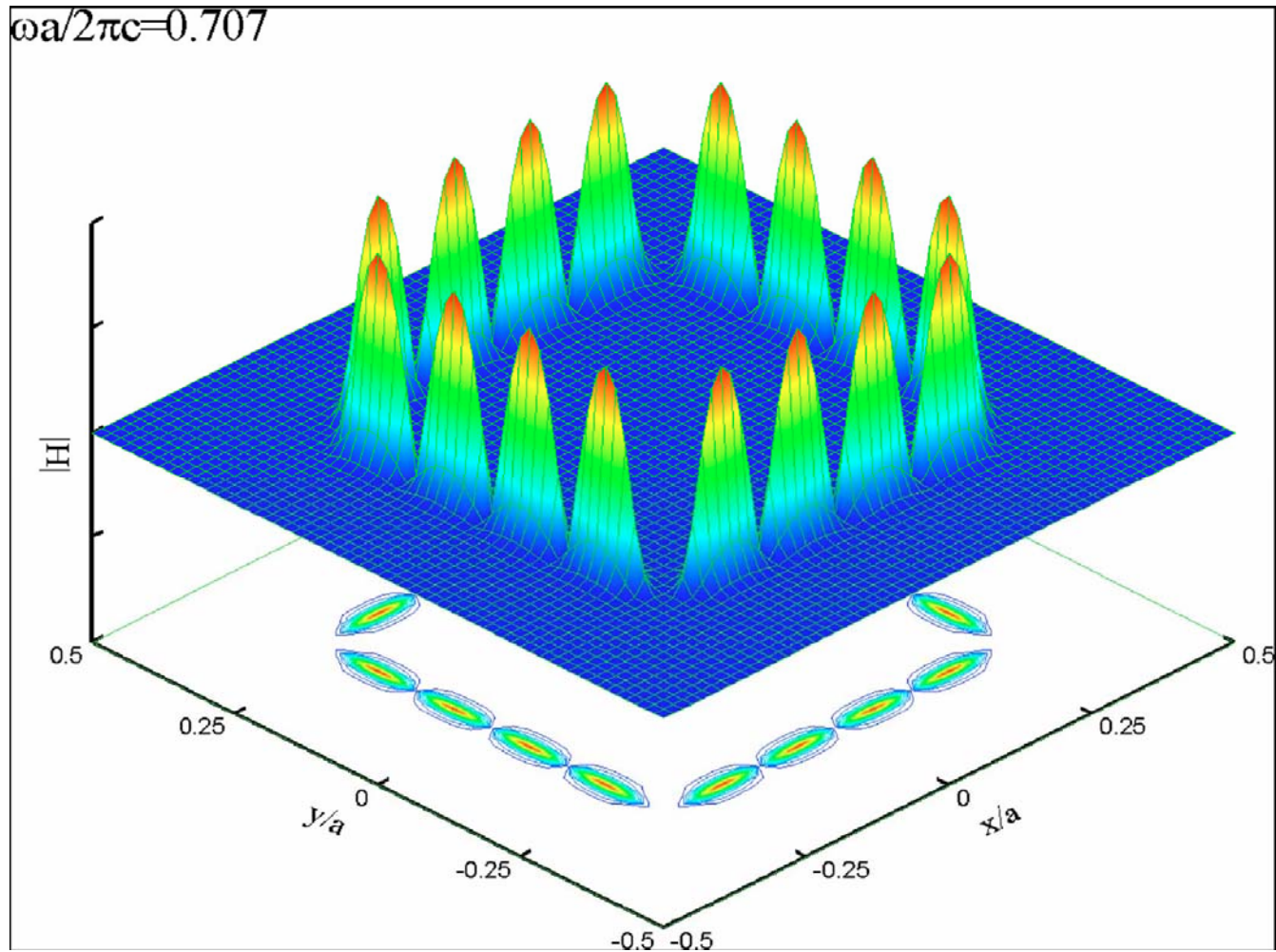
$$\begin{cases} E_z(x+L, y+L) = E_z(x, y) e^{i(k_x L + k_y L)} \\ H_z(x+L, y+L) = H_z(x, y) e^{i(k_x L + k_y L)} \end{cases}$$

Interface conditions:

$$[E_z] = [H_z] = 0$$

$$\begin{cases} \left[\frac{\varepsilon}{\Lambda} \nabla E_z \cdot \mathbf{n} \right] = - \left[\frac{k}{\Lambda \omega} \nabla H_z \cdot \mathbf{s} \right] \\ \left[\frac{\mu}{\Lambda} \nabla H_z \cdot \mathbf{n} \right] = \left[\frac{k}{\Lambda \omega} \nabla E_z \cdot \mathbf{s} \right] \end{cases}$$

Surface Plasmon:



EM wave are confined on surface.

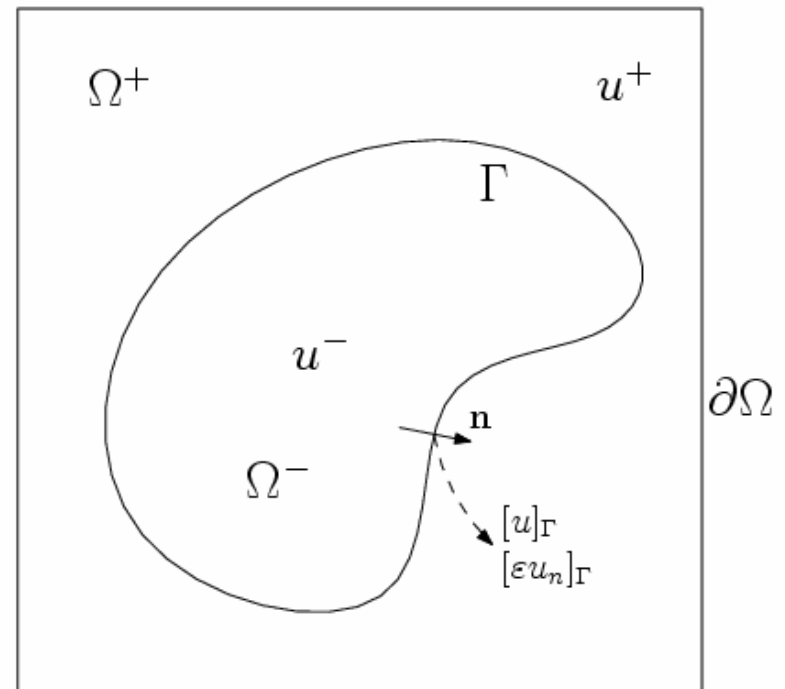
Elliptic Interface Problems

$$-\nabla \cdot (\varepsilon(\mathbf{x}) \nabla u(\mathbf{x})) = f(\mathbf{x}), \quad \mathbf{x} \in \Omega \setminus \Gamma,$$

$$[u] = \tau, \quad [\varepsilon u_n] = \sigma \quad \text{on } \Gamma,$$

$$u = g \quad \text{on } \partial\Omega.$$

ε and u are discontinuous,
 f is singular across Γ



Three classes of approaches

- Boundary integral approach
 - Finite element approach:
 - Finite Difference approach:
 - Body-fitting approach
 - Fixed underlying grid: more flexible for moving interface problems
-

Regular Grid Methods for Solving Elliptic Interface Problems

- **Regularization approach** (Tornberg-Engquist, 2003)
 - Harmonic Averaging (Tikhonov-Samarskii, 1962)
 - Immersed Boundary Method (IB Method) (Peskin, 1974)
 - Phase field method
- **Dimension un-splitting approach**
 - Immersed Interface Method (IIM) (LeVeque-Li, 1994)
 - Maximum Principle Preserving IIM (MIIM) (Li-Ito, 2001)
 - Fast iterative IIM (FIIM) (Li, 1998)
- **Dimension splitting approach**
 - Ghost Fluid Method (Fedkiw et al., 1999, Liu et al. 2000)
 - Decomposed Immersed Interface Method (DIIM) (Berthelsen, 2004)
 - Matched Interface and Boundary Method (MIB) (YC Zhou et al., 2006)
 - **Coupling interface method (CIM) (Chern and Shu 2007)**

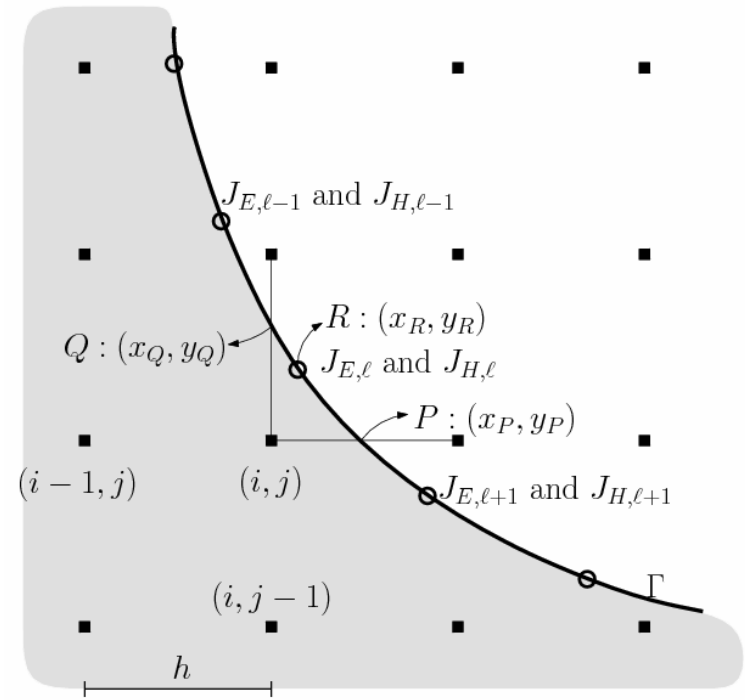
Coupling Interface Method (CIM)

■ CIM

- CIM1 (first order)
- CIM2 (2nd order)
- Hybrid CIM (CIM1 + CIM2)
for complex interface problems

■ Augmented CIM

- Auxiliary variables on interfaces



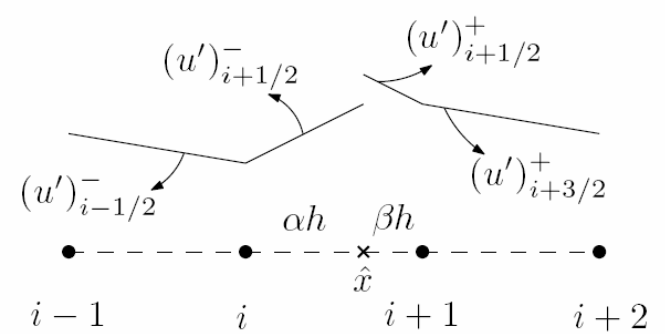
Numerical Issues for dealing with interface problems

- Accuracy: second-order in maximum norm.
 - Simplicity: easy to derive and program.
 - Stability: nice stencil coefficients for linear solvers.
 - Robustness: capable to handle complex interfaces.
 - Speed: linear computational complexity
-

CIM outline

- 1d: CIM1, CIM2
 - 2d: CIM2
 - 2d: Augmented CIM
 - d dimension
 - Hybrid CIM
 - Numerical validation
-

CIM1: one dimension



$$\begin{cases} u^-(x) := u_i + (u')_{i+1/2}^-(x - x_i) & \text{for } x_i \leq x < \hat{x} \\ u^+(x) := u_{i+1} + (u')_{i+1/2}^+(x - x_{i+1}) & \text{for } \hat{x} < x < x_{i+1}. \end{cases}$$

$$(u_{i+1} - \beta h (u')_{i+1/2}^+) - (u_i + \alpha h (u')_{i+1/2}^-) \approx \tau$$

$$\varepsilon^+ (u')_{i+1/2}^+ - \varepsilon^- (u')_{i+1/2}^- \approx \sigma.$$

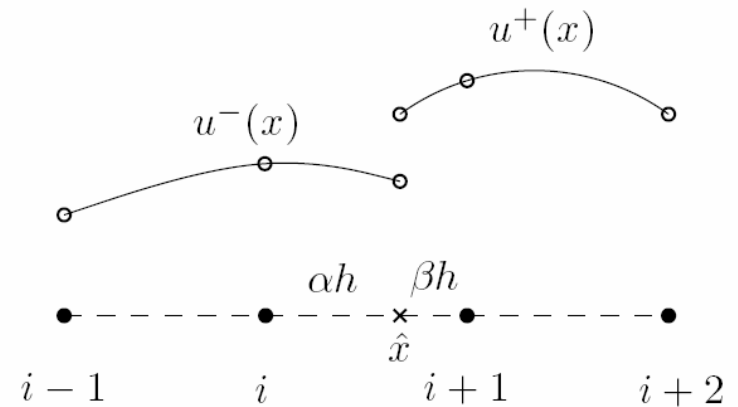
$$(u')_{i+1/2}^- = \frac{1}{h} \left(\bar{\rho}^+ (u_{i+1} - u_i) - \bar{\rho}^+ \tau - \beta h \frac{\sigma}{\bar{\varepsilon}} \right) + O(h)$$

$$(u')_{i+1/2}^+ = \frac{1}{h} \left(\bar{\rho}^- (u_{i+1} - u_i) - \bar{\rho}^- \tau + \alpha h \frac{\sigma}{\bar{\varepsilon}} \right) + O(h)$$

$$\bar{\varepsilon} = \alpha \varepsilon^+ + \beta \varepsilon^-, \quad \bar{\rho}^\pm = \varepsilon^\pm / \bar{\varepsilon}.$$

$$- (\varepsilon u')'(x_i) = -\frac{1}{h} \varepsilon_i \left((u')_{i+1/2}^- - (u')_{i-1/2}^- \right) + O(1).$$

CIM2: One dimension



- Quadratic approximation and match two grid data on each side

$$u_\ell(x) = u_i + \left(\frac{u_i - u_{i-1}}{h} + \frac{1}{2} h \underline{u''_i} \right) (x - x_i) + \frac{1}{2} \underline{u''_i} (x - x_i)^2 + O(h^3),$$

$$u_r(x) = u_{i+1} + \left(\frac{u_{i+2} - u_{i+1}}{h} - \frac{1}{2} h \underline{u''_{i+1}} \right) (x - x_{i+1}) + \frac{1}{2} \underline{u''_{i+1}} (x - x_{i+1})^2 + O(h^3)$$

- Match two jump conditions

$$u_r(\hat{x}) - u_\ell(\hat{x}) = \tau, \quad \hat{\varepsilon}^+ u'_r(\hat{x}) - \hat{\varepsilon}^- u'_\ell(\hat{x}) = \sigma,$$

CIM2: One dimension

$$u_i'' = \frac{1}{h^2} \left(L^{(\ell)} u_i + J_i^{(\ell)} \right) + O(h)$$

$$u_{i+1}'' = \frac{1}{h^2} \left(L^{(r)} u_{i+1} + J_{i+1}^{(r)} \right) + O(h),$$

$$L^{(\ell)} u_i := a_{i,-1} u_{i-1} + a_{i,0} u_i + a_{i,1} u_{i+1} + a_{i,2} u_{i+2}$$

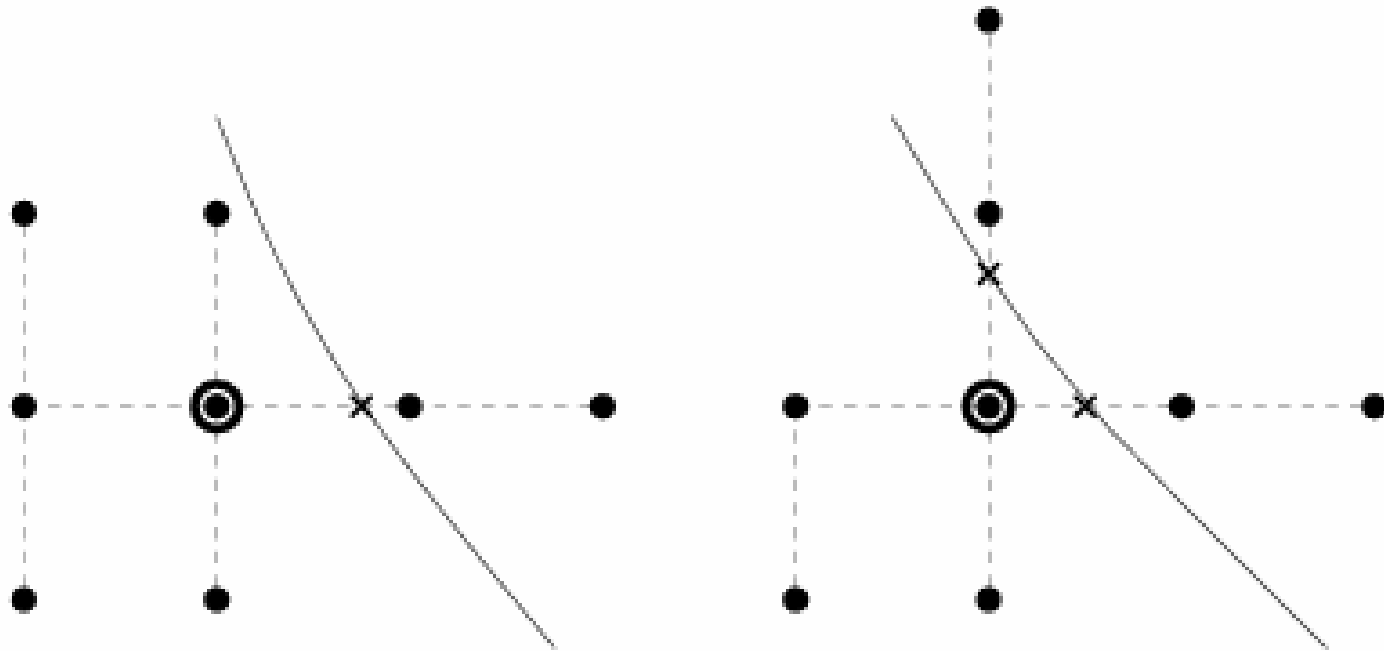
$$L^{(r)} u_{i+1} := a_{i+1,-2} u_{i-1} + a_{i+1,-1} u_i + a_{i+1,0} u_{i+1} + a_{i+1,1} u_{i+2}$$

$$J_i^{(\ell)} := a_{i,\tau} \frac{\tau}{h^2} + a_{i,\sigma} \frac{\sigma}{\hat{\varepsilon} h}$$

$$J_{i+1}^{(r)} := -a_{i+1,\tau} \frac{\tau}{h^2} + a_{i+1,\sigma} \frac{\sigma}{\hat{\varepsilon} h}.$$

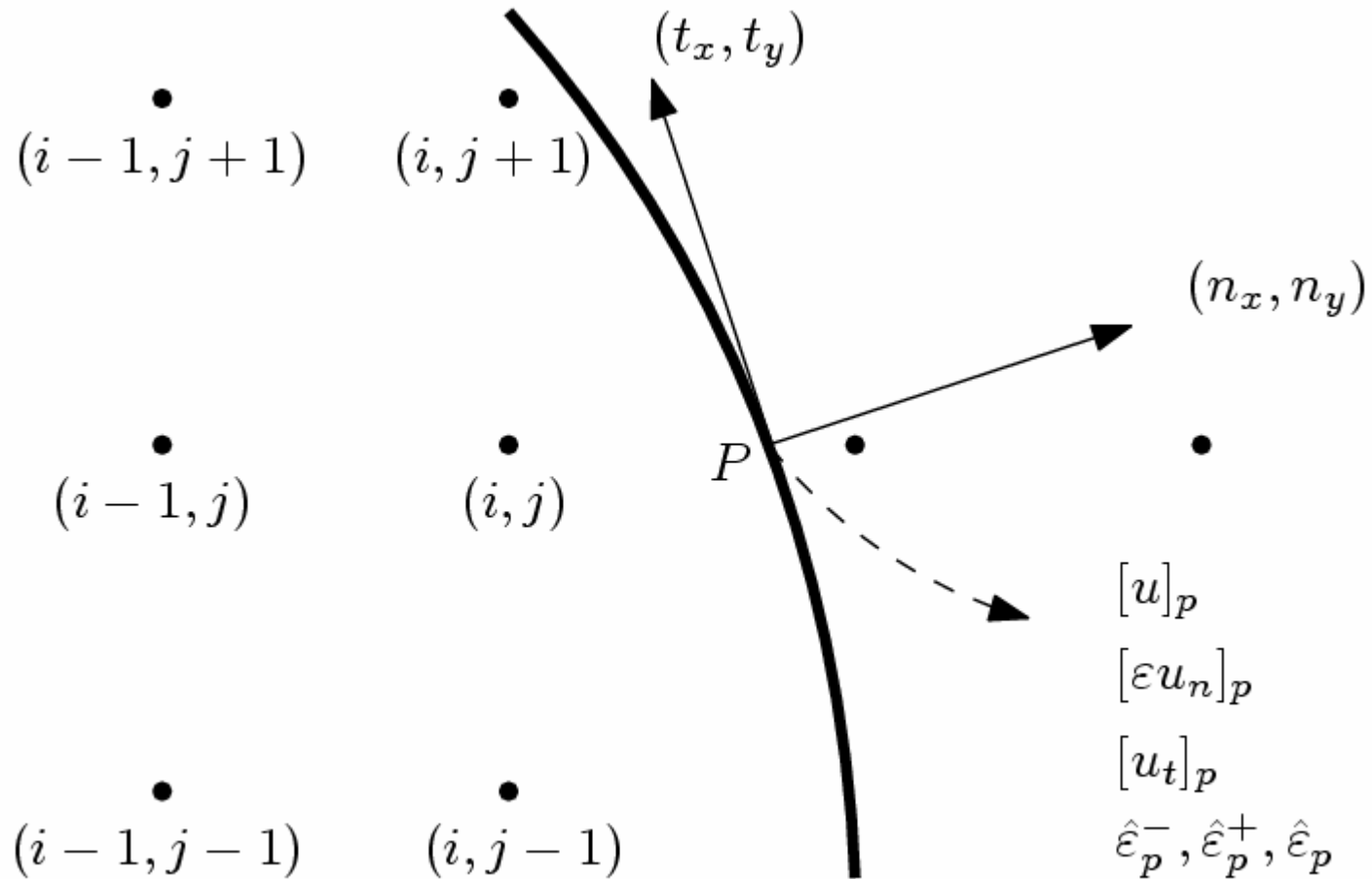
CIM2: 2 dimensions

Stencil at a normal on-front points (bullet) (8 points stencil)

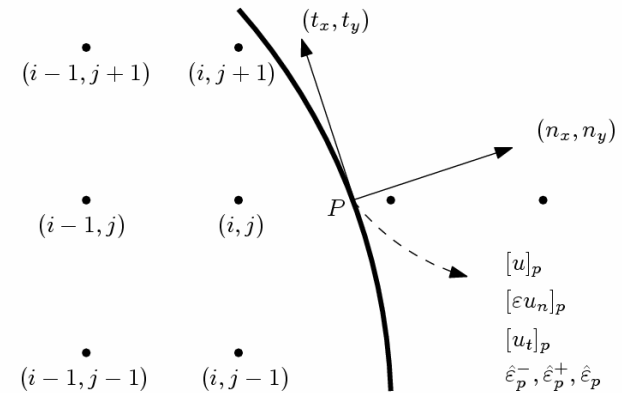


(a) Two dimension: 2 cases

CIM2 Case 1:



CIM2 (Case 1):



- Dimension splitting approach

$$\underline{u_{xx}} = \frac{1}{h^2} \left(Lu + a_\tau [u]_p + a_\sigma h \frac{[\varepsilon u_x]_p}{\hat{\varepsilon}_p} \right) + O(h)$$

- Decomposition of jump condition

$$[\varepsilon u_x]_p = [\varepsilon u_n]_p n_x + (\hat{\varepsilon}_p^+ [u_t]_p + (\hat{\varepsilon}_p^+ - \hat{\varepsilon}_p^-) (u_t^-)_p) t_x$$

- One side interpolation

$$\begin{aligned} (u_t^-)_p &\leftarrow \left(\frac{u_{i,j} - u_{i-1,j}}{h} + \left(\frac{1}{2} + \alpha \right) h \underline{u_{xx}} \right) t_x \\ &+ \left((1 + \alpha) \frac{u_{i,j+1} - u_{i,j-1}}{2h} - \alpha \frac{u_{i-1,j+1} - u_{i-1,j-1}}{2h} \right) t_y + O(h^2) \\ &= \frac{1}{h} T u + h \left(\frac{1}{2} + \alpha \right) t_x u_{xx} + O(h^2) \end{aligned}$$

CIM2 (Case 1):

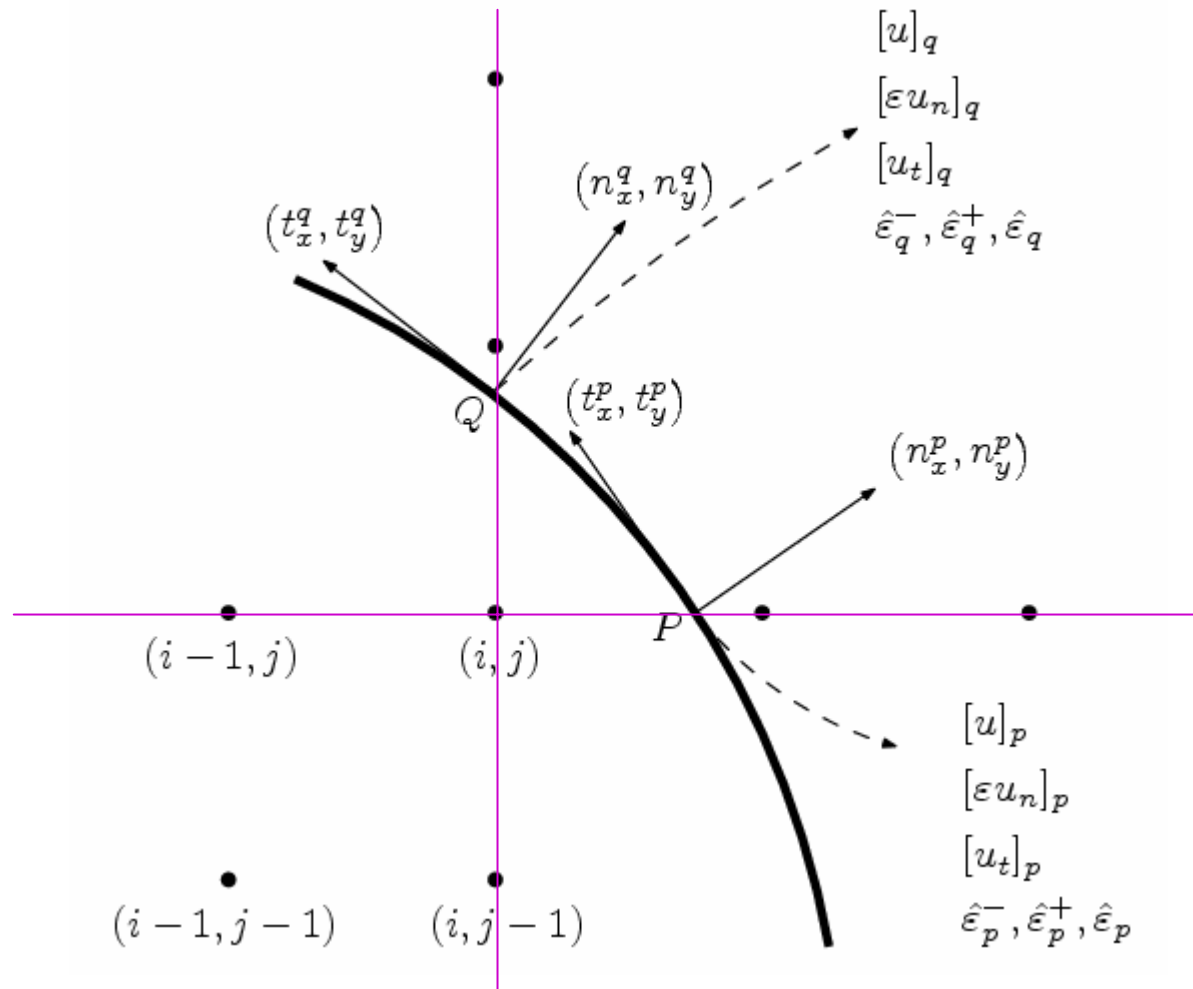
Bounded by 1 and $\varepsilon^+/\varepsilon^-$.

$$\left(1 - \left(\frac{1}{2} + \alpha\right)a_t t_x\right) u_{xx} = \frac{1}{h^2} (Lu + a_t T u + J)$$

$$a_t = a_\sigma (\rho^+ - \rho^-) t_x, \rho^\pm = \hat{\varepsilon}_p^\pm / \hat{\varepsilon}_p,$$

$$J = a_\tau [u]_p + a_\sigma h \left(\frac{[\varepsilon u_n]}{\hat{\varepsilon}} n_x + \rho^+ [u_t] t_x \right)$$

CIM2 (Case 2):

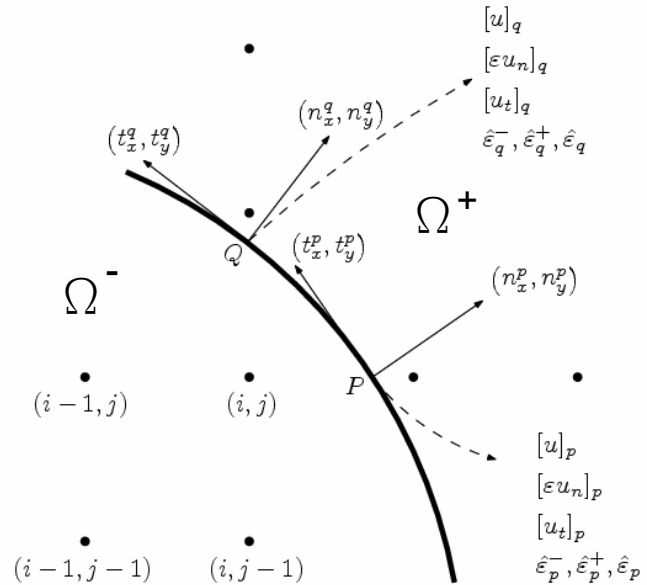


CIM2 (Case 2):

Dimension splitting approach

$$\underline{u_{xx}} = \frac{1}{h^2} \left(L_x u + a_{\tau,p} [u]_p + a_{\sigma,p} h \frac{[\varepsilon u_x]_p}{\hat{\varepsilon}_p} \right) + O(h)$$

$$\underline{u_{yy}} = \frac{1}{h^2} \left(L_y u + a_{\tau,q} [u]_q + a_{\sigma,q} h \frac{[\varepsilon u_y]_q}{\hat{\varepsilon}_q} \right) + O(h)$$



Decomposition of jump conditions

$$[\varepsilon u_x]_p = [\varepsilon u_n]_p n_x^p + (\hat{\varepsilon}_p^+ [u_t]_p + (\hat{\varepsilon}_p^+ - \hat{\varepsilon}_p^-) (u_t^-)_p) (t_x^p)$$

$$[\varepsilon u_y]_q = [\varepsilon u_n]_q n_y^q + (\hat{\varepsilon}_q^+ [u_t]_q + (\hat{\varepsilon}_q^+ - \hat{\varepsilon}_q^-) (u_t^-)_q) (t_y^q)$$

One-side interpolation

$$(u_t^-)_p \approx \left(\frac{u_{i,j} - u_{i-1,j}}{h} + \left(\frac{1}{2} + \alpha_p \right) \underline{u_{xx}} \right) t_x^p + \left((1 + \alpha_p) \frac{u_{i,j} - u_{i,j-1}}{h} - \alpha_p \frac{u_{i-1,j} - u_{i-1,j-1}}{h} + \frac{1}{2} \underline{u_{yy}} \right) t_y^p$$

$$(u_t^-)_q \approx \left(\frac{u_{i,j} - u_{i,j-1}}{h} + \left(\frac{1}{2} + \alpha_q \right) \underline{u_{yy}} \right) t_y^q + \left((1 + \alpha_q) \frac{u_{i,j} - u_{i-1,j}}{h} - \alpha_q \frac{u_{i,j-1} - u_{i-1,j-1}}{h} + \frac{1}{2} \underline{u_{xx}} \right) t_x^q$$

The second order derivatives are coupled by jump conditions

CIM2 (Case 2): results a coupling matrix

$$\mathbf{M} \begin{bmatrix} u_{xx} \\ u_{yy} \end{bmatrix} = \begin{bmatrix} L_x u + a_{t,p} T_p u + J_p \\ L_y u + a_{t,q} T_q u + J_q \end{bmatrix}$$

$$\mathbf{M} = \begin{bmatrix} 1 - (\frac{1}{2} + \alpha_p) a_{t,p} t_x^p & -\frac{1}{2} a_{t,p} t_y^p \\ -\frac{1}{2} a_{t,q} t_x^q & 1 - (\frac{1}{2} + \alpha_q) t_y^q \end{bmatrix}$$

$$a_{t,p} = a_{\sigma,p} (\rho_p^+ - \rho_q^-) t_x^p$$

$$a_{t,q} = a_{\sigma,q} (\rho_q^+ - \rho_q^-) t_y^q$$

$$\rho_p^\pm = \hat{\varepsilon}_p^\pm / \hat{\varepsilon}_p$$

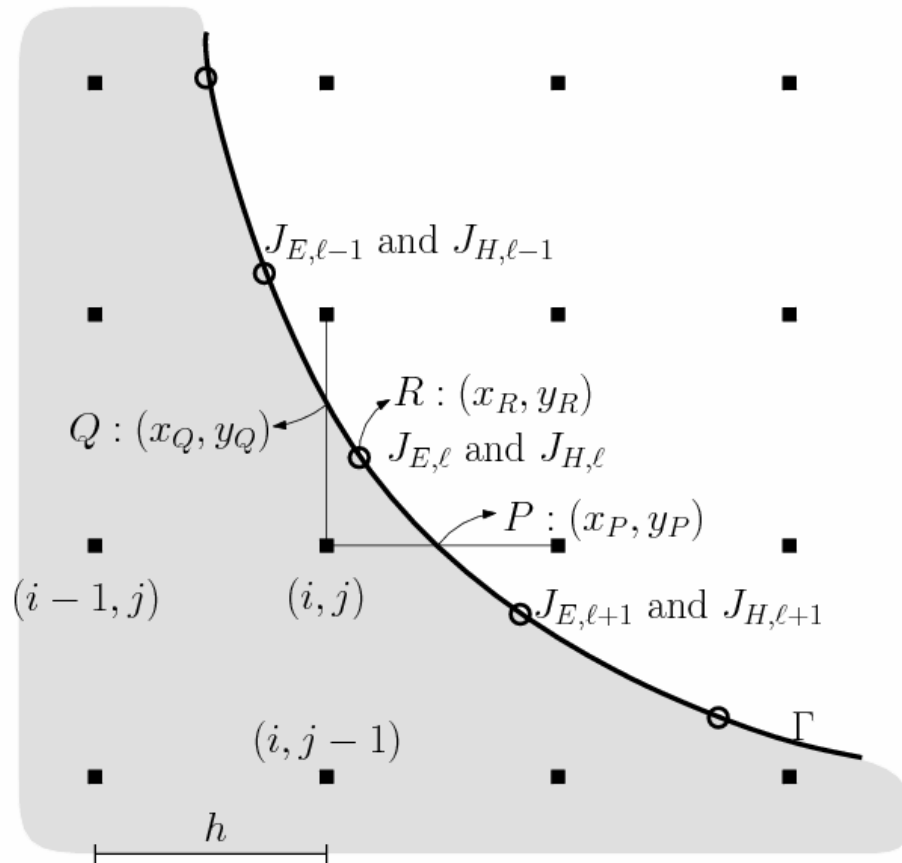
$$\rho_q^\pm = \hat{\varepsilon}_q^\pm / \hat{\varepsilon}_q$$

$$J_p = a_{\tau,p} [u]_p + a_{\sigma,p} h \left(\frac{[\varepsilon u_n]_p}{\hat{\varepsilon}_p} n_x^p + \rho_p^+ [u_t]_p t_x^p \right)$$

$$J_q = a_{\tau,q} [u]_q + a_{\sigma,q} h \left(\frac{[\varepsilon u_n]_q}{\hat{\varepsilon}_q} n_y^q + \rho_q^+ [u_t]_q t_y^q \right)$$

Theorem: $\det(\mathbf{M})$ is positive when local curvature is zero or h is small

Augmented CIM



Augmented CIM

- Auxiliary interfacial variables are distributed on the interface almost uniformly.
 - The jump information at the intersections of grid line and interface is expressed in terms of interfacial variables at nearby interfacial grid.
-

Apply 1-d method in x- and y-directions

$$\frac{\partial^2 E}{\partial x^2} \Big|_{i,j} = L_{i,j,x} (E_{i-1:i+2,j}, [\varepsilon u_x]_P)$$

$$\frac{\partial^2 E}{\partial y^2} \Big|_{i,j} = L_{i,j,y} (E_{i,j-1:j+2}, [\varepsilon u_y]_Q)$$

$$\left[\varepsilon \frac{\partial E}{\partial x} \right]_P = \left[\varepsilon \frac{\partial E}{\partial x} \right]_R + (x_P - x_R) \left[\varepsilon \frac{\partial^2 E}{\partial x^2} \right]_R + (y_P - y_R) \left[\varepsilon \frac{\partial^2 E}{\partial x \partial y} \right]_R$$

$$\left[\varepsilon \frac{\partial E}{\partial y} \right]_Q = \left[\varepsilon \frac{\partial E}{\partial x} \right]_R + (y_Q - y_R) \left[\varepsilon \frac{\partial^2 E}{\partial y^2} \right]_R + (x_P - x_R) \left[\varepsilon \frac{\partial^2 E}{\partial x \partial y} \right]_R$$

Resulting scheme

$$\frac{\partial^2 E}{\partial x^2} \Big|_{i,j} \approx \mathcal{L}'_{E_{xx}} (E_{i-1:i+2, j-1, j+2}, J_{E, \ell}),$$

$$\frac{\partial^2 E}{\partial y^2} \Big|_{i,j} \approx \mathcal{L}'_{E_{yy}} (E_{i-1:i+2, j-1, j+2}, J_{E, \ell}),$$

$$\nabla^2 E_{i,j} \approx (\mathcal{L}'_{E_{xx}} + \mathcal{L}'_{E_{yy}})(E_{i-1:i+2, j-1, j+2}, J_{E, \ell}).$$

CIM1: d dimensions

■ Dimension splitting approach

$$\begin{aligned}\frac{\partial}{\partial x_k} u(\mathbf{x} + \frac{1}{2} h \mathbf{e}_k) &\approx \frac{1}{h} \left(\bar{\rho}_{k+}^+ (u(\mathbf{x} + h \mathbf{e}_k) - u(\mathbf{x})) - \bar{\rho}_{k+}^+ [u]_{\hat{\mathbf{x}}_{k+}} - \beta_{k+} h \frac{[\varepsilon \nabla u \cdot \mathbf{e}_k]_{\hat{\mathbf{x}}_{k+}}}{\bar{\varepsilon}_{k+}} \right) \\ \frac{\partial}{\partial x_k} u(\mathbf{x} - \frac{1}{2} h \mathbf{e}_k) &\approx \frac{1}{h} \left(\bar{\rho}_{k-}^+ (u(\mathbf{x}) - u(\mathbf{x} - h \mathbf{e}_k)) + \bar{\rho}_{k-}^+ [u]_{\hat{\mathbf{x}}_{k-}} - \beta_{k-} h \frac{[\varepsilon \nabla u \cdot \mathbf{e}_k]_{\hat{\mathbf{x}}_{k-}}}{\bar{\varepsilon}_{k-}} \right)\end{aligned}$$

■ Decomposition of jump conditions

$$[\varepsilon \nabla u \cdot \mathbf{e}_k]_{\hat{\mathbf{x}}_k} = [\varepsilon \nabla u \cdot \mathbf{n}_k]_{\hat{\mathbf{x}}_k} (\mathbf{n}_k \cdot \mathbf{e}_k) + [\varepsilon \nabla u \cdot \mathbf{t}_k]_{\hat{\mathbf{x}}_k} (\mathbf{t}_k \cdot \mathbf{e}_k)$$

$$= \sigma_k (\mathbf{n}_k \cdot \mathbf{e}_k) + (\hat{\varepsilon}_k^+ [\nabla u \cdot \mathbf{t}_k]_{\hat{\mathbf{x}}_k} + (\hat{\varepsilon}_k^+ - \hat{\varepsilon}_k^-) \nabla u^-(\hat{\mathbf{x}}_k) \cdot \mathbf{t}_k) (\mathbf{t}_k \cdot \mathbf{e}_k)$$

■ One-side interpolation

- $j = k$: $\frac{\partial}{\partial x_k} u^-(\hat{\mathbf{x}}_{k\pm}) \approx \frac{\partial}{\partial x_k} u(\mathbf{x} \pm \frac{1}{2} h \mathbf{e}_k)$

- $j \neq k$: $\frac{\partial}{\partial x_j} u^-(\hat{\mathbf{x}}_{k\pm}) = \begin{cases} D_j^{(s_j)} u(\mathbf{x}) & \text{if } \gamma_{j+\frac{1}{2}} + \gamma_{j-\frac{1}{2}} < 2 \\ \frac{\partial}{\partial x_j} u^-(\mathbf{x} \pm \frac{1}{2} h \mathbf{e}_j) & \text{if } \gamma_{j+\frac{1}{2}} + \gamma_{j-\frac{1}{2}} = 2 \end{cases}$

CIM2: d dimensions

- Dimension splitting approach

$$\frac{\partial^2}{\partial x_k^2} u(\mathbf{x}) = \frac{1}{h^2} \left(L_k^{(s_k)} u(\mathbf{x}) + a_{\tau,k} [u]_{\hat{\mathbf{x}}_k} + s_k a_{\sigma,k} h \frac{[\varepsilon \nabla u \cdot \mathbf{e}_k]_{\hat{\mathbf{x}}_k}}{\hat{\varepsilon}_k} \right) + O(h)$$

- Decomposition of jump conditions

$$[\varepsilon \nabla u \cdot \mathbf{e}_k]_{\hat{\mathbf{x}}_k} = [\varepsilon \nabla u \cdot \mathbf{n}_k]_{\hat{\mathbf{x}}_k} (\mathbf{n}_k \cdot \mathbf{e}_k) + [\varepsilon \nabla u \cdot \mathbf{t}_k]_{\hat{\mathbf{x}}_k} (\mathbf{t}_k \cdot \mathbf{e}_k)$$

$$= \sigma_k (\mathbf{n}_k \cdot \mathbf{e}_k) + (\hat{\varepsilon}_k^+ [\nabla u \cdot \mathbf{t}_k]_{\hat{\mathbf{x}}_k} + (\hat{\varepsilon}_k^+ - \hat{\varepsilon}_k^-) \nabla u^-(\hat{\mathbf{x}}_k) \cdot \mathbf{t}_k) (\mathbf{t}_k \cdot \mathbf{e}_k)$$

- One-side interpolation

$$\begin{aligned} & \nabla u^-(\hat{\mathbf{x}}_k) \cdot \mathbf{t}_k \\ &= \frac{1}{h} T_k u(\mathbf{x}) + h \left(s_k \left(\frac{1}{2} + \alpha_k \right) (\mathbf{t}_k \cdot \mathbf{e}_k) \frac{\partial^2}{\partial x_k^2} u(\mathbf{x}) + \frac{1}{2} \sum_{j=1, j \neq k}^d s_j (\mathbf{t}_k \cdot \mathbf{e}_j) \frac{\partial^2}{\partial x_j^2} u(\mathbf{x}) \right) \end{aligned}$$

CIM2: d dimensions, coupling matrix

$$\mathbf{M} \left(\frac{\partial^2}{\partial x_k^2} u(\mathbf{x}) \right)_{k=1}^d = \frac{1}{h^2} (Lu(\mathbf{x}) + Tu(\mathbf{x}) + J),$$

$$m_{k,j} = \begin{cases} 1 - |s_k|(\frac{1}{2} + \alpha_k) a_{t,k} (\mathbf{t}_k \cdot \mathbf{e}_k) & j = k \\ -\frac{1}{2} s_j s_k a_{t,k} (\mathbf{t}_k \cdot \mathbf{e}_j) & j \neq k, \end{cases}$$

$$L = (L_1, \dots, L_d)^T,$$

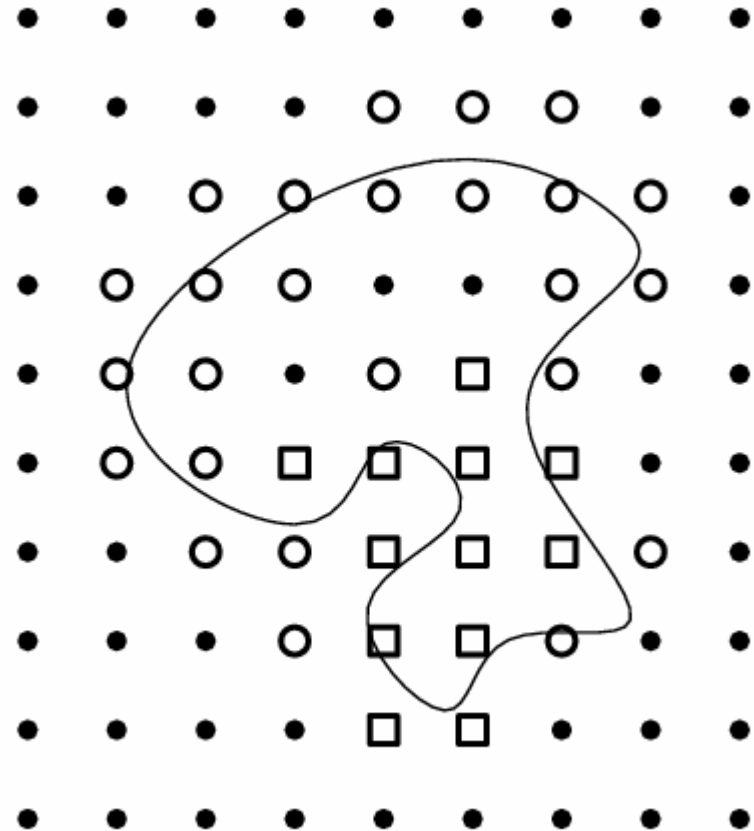
$$T = (s_1 a_{t,1} T_1, \dots, s_d a_{t,d} T_d)^T$$

$$J = (J_1, \dots, J_d)^T.$$

Complex interface problems

Classification of grid

- Interior points (bullet)
(contral finite difference)
 - Nearest neighbors are in the same side
- On-front points (circle and box)
 - Normal (circle) (CIM2).
 - Exceptional (box) (CIM1).



Classification of grids for complex interface (number of grids)

- Interior grids: $O(h^{-d})$
 - Normal on-fronts (CIM2): $O(h^{1-d})$
 - Exceptional (CIM1): $O(1)$

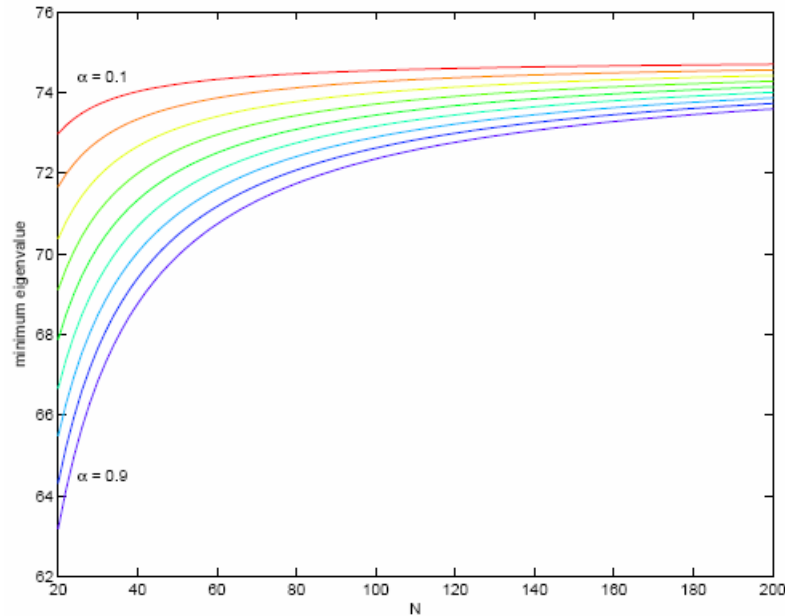
 - The resulting scheme is still **2nd order**
-

Numerical Validation

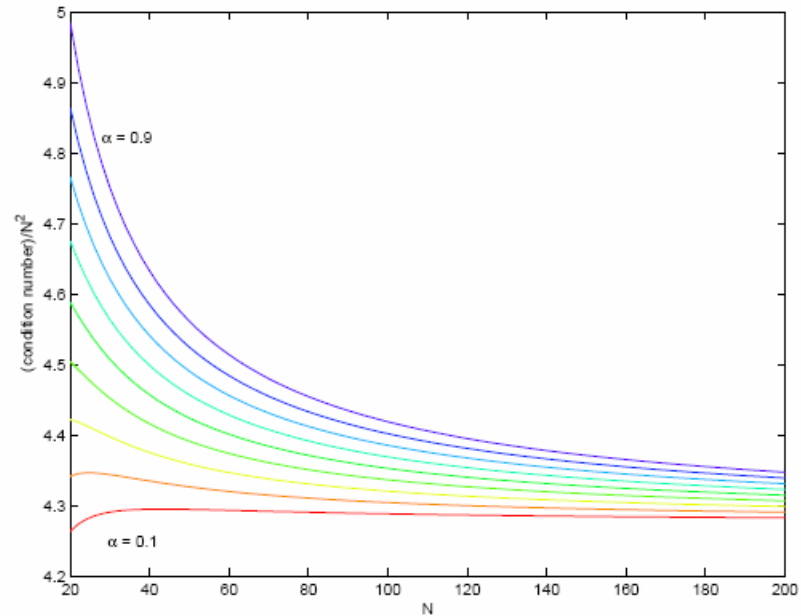
- Stability of CIM2 in 1d
 - Orientation error of CIM2 in 2d
 - Convergence tests of CIM1
 - Comparison results (CIM2)
 - Complex interfaces results (Hybrid CIM)
-

Stability Issue of CIM2 in 1-d

Let $A(\alpha, N)$ be the resulting matrix.



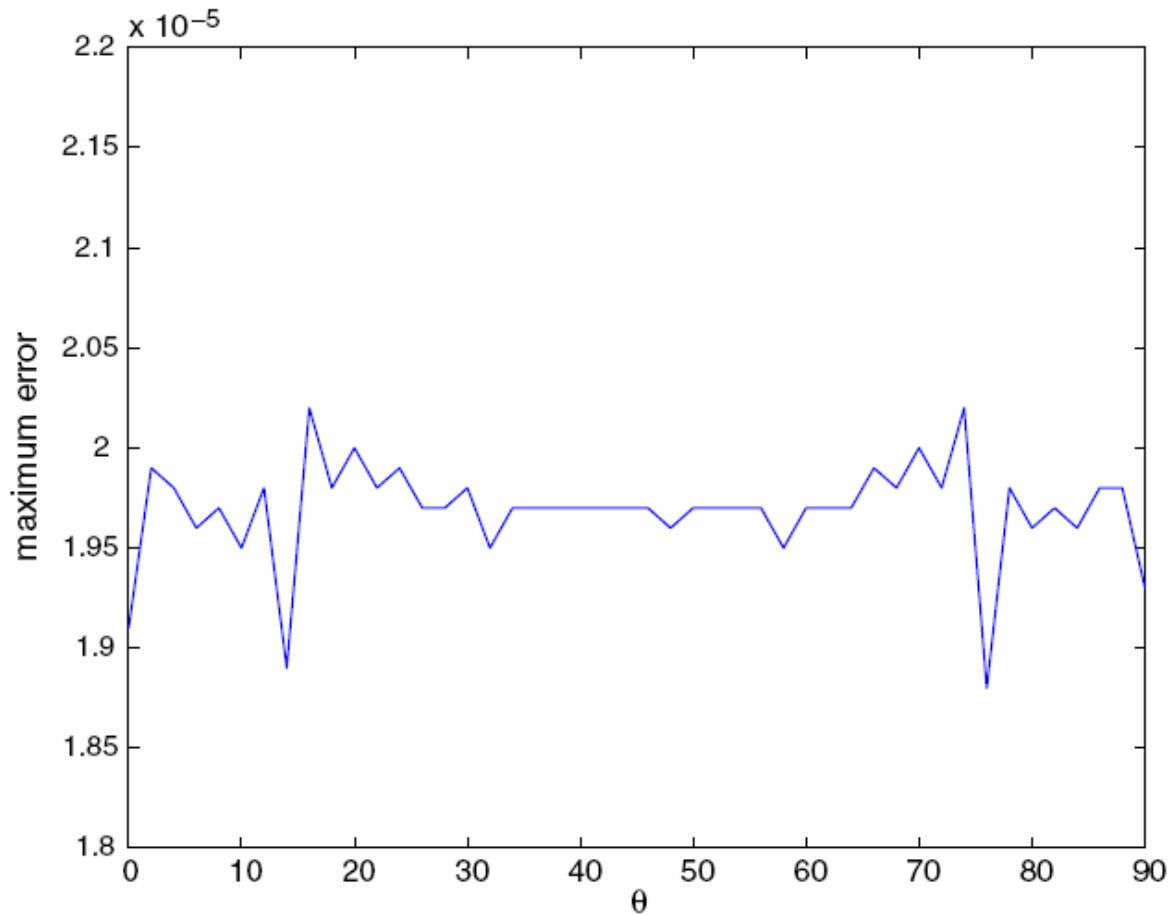
(a) Minimal eigenvalue $\lambda_{min}(\alpha, N)$



(b) Scaled condition number $condA(\alpha, N)/N^2$

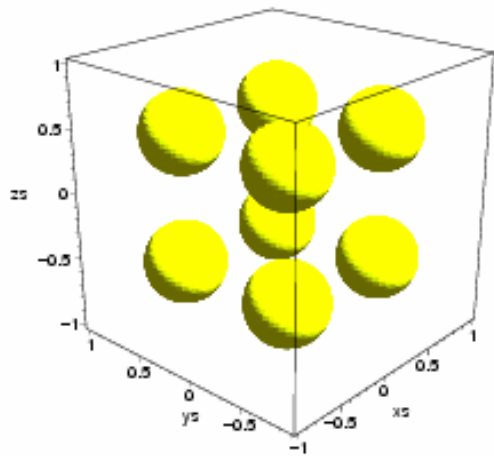
Insensitive to the location of the interface in a cell.

Orientation error from CIM2 is small

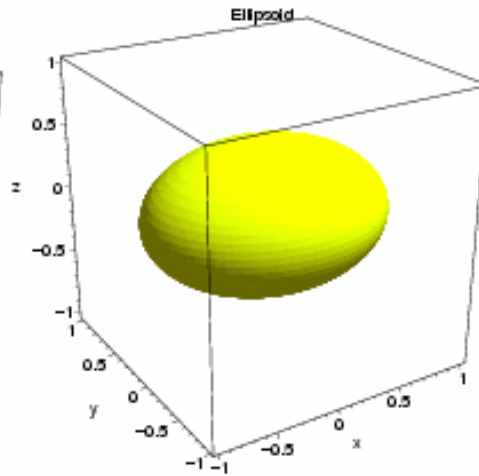


Insensitive to the orientation of the interface.

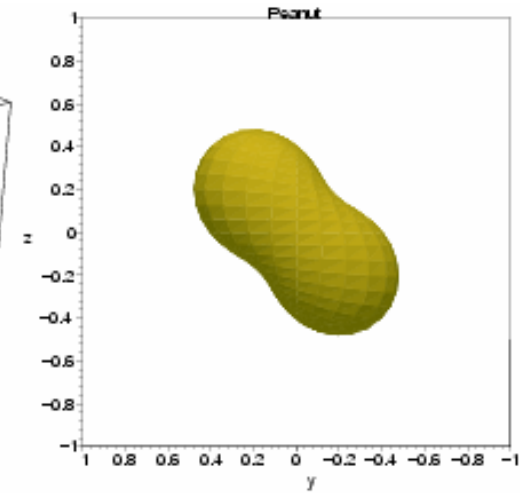
Convergence tests for CIM1: interfaces



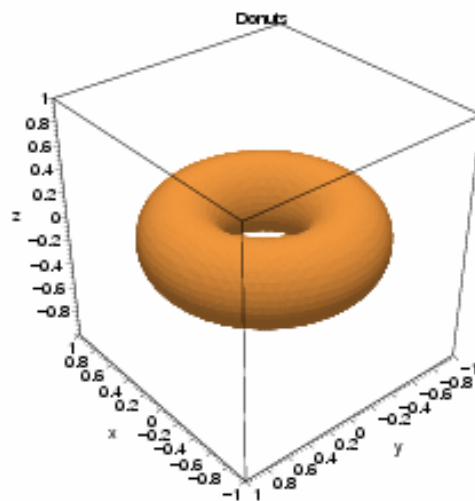
(a) 8 balls



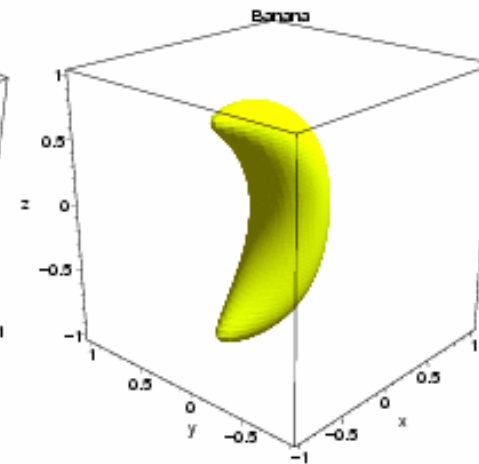
(b) Ellipsoid



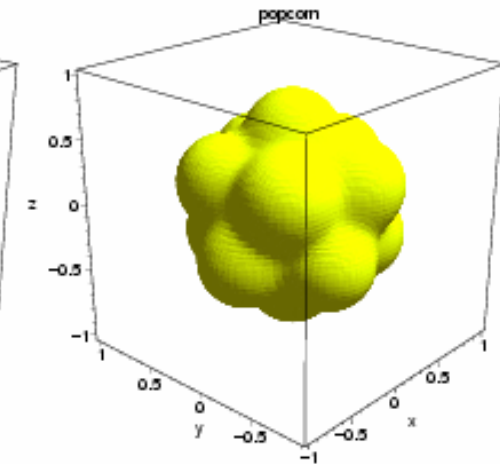
(c) Peanut



(d) Donut



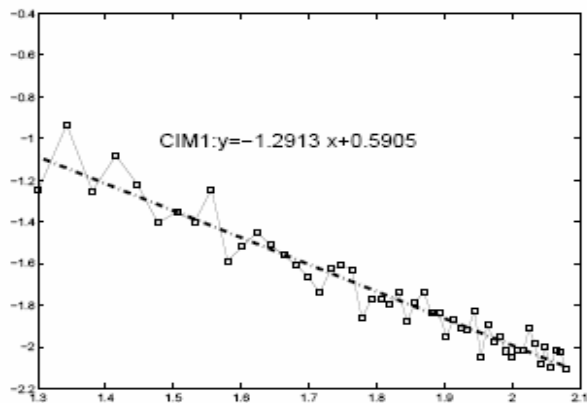
(e) Banana



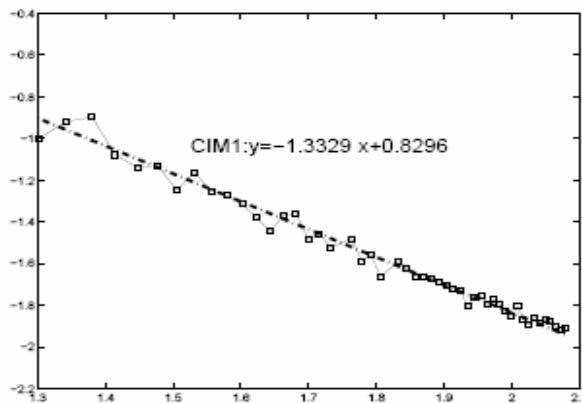
(f) Popcorn

Convergence of CIM1 (2) (order 1.3)

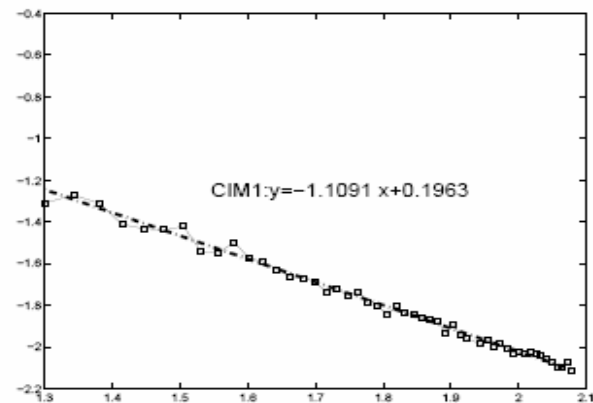
log-log plot of error versus N



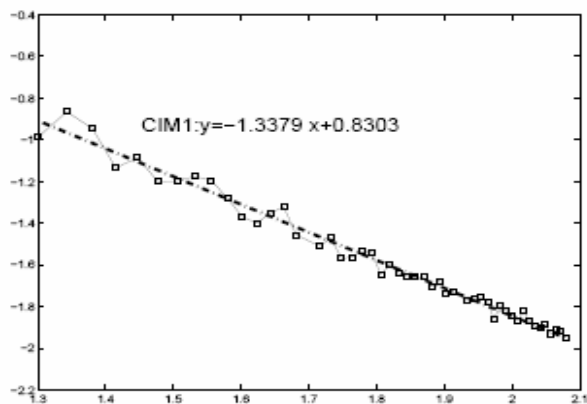
(a) 8 balls



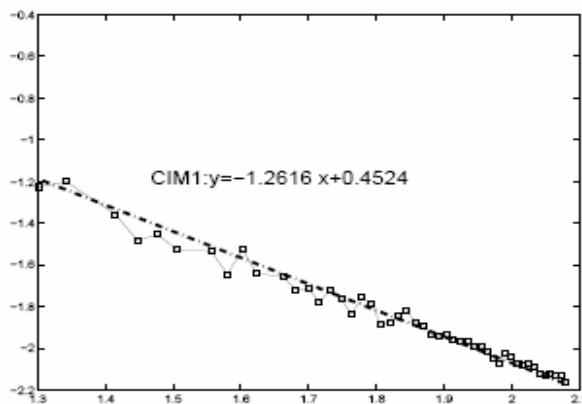
(b) Ellipsoid



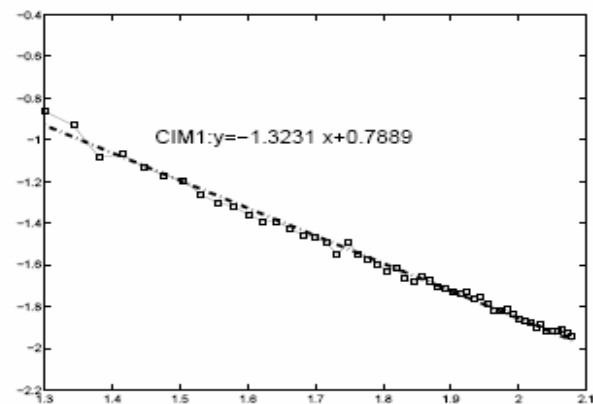
(c) Peanut



(d) Donut



(e) Banana



(f) Popcorn

Example 5 (for CIM2)

$$\phi(x, y, z) = r - 0.5, \quad \Omega^- = \{(x, y, z) | \phi(x, y, z) < 0\}, \quad \Omega^+ = \{(x, y, z) | \phi(x, y, z) > 0\}$$

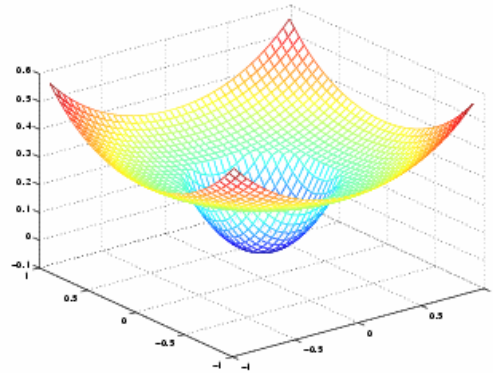
$$\varepsilon(x, y, z) = \begin{cases} 1 + r^2 & (x, y, z) \in \Omega^- \\ b & (x, y, z) \in \Omega^+ \end{cases}$$

$$u_e(x, y, z) = \begin{cases} r^2 & (x, y, z) \in \Omega^- \\ (r^4/2 + r^2)/b - (0.5^4/2 + 0.5^2)/b + 0.5^2 & (x, y, z) \in \Omega^+ \end{cases}$$

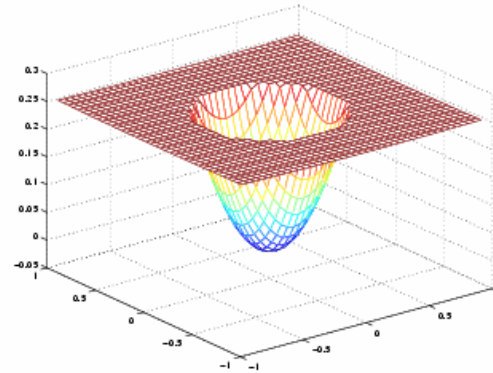
$$f(x, y, z) = -(10r^2 + 6),$$

$$b = 1, 10, 1000$$

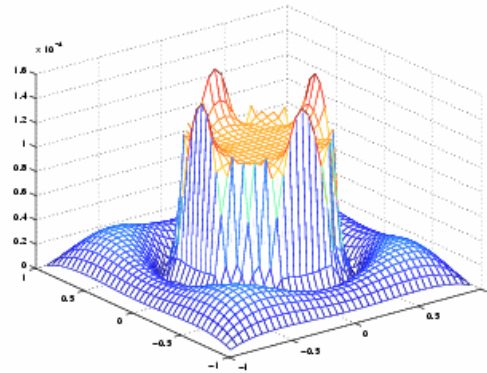
Example 5, figures



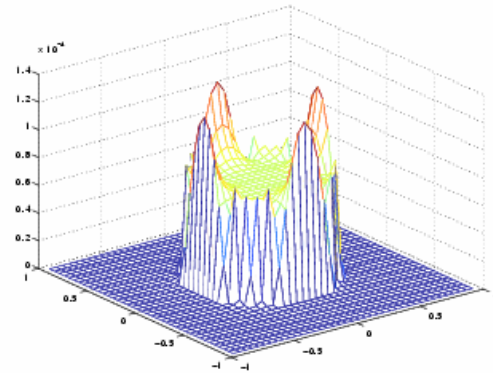
(a) Exact Solution: $b = 10$



(b) Exact Solution: $b = 1000$



(c) $|u - u_e|$: $b = 10$



(d) $|u - u_e|$: $b = 1000$

Example 5 (for CIM2)

| n | CPU | CIM | | | MIIM, 27 points | |
|-----|------|--|---|-------|---|-------|
| | | $\ \nabla u - \nabla u_e\ _{\infty, \Gamma}$ | $\ u_a - u_e\ _{\infty} / \ u_e\ _{\infty}$ | Order | $\ u_a - u_e\ _{\infty} / \ u_e\ _{\infty}$ | Order |
| 26 | 1.52 | 1.005×10^{-2} | 1.822×10^{-4} | | 1.247×10^{-3} | |
| 52 | 20.5 | 3.685×10^{-3} | 4.153×10^{-5} | 2.133 | 3.979×10^{-3} | 1.648 |
| 104 | 212 | 9.729×10^{-4} | 9.529×10^{-6} | 2.124 | 9.592×10^{-4} | 2.052 |
| 208 | 2355 | 2.540×10^{-4} | 2.230×10^{-6} | 2.095 | – | – |

Table 10: Example 4: $b = 1$

Example 5 (CIM2)

| n | CIM | | | | MIIM, 27 points | |
|-----|-------|--|---|-------|---|-------|
| | CPU | $\ \nabla u - \nabla u_e\ _{\infty, \Gamma}$ | $\ u_a - u_e\ _{\infty} / \ u_e\ _{\infty}$ | Order | $\ u_a - u_e\ _{\infty} / \ u_e\ _{\infty}$ | Order |
| 26 | 1.45 | 7.174×10^{-3} | 4.332×10^{-4} | | 1.525×10^{-3} | |
| 52 | 19.14 | 2.693×10^{-3} | 9.240×10^{-5} | 2.229 | 5.240×10^{-4} | 1.541 |
| 104 | 161 | 7.401×10^{-4} | 1.636×10^{-5} | 2.498 | 1.010×10^{-4} | 2.375 |
| 208 | 1867 | 1.979×10^{-4} | 3.330×10^{-6} | 2.297 | — | — |

Table 11: Example 4: $b = 10$

Example 5 (CIM2)

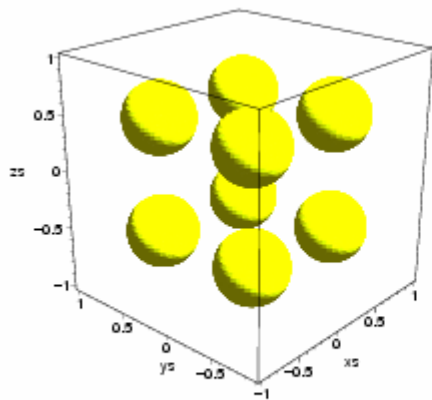
| n | CIM | | | | MIIM, 27 points | |
|-----|-------|--|---|-------|---|-------|
| | CPU | $\ \nabla u - \nabla u_e\ _{\infty, \Gamma}$ | $\ u_a - u_e\ _{\infty} / \ u_e\ _{\infty}$ | Order | $\ u_a - u_e\ _{\infty} / \ u_e\ _{\infty}$ | Order |
| 26 | 1.48 | 6.825×10^{-3} | 9.133×10^{-4} | | 3.845×10^{-3} | |
| 52 | 24.54 | 2.594×10^{-3} | 2.466×10^{-4} | 1.889 | 1.111×10^{-3} | 1.649 |
| 104 | 209 | 7.183×10^{-4} | 3.447×10^{-5} | 2.839 | 1.605×10^{-4} | 2.791 |
| 208 | 3299 | 1.925×10^{-4} | 4.727×10^{-6} | 2.866 | — | — |

Table 12: Example 4: $b = 1000$

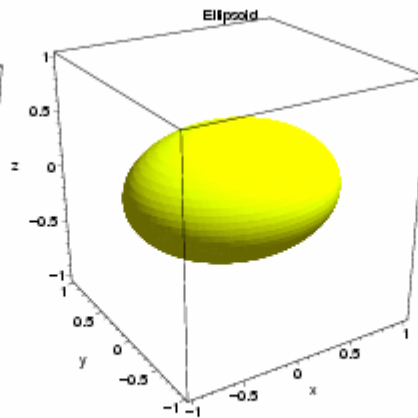
Comparison results

- Second order for u and its gradients in maximum norm for CIM2
 - Insensitive to the contrast of epsilon
 - Less absolute error despite of using smaller size of stencil
 - Linear computational complexity
-

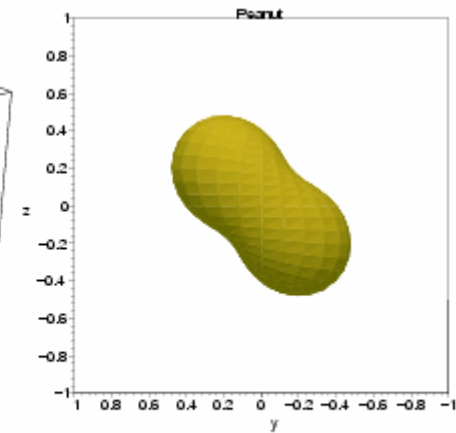
Hybrid CIM



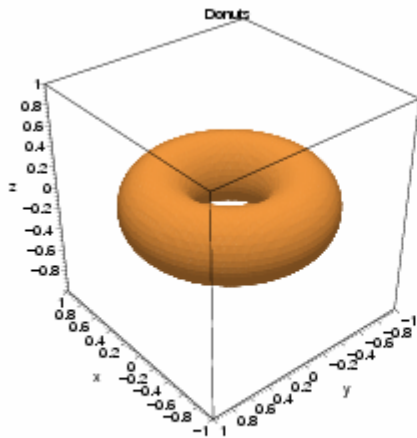
(a) 8 balls



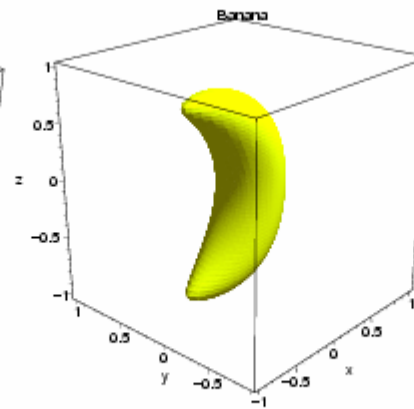
(b) Ellipsoid



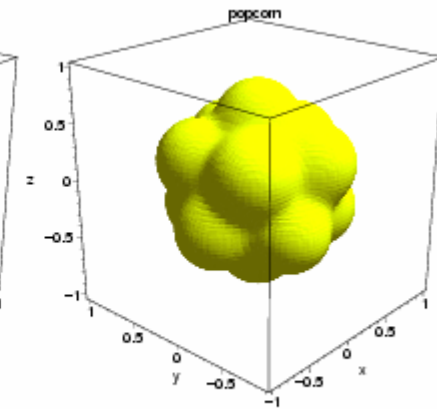
(c) Peanut



(d) Donut



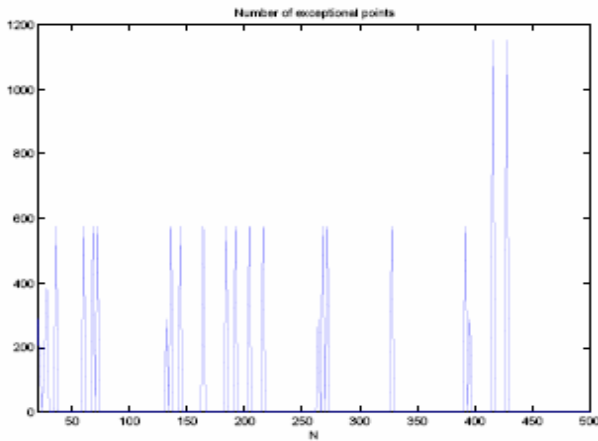
(e) Banana



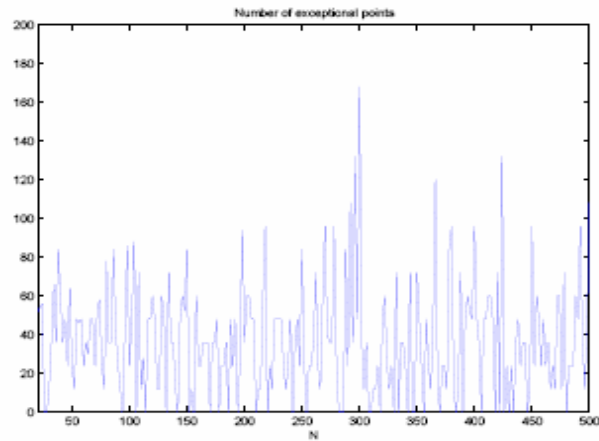
(f) Popcorn

Number of exceptional points

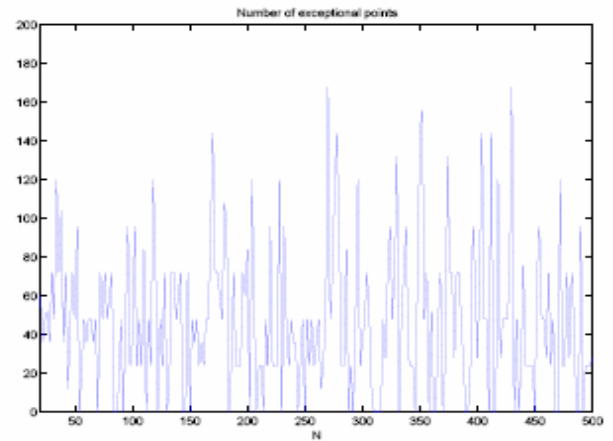
$O(1)$ in general



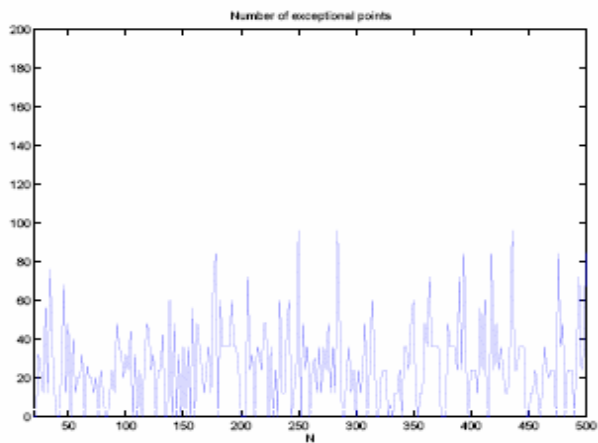
(a) 8 balls



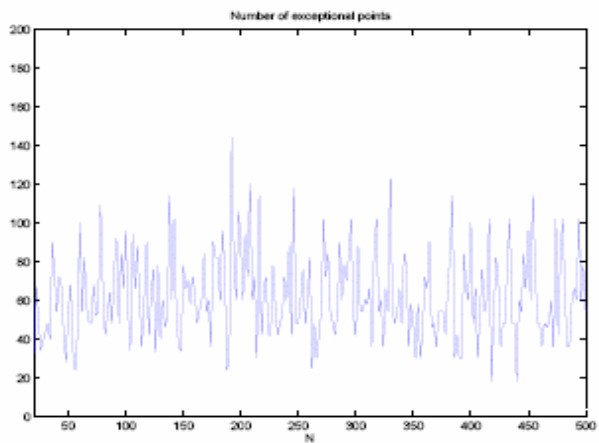
(b) Ellipsoid



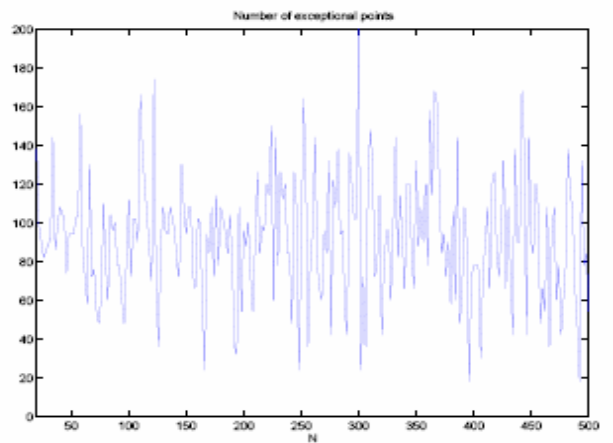
(c) Donuts



(d) Peanut

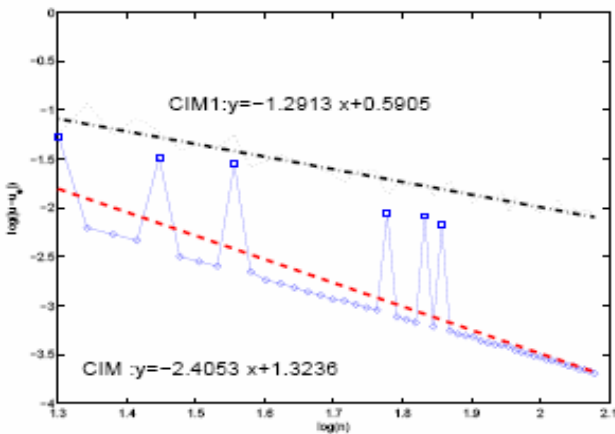


(e) Banana

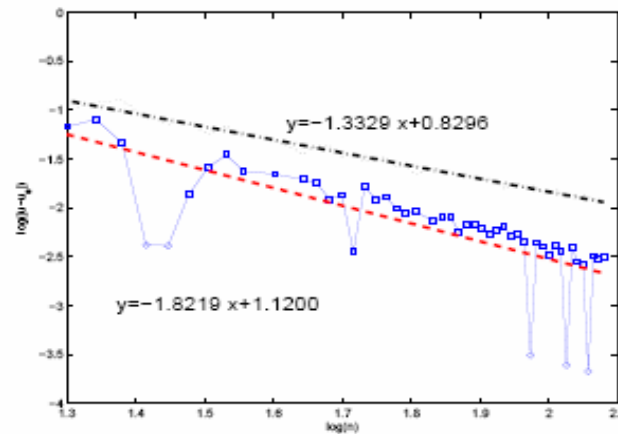


(f) Popcorn

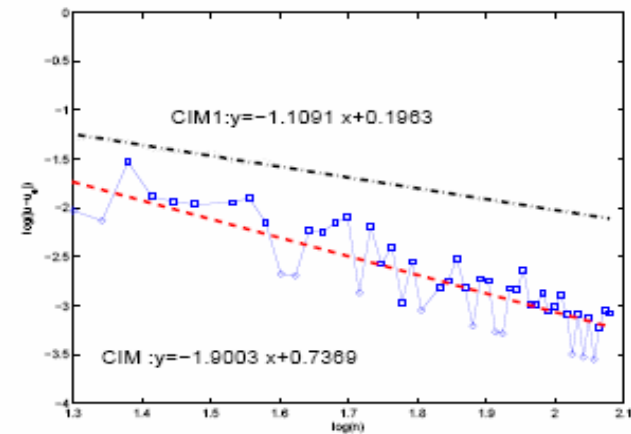
Convergence of hybrid CIM (order 1.8)



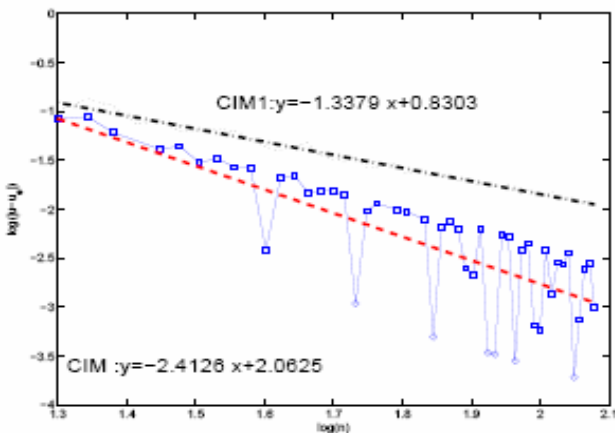
(a) 8 balls



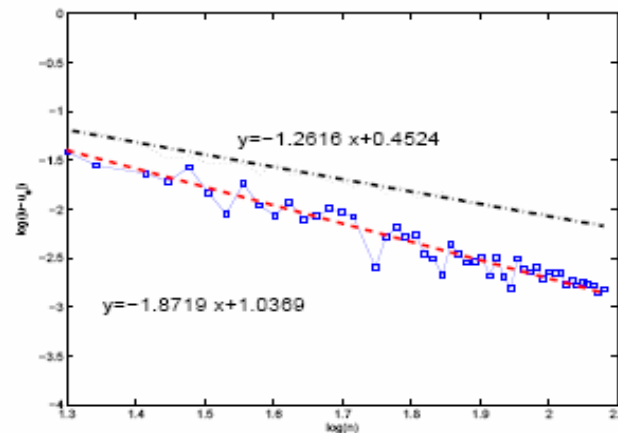
(b) Ellipsoid



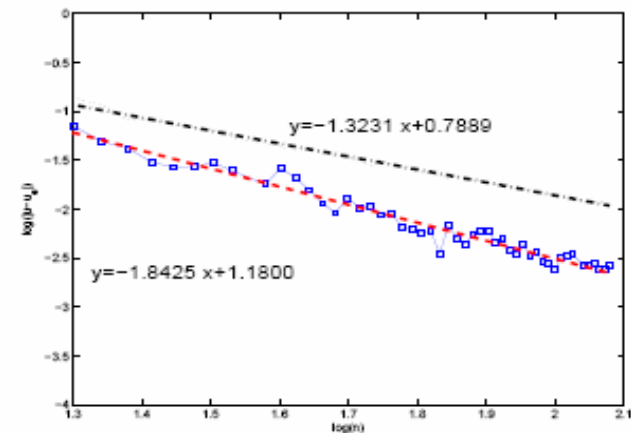
(c) Peanut



(d) Donut



(e) Banana



(f) Popcorn

Hybrid CIM

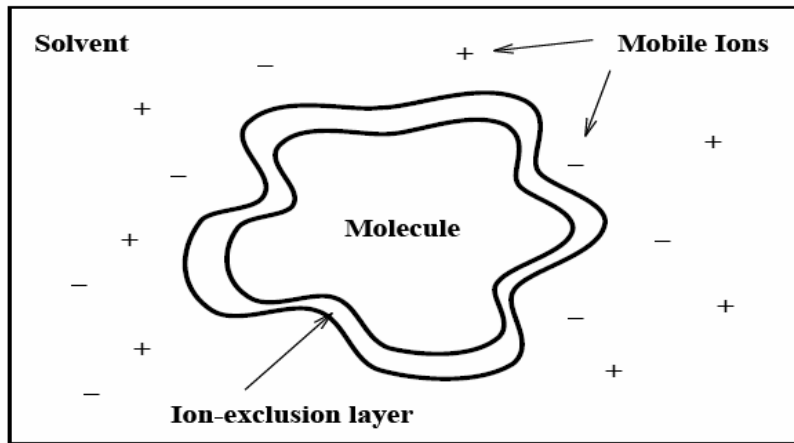
- Capable to handle complex interface problems in three dimensions
 - Produce less absolute error than FIIM.
 - Second order accuracy due to number of exceptional points is $O(1)$ in most applications.
-

Some applications

- Find electrostatic potential for macromolecule in solvent
 - Tumor growth simulation
 - Finding dispersion relation for surface plasmonic wave propagation
-

Biomolecule in solvent: Poisson-Boltzmann Equation

$$-\nabla \cdot (\epsilon(x) \nabla u(x)) + \bar{\kappa}^2(x) \sinh(u(x)) = \frac{4\pi e_c^2}{k_B T} \sum_{i=1}^{N_m} z_i \delta(x - \bar{x}_i)$$



positive ion distribution : e^{-u}

negative ion distribution : $-e^u$

N. Baker, M. Holst, and F. Wang, [Adaptive multilevel finite element solution of the Poisson-Boltzmann equation II: refinement at solvent accessible surfaces in biomolecular systems](#). J. Comput. Chem., 21 (2000), pp. 1343-1352. (Paper at Wiley)

Poisson-Boltzmann equation

$$-\nabla[\epsilon(r)\nabla\phi(r)] + K(r) \sinh(\phi(r)) = Q(r)$$

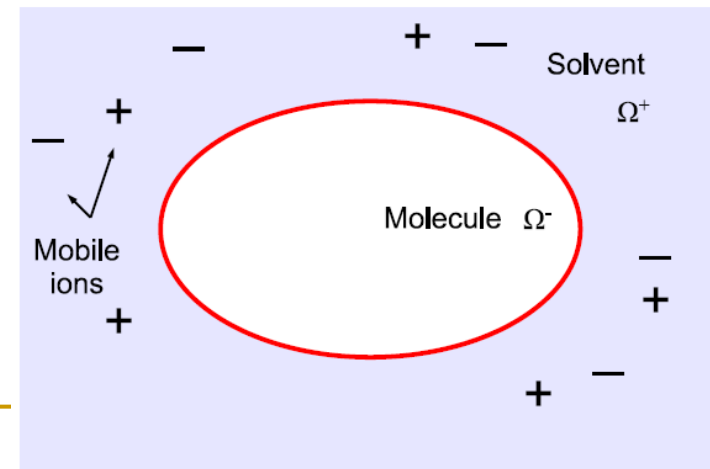
$$Q(r) = C \sum_{i=1}^{N_m} q_i \delta(r - r_i), \quad C = \frac{4\pi e_c^2}{k_B T}$$

$$\epsilon_1 \approx 1 \sim 2, \quad \epsilon_2 \approx 80,$$

$$5249.0 \leq C \leq 10500.0,$$

$$-1 \leq q_i \leq 1,$$

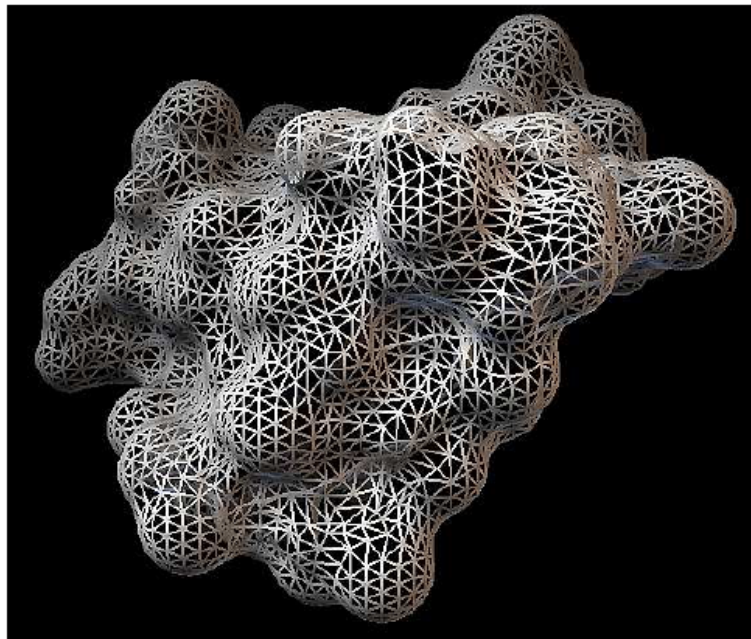
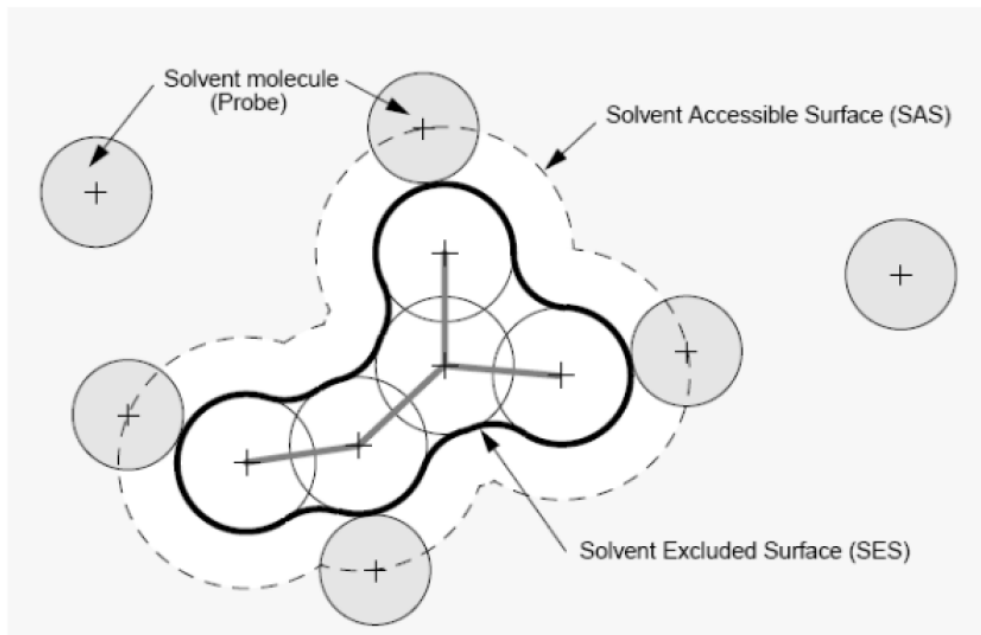
$$K = \bar{\kappa}^2 = 8.486902807 \text{ \AA}^{-2} I_s,$$



Numerical procedure

- Construction of molecular surface (by MSMS)
- Treatment of singular charges $C \sum q_i (x - x_i)$
- Nonlinear iteration by damped Newton's method for the perturbed equation
- Coupling interface method to solve elliptic interface problem
- Algebraic multigrid for solving linear systems

Construction of molecular surface: MSMS



The interface calculated by computer software MSMS of molecule 1crn with probe radius 1.4 and triangulation density 3.0.

Treatment of Singularity

$$\bar{\phi}(r) = \begin{cases} \phi^*(r) & r \in \Omega^- \\ 0 & r \in \Omega^+ \end{cases}$$

$$\phi^*(r) = \begin{cases} C \sum_{i=1}^{N_m} \frac{q_i}{4\pi\epsilon_1} \frac{1}{|r - r_i|} & r \in R^3 \\ C \sum_{i=1}^{N_m} -\frac{q_i}{2\pi\epsilon_1} \log(|r - r_i|) & r \in R^2 \end{cases}$$

$$\tilde{\phi} = \phi - \bar{\phi}$$

$$-\nabla(\epsilon(r)\nabla\tilde{\phi}(r)) + K(r)\sinh(\bar{\phi}(r) + \tilde{\phi}(r)) = [\epsilon\bar{\phi}_n]_{\Gamma}\delta_{\Gamma}$$

Damped Newton's method

$$-\nabla \cdot (\epsilon(r) \nabla v^l) + K(r) \cosh(\phi^l) v^l = \nabla \cdot (\epsilon(r) \nabla \tilde{\phi}^l) - K(r) \sinh(\phi^l) + [\epsilon \bar{\phi}_n]_{\Gamma} \delta_{\Gamma}$$

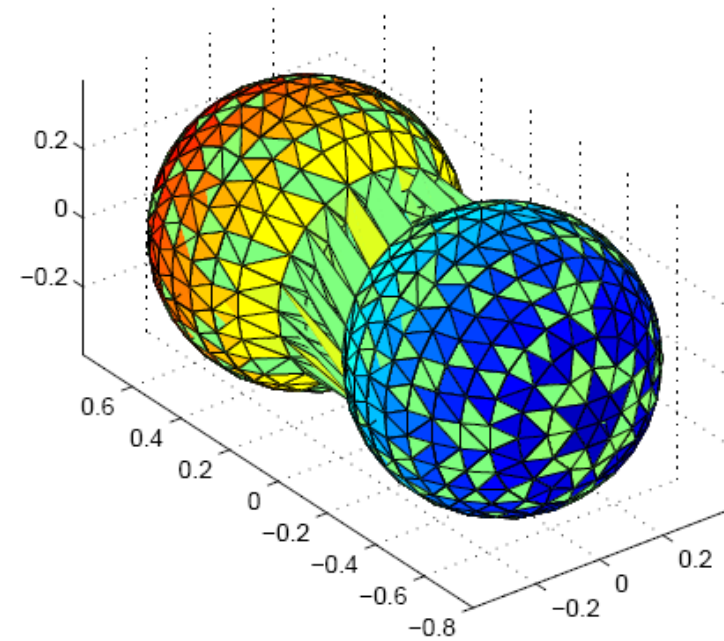
$$\phi^{l+1} = \tilde{\phi}^l + \lambda^l v^l$$

$$E(\phi^l + \lambda^l v^l) < E(\phi^l) \text{ for small } \lambda > 0$$

Ref. Holst

Numerical Validation—Artificial molecule

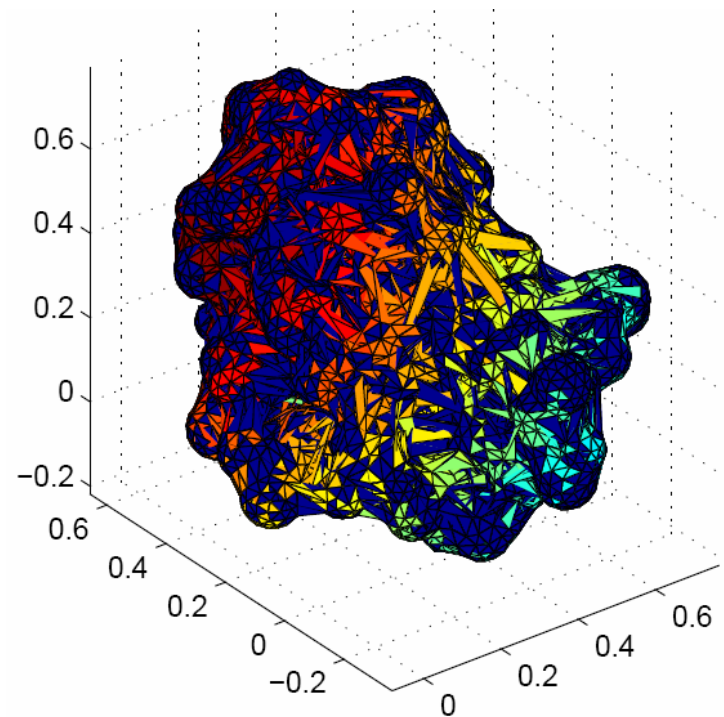
$$u_e(r) = \begin{cases} e^{-(x^2+y^2+z^2)} & r \in \Omega^- \\ 0 & r \in \Omega^+ \end{cases}$$



| N | Newton iteration | $\ \nabla u - \nabla u_e\ _{\infty, \Gamma}$ | order | $\ u - u_e\ _{\infty}$ | order |
|----|------------------|--|--------|------------------------|--------|
| 10 | 4 | 6.572e-002 | — | 8.136e-003 | — |
| 20 | 3 | 1.378e-002 | 2.2538 | 2.025e-003 | 2.0064 |
| 40 | 3 | 3.115e-003 | 2.1292 | 4.901e-004 | 2.0467 |

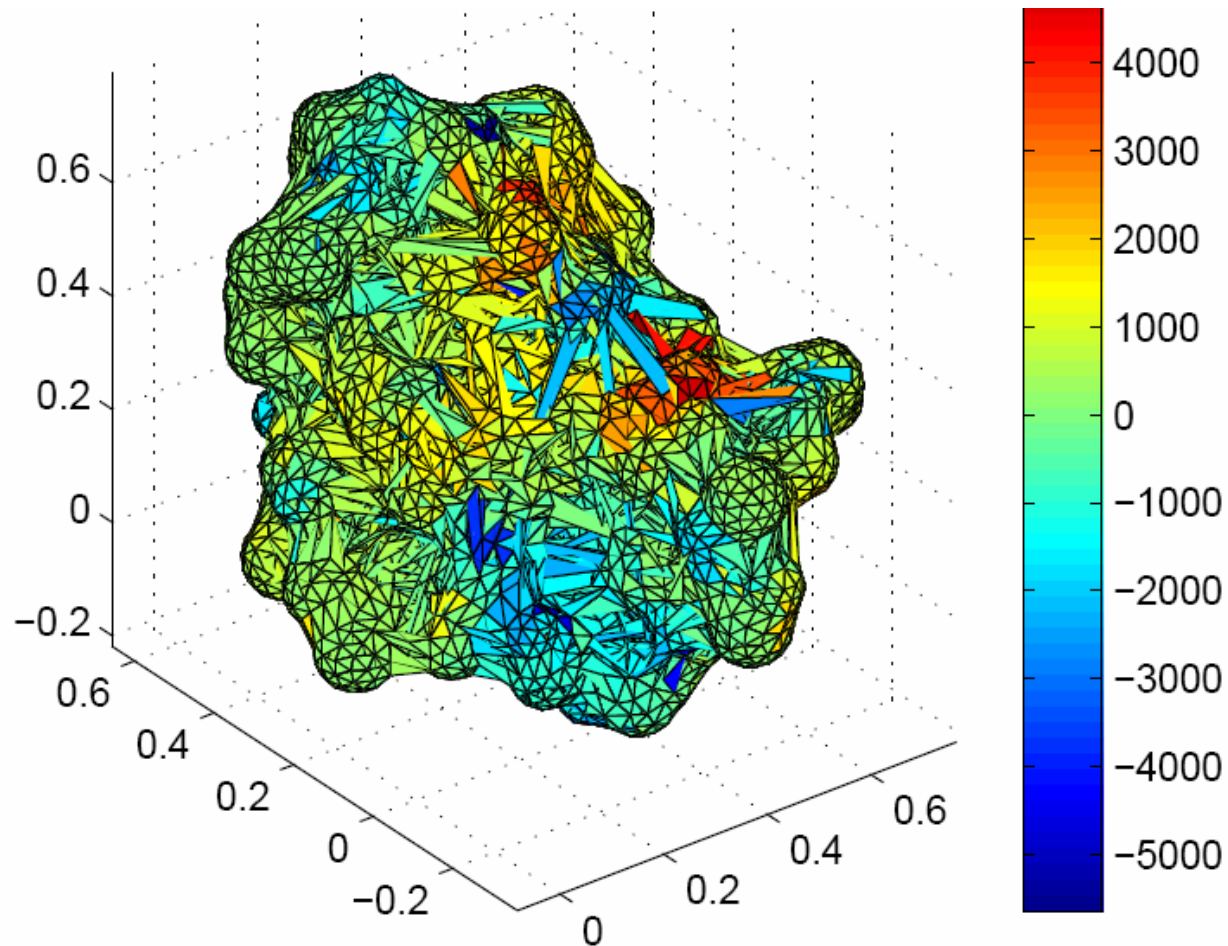
Numerical Validation

$$u_e(r) = \begin{cases} e^{-(x^2+y^2+z^2)} & r \in \Omega^- \\ 0 & r \in \Omega^+ \end{cases}$$



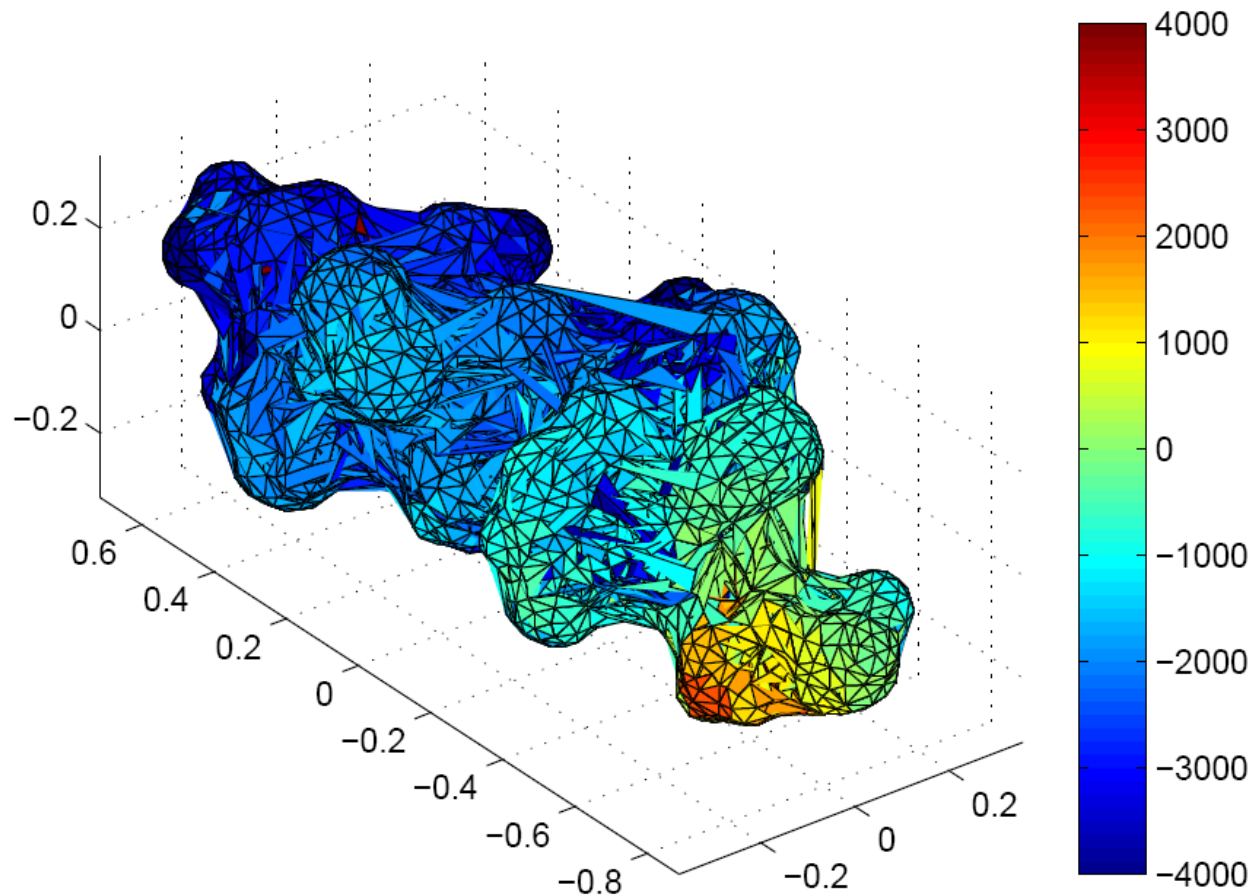
| N | Newton iteration | $\ \nabla u - \nabla u_e\ _{\infty, \Gamma}$ | order | $\ u - u_e\ _{\infty}$ | order |
|----|------------------|--|--------|------------------------|--------|
| 10 | 3 | 1.145e-001 | — | 2.161e-002 | — |
| 20 | 3 | 6.706e-002 | 0.7718 | 5.803e-003 | 1.8968 |
| 40 | 3 | 3.586e-002 | 0.9031 | 1.671e-003 | 1.7958 |

Hydrophobic protein (PDB ID: 1 crn)



*Computed solution of a hydrophobic protein (PDB ID:1crn)
with the number of charges $N_m = 642$.*

Hydrophilic protein (PDB ID: 1DGN)



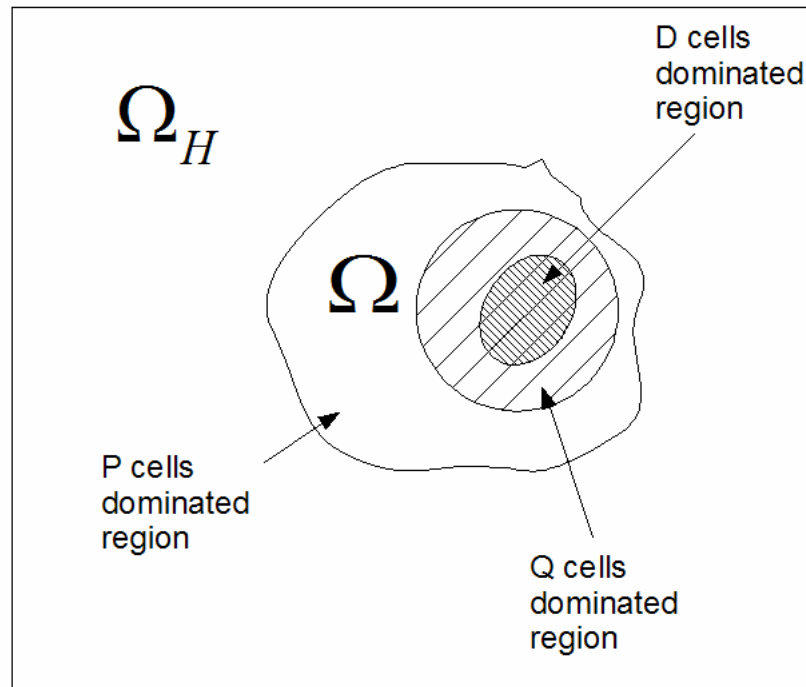
*Computed solution of a hydrophilic protein (PDB ID:1DNG)
with the number of charges $N_m = 207$.*

Summary of computing

Poisson-Boltzmann equation

- Ingredients: CIM + AMG + damped Newton's iteration
 - Second order accuracy for potential and electric field for molecules with smooth surfaces
 - 3-4 Newton's iterations only
-

Tumor growth Simulation



Lowengrub et al.

Tumor growth model (1)

Nutrient model

Assume the tumor depends on only one kind of nutrient σ .

The governing equation of σ is

$$\frac{\partial \sigma}{\partial t} = D_{\sigma} \nabla^2 \sigma + \Gamma,$$

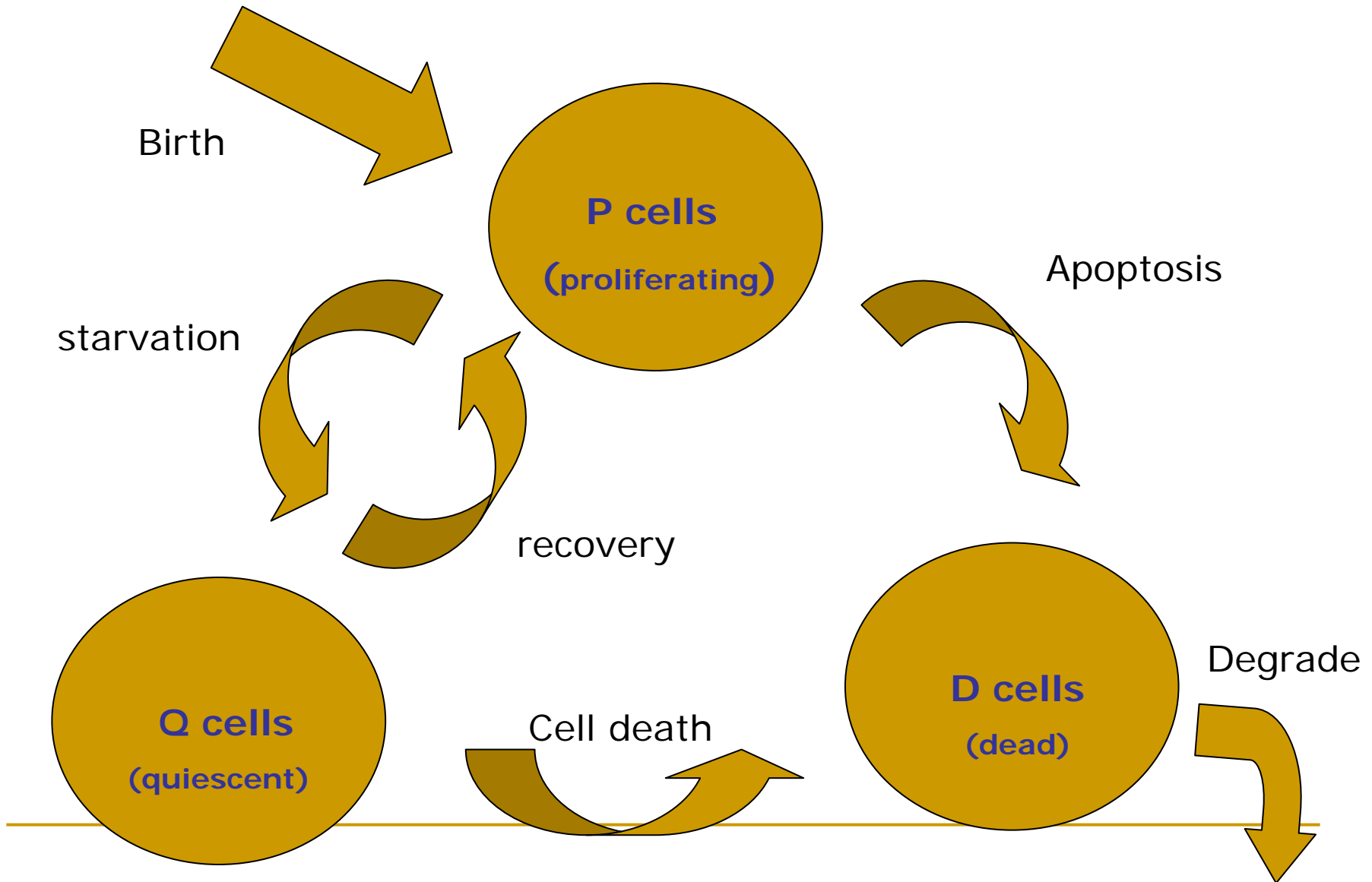
where $\Gamma = -\lambda_B(\sigma - \sigma_B) - \lambda\sigma$.

D_{σ} : the diffusion coefficient.

$\lambda_B(\sigma - \sigma_B)$: blood-tissue transfer.

$\lambda\sigma$: nutrient consumption of cells.

Cell evolution



Tumor growth model (2)

Reaction diffusion model for cell populations

Then the governing equations

for P, Q and D are

$$\frac{\partial P}{\partial t} + \nabla \cdot (P\bar{v}) = (K_B(\sigma) - K_Q(\sigma) - K_A(\sigma))P + K_P(\sigma)Q$$

$$\frac{\partial Q}{\partial t} + \nabla \cdot (Q\bar{v}) = K_Q(\sigma)P - [K_P(\sigma) + K_D(\sigma)]Q$$

$$\frac{\partial D}{\partial t} + \nabla \cdot (D\bar{v}) = K_A(\sigma)P - K_D(\sigma)Q - K_R D.$$

Since $P+Q+D=1$, in fact we have only two independent equations.

Summing three equations together,

$$\frac{\partial(P+Q+D)}{\partial t} + \nabla \cdot ((P+Q+D)\bar{v}) = \nabla \cdot \bar{v} = K_B(\sigma)P - K_R D.$$

Tumor growth model (3)

- Momentum equation: Darcy's law

$$-\nabla p = \alpha \vec{v}$$

- Boundary condition:

$$p = \gamma \kappa$$

κ is the mean curvature of the interface

Free boundary problem

Quasi-steady approximation

- Assume $Q = 0$ (sufficient nutrient available)
- D is digested very fast $K_R \gg 1$

$$0 \approx \frac{1}{K_R} \left(\frac{\partial D}{\partial t} + \nabla \cdot (D\vec{v}) \right) = \frac{K_A(\sigma)}{K_R} P - D$$

$$P \approx 1, Q = 0, D \approx 0$$

$$\nabla \cdot \mathbf{v} = K_B(\sigma)P - K_R D \approx [K_B(\sigma) - K_A(\sigma)]P$$

Quasi-steady approximation for tumor growth

$$D_\sigma \nabla^2 \sigma = (\lambda_B + \lambda)\sigma - \lambda_B \sigma_B \text{ in } \Omega(t)$$

$$-\mu \nabla^2 p = (k_b + k_a)\sigma - k_a \sigma^\infty \text{ in } \Omega(t)$$

$$\sigma = \sigma^\infty \text{ on } \partial\Omega$$

$$p = \gamma \kappa \text{ on } \partial\Omega(t)$$

$$V_n = -\mu \frac{\partial p}{\partial n} \text{ on } \partial\Omega(t)$$

σ is the nutrient

p is the pressure

Dimensionless formulation

(Lowengrub et al)

$$\nabla^2 \bar{\Gamma} = \bar{\Gamma} \text{ in } \Omega(\bar{t}), \quad \bar{\Gamma}|_{\partial\Omega(\bar{t})} = 1$$

$$\nabla^2 \bar{p} = -G(\bar{\Gamma} - A) \text{ in } \Omega(\bar{t}), \quad \bar{p}|_{\partial\Omega(\bar{t})} = \kappa$$

$$V_n = -\frac{\partial p}{\partial n} \text{ on } \partial\Omega(t)$$

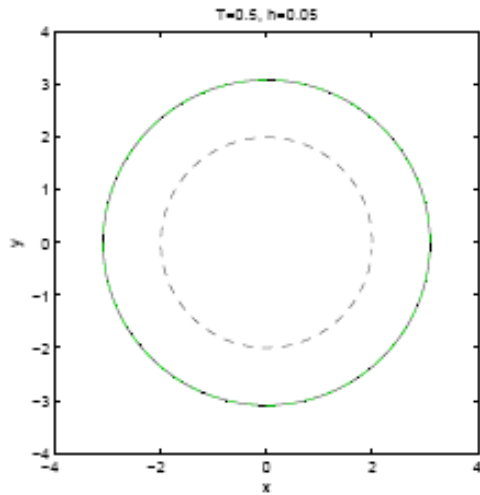
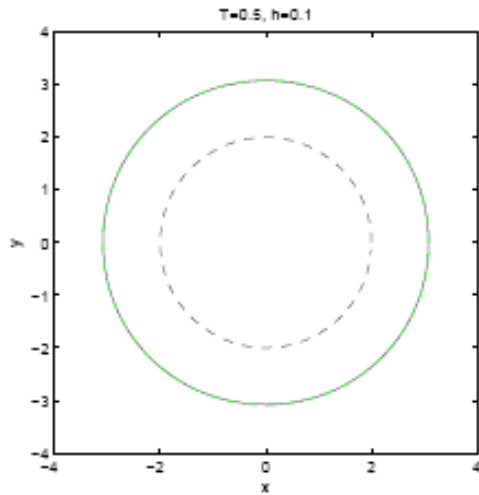
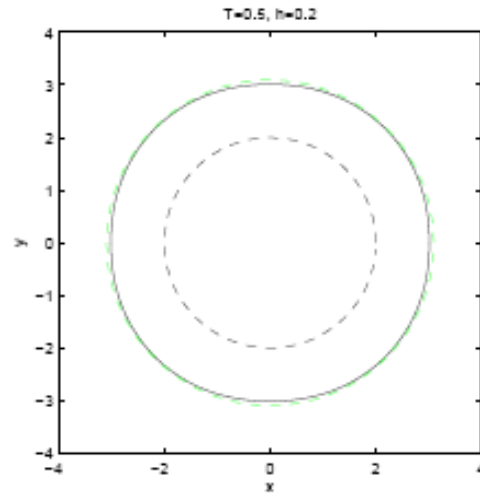
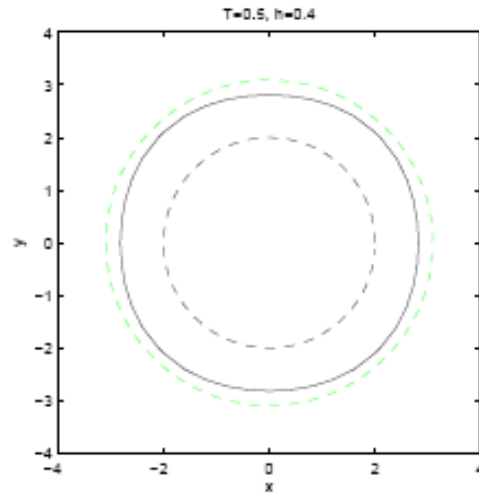
$$G = \frac{(k_a + k_b)\sigma^\infty}{\lambda_R} (1 - B)$$

$$A = \frac{k_a / (k_a + k_b) - B}{1 - B} \quad B = \frac{\sigma_B}{\sigma^\infty} \frac{\lambda_B}{\lambda_B + \lambda}$$

Numerical procedure

- Level set method for interface propagation
 - WENO5 + RK3 for interface propagation
 - Least square method for velocity extension
 - Coupling interface method for elliptic problems on arbitrary domain
-

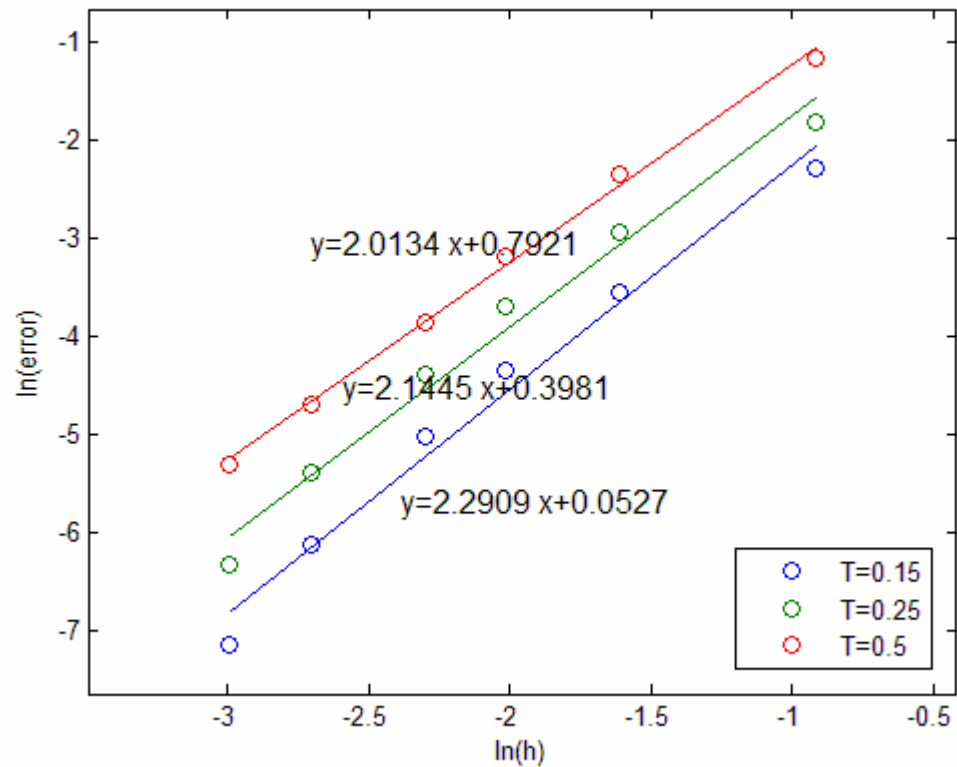
Numerical Validation (1)



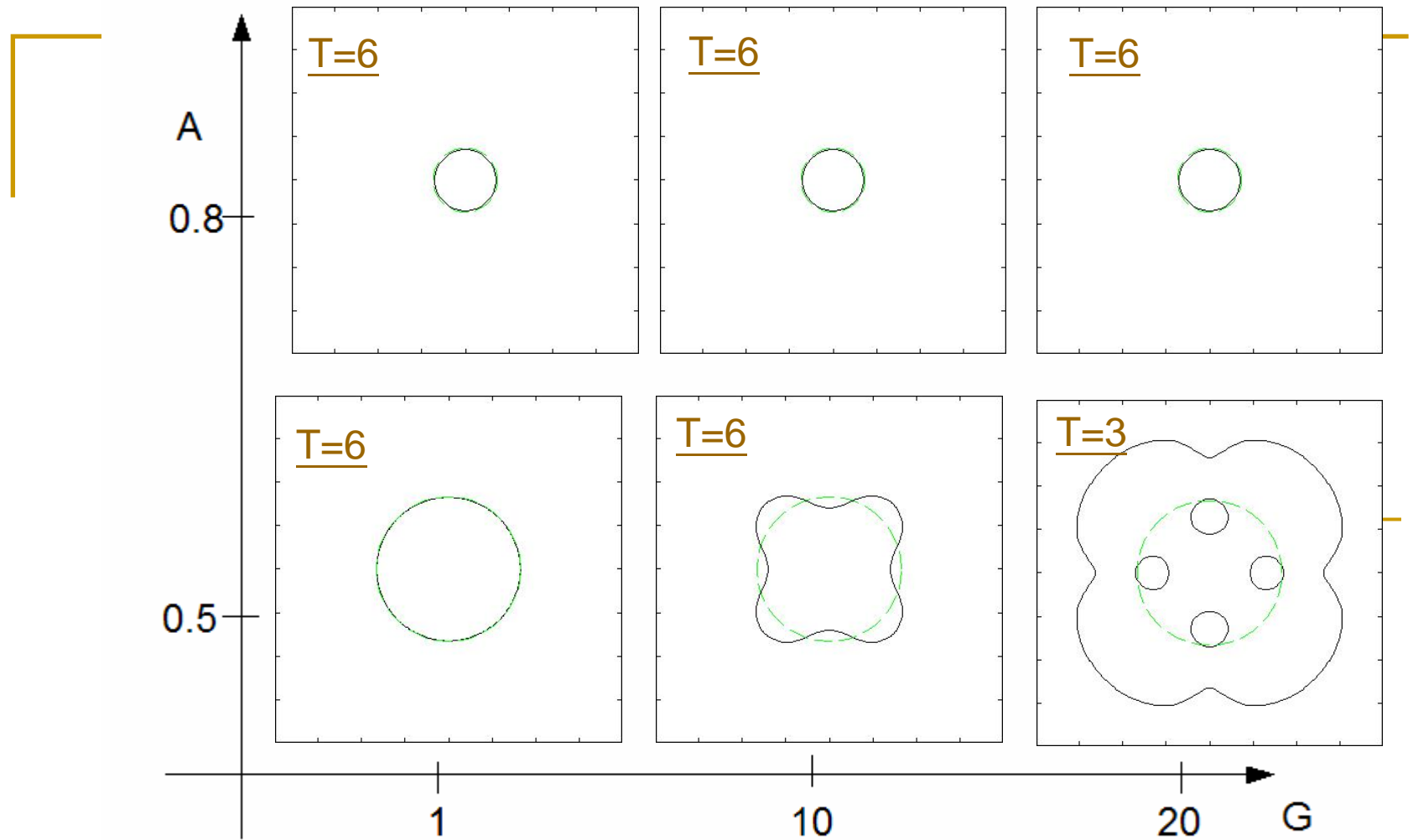
Numerical Validation (2)

| h | $t = 0.15$ | $t = 0.25$ | $t = 0.5$ |
|----------------|----------------|----------------|----------------|
| 0.40000 | $1.01654e - 1$ | $1.62572e - 1$ | $3.14382e - 1$ |
| 0.20000 | $2.89047e - 2$ | $5.33126e - 2$ | $9.59403e - 2$ |
| 0.13333 | $1.29981e - 2$ | $2.48926e - 2$ | $4.14796e - 2$ |
| 0.10000 | $6.63929e - 3$ | $1.26178e - 2$ | $2.13489e - 2$ |
| 0.06667 | $2.23080e - 3$ | $4.62618e - 3$ | $9.25444e - 3$ |
| 0.05000 | $7.97250e - 4$ | $1.78539e - 3$ | $5.00846e - 3$ |
| overall order: | 2.29084 | 2.14448 | 2.01338 |

Numerical Validation (3)



Bifurcation of tumor growth

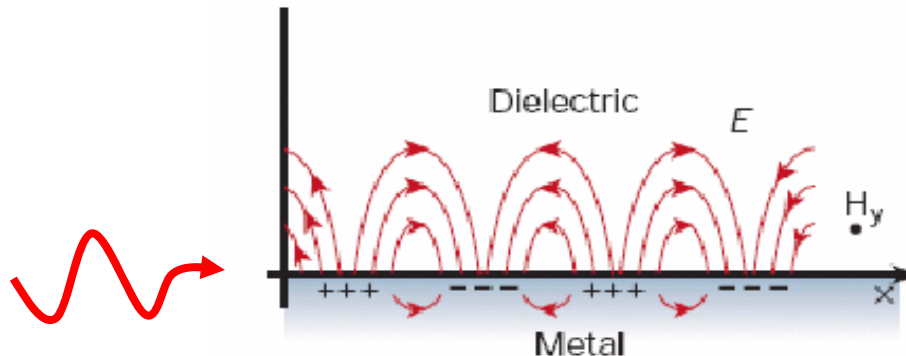


G (growth rate/adhesive force), A (apoptosis)

Initial condition: $R=2$.

Surface plasmons

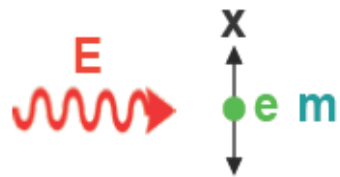
- Surface plasmons are surface electromagnetic waves that propagate parallel along a metal/dielectric (or metal/vacuum) interface.
- E field excites electron motion on metal surface



Drude model

Displacement

$$m(\ddot{\mathbf{x}} + \gamma\dot{\mathbf{x}}) = -e\mathbf{E}$$



$$\mathbf{x} = \frac{e}{m(\omega^2 + i\omega\gamma)} \mathbf{E}$$
$$\mathbf{P} = -ne\mathbf{x}$$

Polarization

$$\mathbf{P} = -\frac{ne^2}{m(\omega^2 + i\omega\gamma)} \mathbf{E}$$

$$\varepsilon(\omega) = \varepsilon_0 \left(1 - \frac{\omega_p^2}{\omega^2 + i\omega\gamma} \right)$$

Dielectric function

$$\varepsilon\mathbf{E} = \varepsilon_0\mathbf{E} + \mathbf{P}$$

$$\nabla \cdot (\varepsilon\mathbf{E}) = 0$$

Assumption:

1. small oscillation
2. no magnetic force

$$\omega_p^2 = \frac{ne^2}{\varepsilon_0 m}$$

Plasma frequency

Plasma frequency

| | $\omega_p \text{ (s}^{-1}\text{)}$ | $\gamma = \omega_\tau \text{ (s}^{-1}\text{)}$ |
|----|------------------------------------|--|
| Au | 1.37×10^{16} | 4.05×10^{13} |
| Ag | 1.37×10^{16} | 2.73×10^{13} |
| Pt | 7.82×10^{15} | 1.05×10^{14} |

Drude model for gold

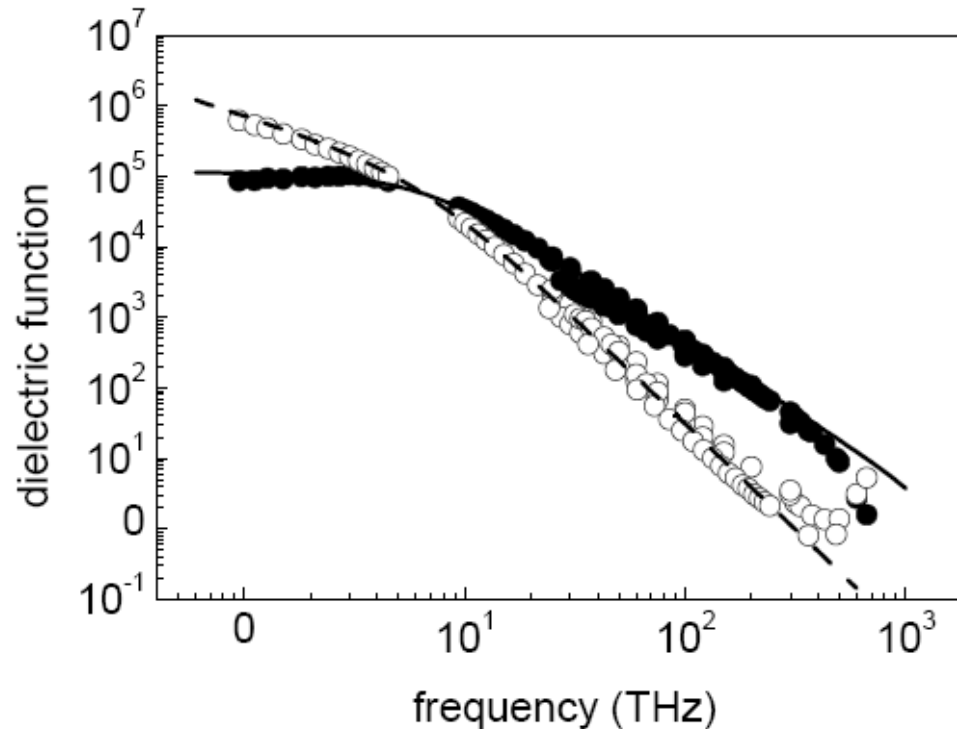
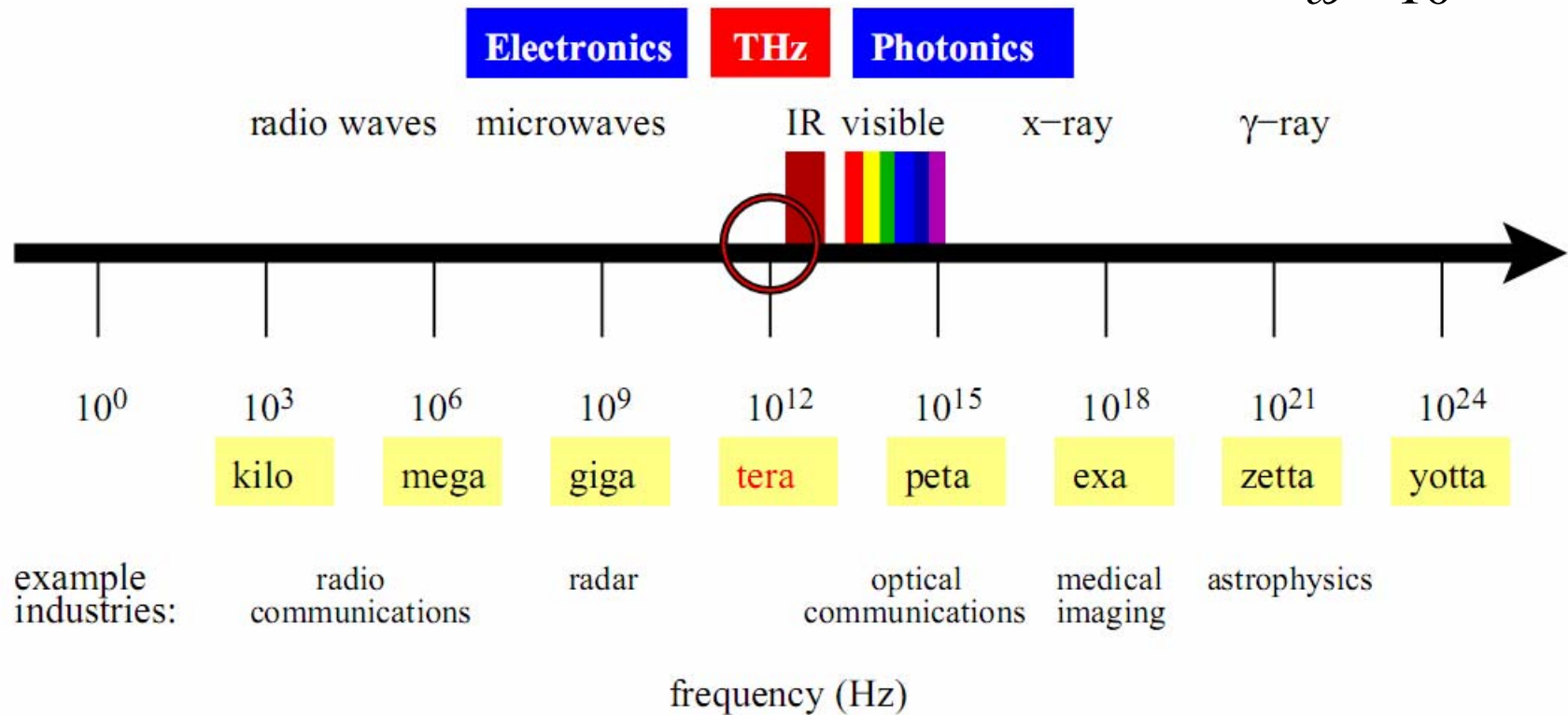


FIG. 2.4: Drude fit of the experimentally obtained real (\bullet) and imaginary (\circ) part of the dielectric function $\varepsilon = \varepsilon' + i\varepsilon''$ of Au. For convenience, the real part has been multiplied by -1 . Data has been taken from [29].

Drude model is good approximation for $\omega_p < 10^{14}$

Optical communication frequency

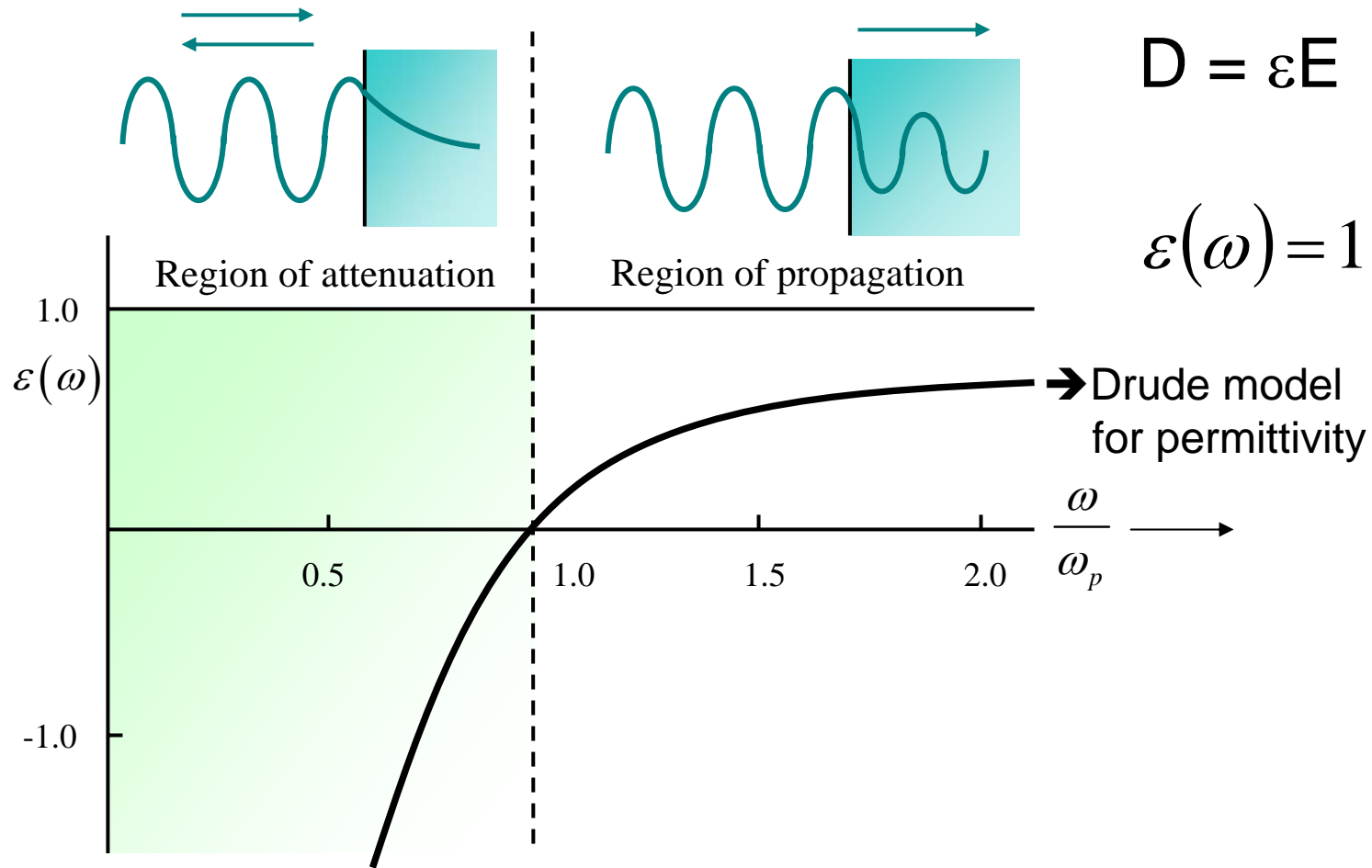
$$\varepsilon_m(\omega) = -10^6,$$
$$\omega = 10^{13}$$



A goal of nanotechnology: fabrication of nanoscale photonic circuits operating at optical frequencies. Faster and Smaller devices.

Quoted from Jorg Saxler 2003

Wave propagation in metal



ω_p is the frequency of collective oscillations of the electron gas.

Maxwell equation in matter

- Macroscopic Maxwell Equation

$$\left\{ \begin{array}{l} \nabla \cdot D = 0 \\ \nabla \cdot B = 0 \\ \nabla \times E = -B_t \\ \nabla \times H = D_t \end{array} \right.$$

$$\begin{array}{l} D = \varepsilon E \\ B = \mu H \end{array}$$

$$\begin{array}{l} \varepsilon(\omega) = \varepsilon_0 \left(1 - \frac{\omega_p^2}{\omega(\omega + i\gamma)} \right) \\ \mu = \mu_0 \end{array}$$

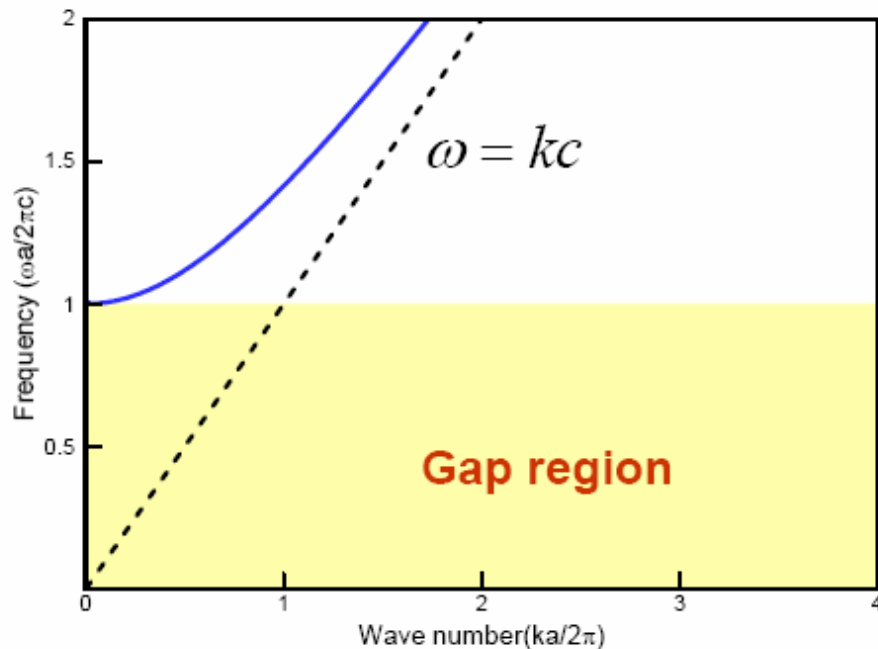
Interface condition

$$\begin{array}{l} [E] \cdot t = 0 \\ [H] \cdot t = 0 \end{array}$$

Dispersion relation: Bulk case

- No SP mode

$$\omega = \left(\omega_p^2 + k^2 c^2 \right)^{1/2}$$



$$\epsilon_m = 1 - \omega_p^2 / \omega^2$$

ω_p

$$(E, H) = (E_0, H_0) e^{i(kz - \omega t)}$$

Dispersion relation: 1 interface

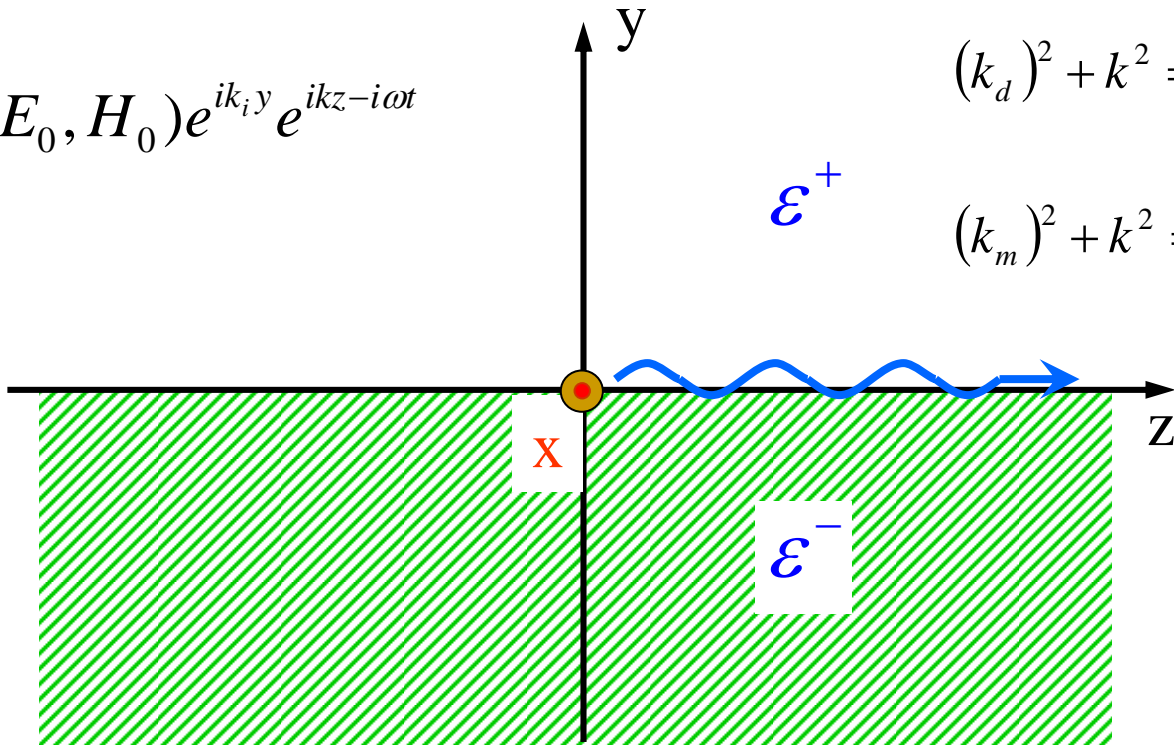
Surface Plasmon modes

$$(E, H) = (E_0, H_0) e^{ik_i y} e^{ikz - i\omega t}$$

$$i = d, m$$

$$(k_d)^2 + k^2 = \epsilon_d \left(\frac{\omega}{c} \right)^2$$

$$(k_m)^2 + k^2 = \epsilon_m \left(\frac{\omega}{c} \right)^2$$



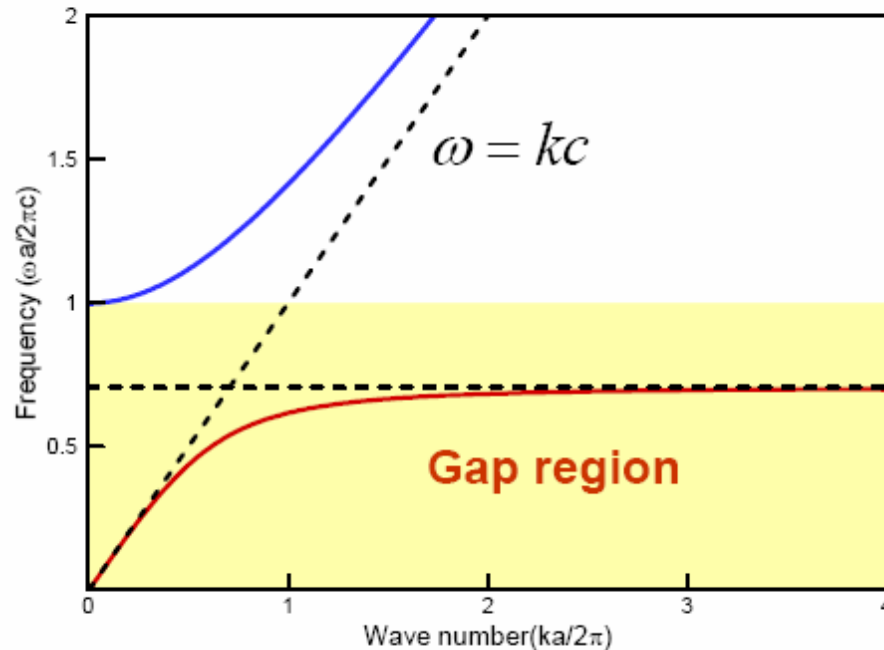
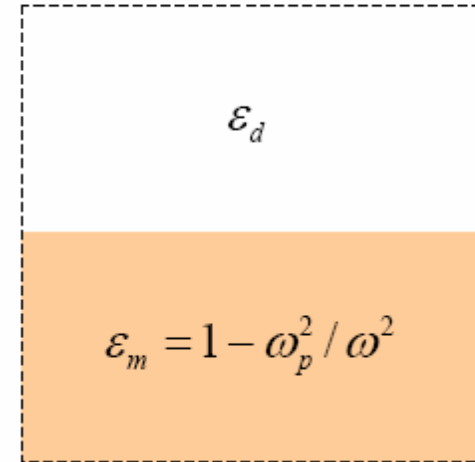
ϵ^+ : dielectric

$\epsilon^- (< 0)$: metal

Dispersion relation: 1 interface case

- 1 SP mode (1 interface)

$$\frac{k_d^\perp}{\epsilon_d} + \frac{k_m^\perp}{\epsilon_m} = 0$$



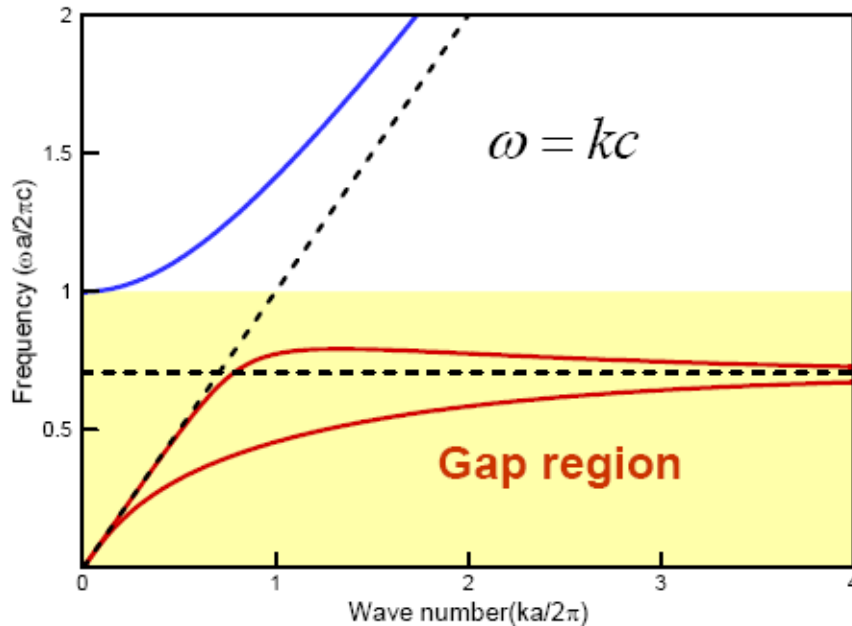
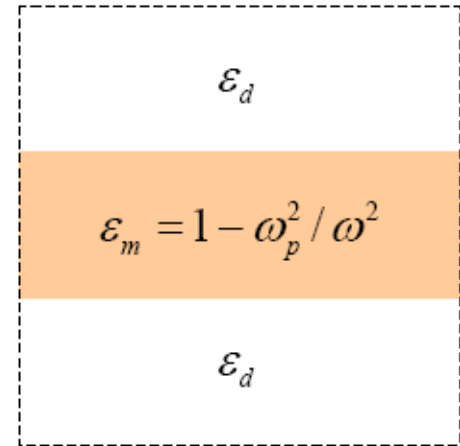
$$\omega_{sp} = \frac{\omega_p}{\sqrt{1 + \epsilon_d}}$$

Surface plasma frequency

Dispersion relation: Slab -1

- 2 SP modes (2 interfaces)

$$\frac{k_d^\perp}{\epsilon_d} + \frac{k_m^\perp}{\epsilon_m} \tanh\left(\frac{k_m^\perp d}{2i}\right) = 0, \quad \frac{k_d^\perp}{\epsilon_d} + \frac{k_m^\perp}{\epsilon_m} \coth\left(\frac{k_m^\perp d}{2i}\right) = 0$$



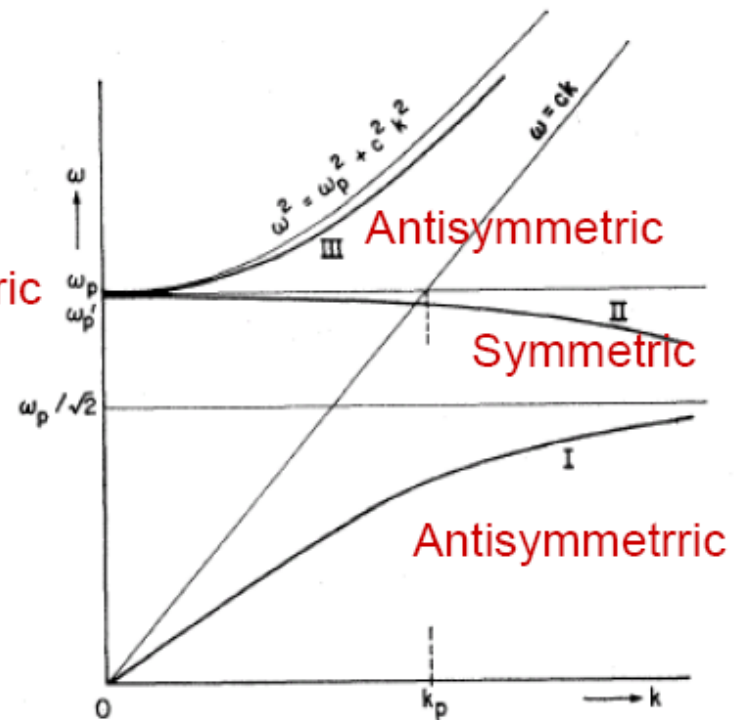
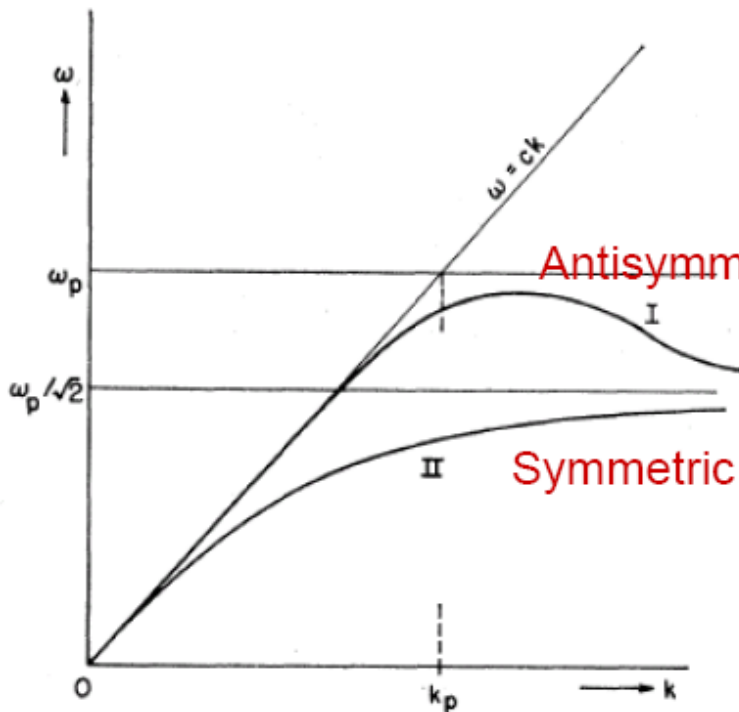
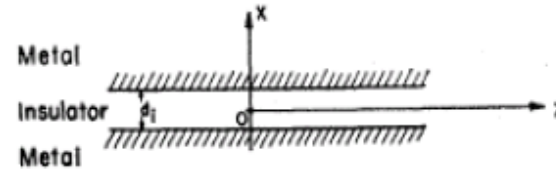
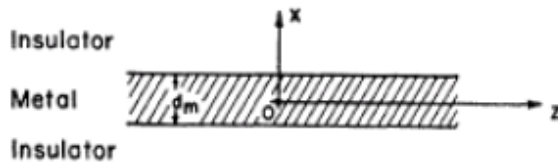
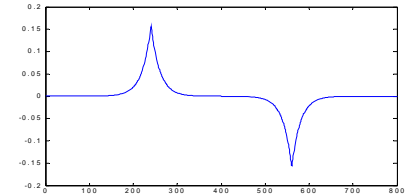
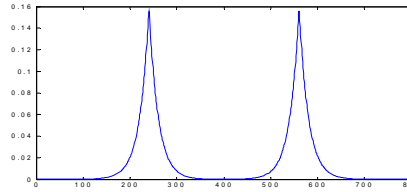
$$\omega_{sp} = \frac{\omega_p}{\sqrt{1 + \epsilon_d}}$$

Surface plasma frequency

$$(k_d^\perp)^2 + (k^\parallel)^2 = \epsilon_d (\omega/c)^2$$

$$(k_m^\perp)^2 + (k^\parallel)^2 = \epsilon_m (\omega/c)^2$$

Slab-2

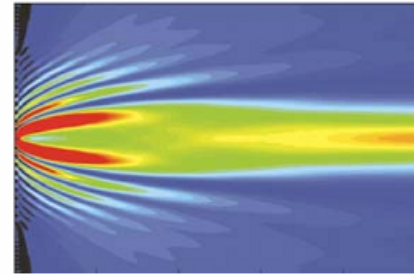
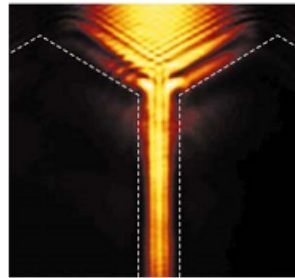


Surface plasmons

- From Wikipedia, the free encyclopedia
 - The excitation of surface plasmons by light is denoted as a **surface plasmon resonance** (SPR) for planar surfaces or **localized surface plasmon resonance** (LSPR) for nanometer-sized metallic structures.
 - Since the wave is on the boundary of the metal and the external medium (air or water for example), these oscillations are very sensitive to any change of this boundary, such as the adsorption of molecules to the metal surface.
 - This phenomenon is the basis of many standard tools for measuring adsorption of material onto planar metal (typically gold and silver) surfaces or onto the surface of metal nanoparticles. It is behind many color based biosensor applications and different lab-on-a-chip sensors.
-

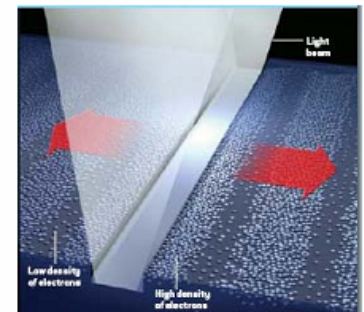
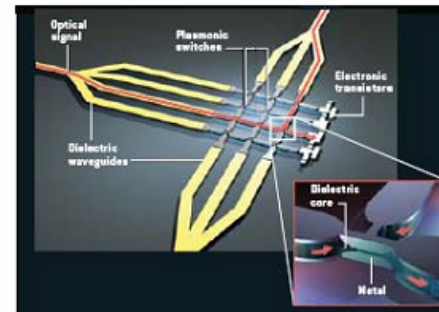
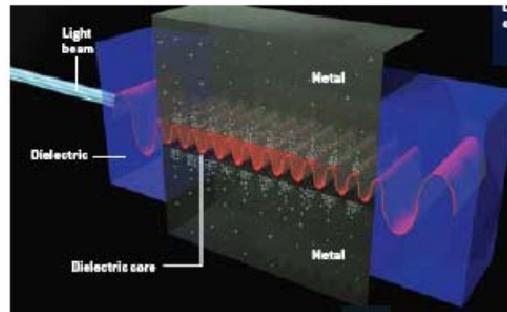
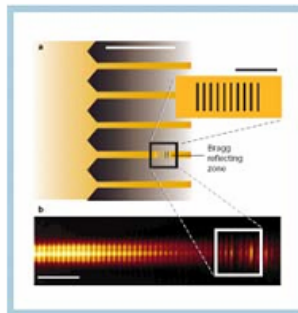
Surface plasmon

- **Property:** field confinement & field enhancement



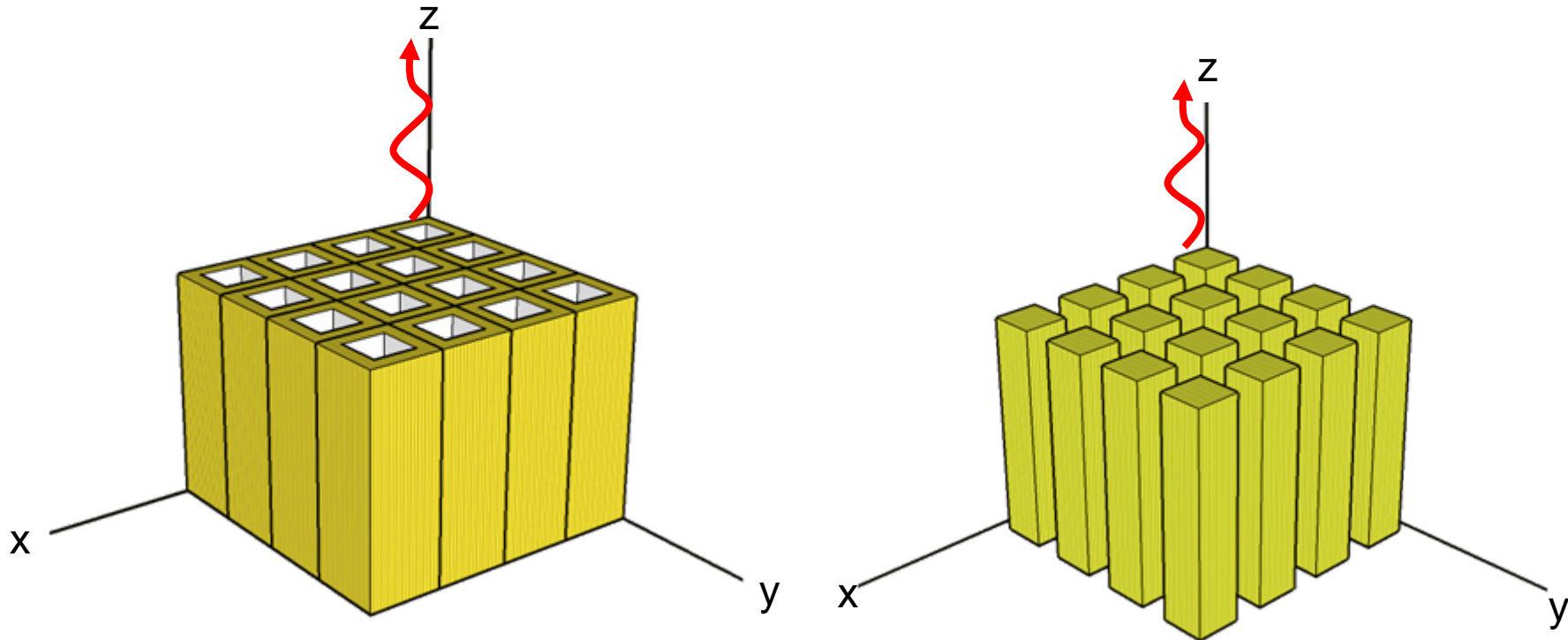
- **Application:**

optical data storage, detection, sensing, imaging, circuit, light generation, harvest, emission



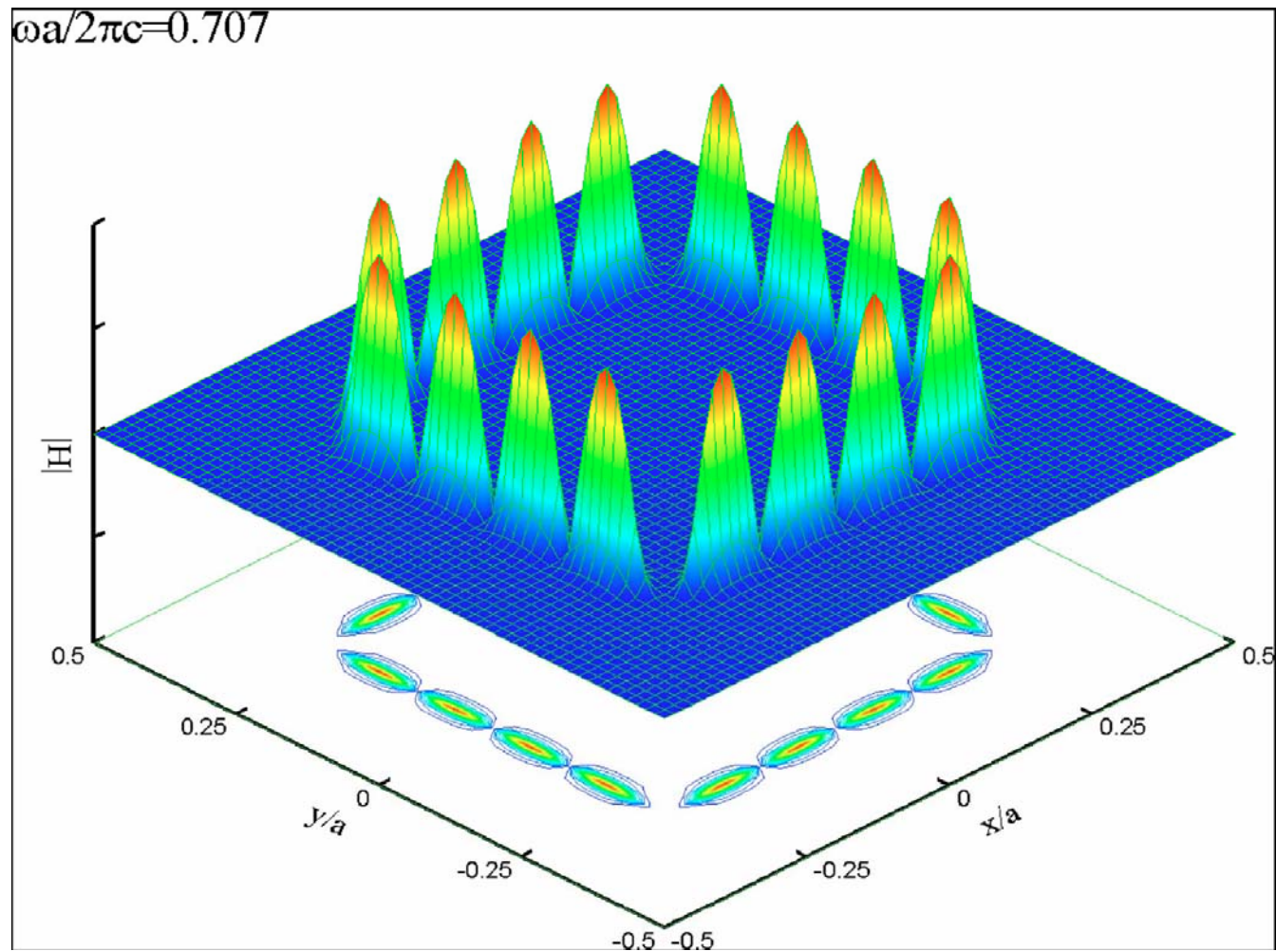
pictures from Scientific American (2007/04)

Wave propagation in periodic nano structure



Metal-dielectric materials

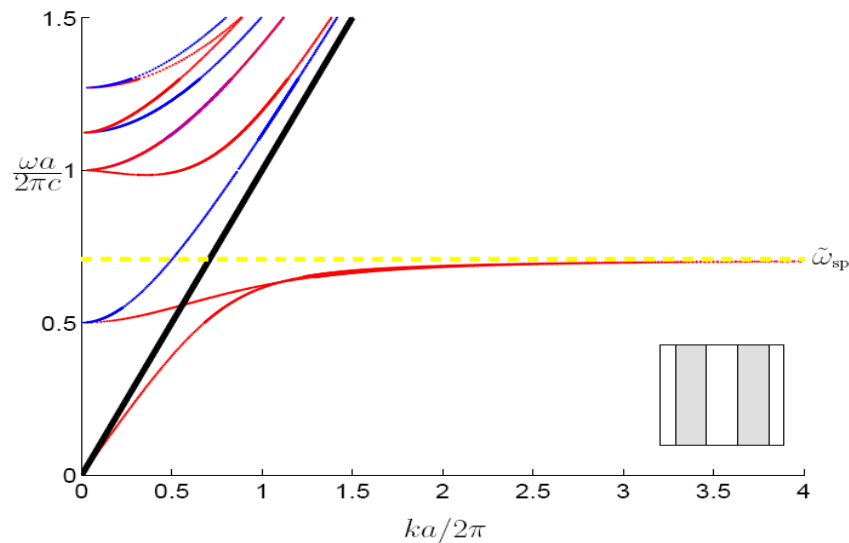
Surface Plasmon



EM wave are confined on surface.

Goal: study band structure

- Signal propagation via surface plasmonic waves
- Energy absorbing problem

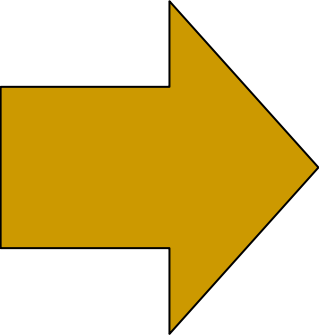


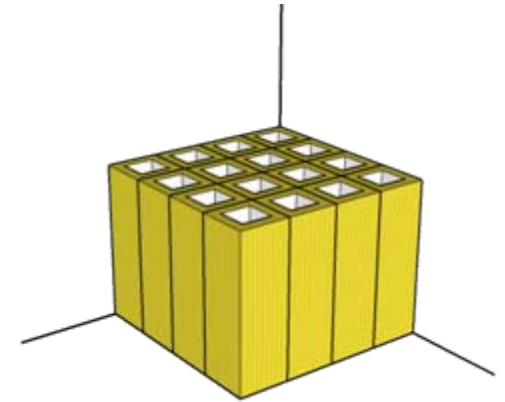
$$k = k(\omega)$$

Waveguide: homogeneous in z direction

$$E = (E_x, E_y, E_z) e^{i(kz - \omega t)},$$

$$H = (H_x, H_y, H_z) e^{i(kz - \omega t)}$$


$$\left\{ \begin{array}{l} E_x = \frac{i}{\Lambda} \left(k \frac{\partial E_z}{\partial x} + \omega \mu \frac{\partial H_z}{\partial y} \right) \\ E_y = \frac{i}{\Lambda} \left(k \frac{\partial E_z}{\partial y} - \omega \mu \frac{\partial H_z}{\partial x} \right) \\ H_x = \frac{i}{\Lambda} \left(k \frac{\partial H_z}{\partial x} - \omega \varepsilon \frac{\partial E_z}{\partial y} \right) \\ H_y = \frac{i}{\Lambda} \left(k \frac{\partial H_z}{\partial y} + \omega \varepsilon \frac{\partial E_z}{\partial x} \right) \end{array} \right.$$



$$\Lambda = \omega^2 \varepsilon \mu - k^2$$

Reduced equations for (E_z, H_z)

From Faraday's Law and Ampere's Law(curl equations)

$$\begin{cases} \nabla_2 \cdot \left(\frac{\varepsilon \nabla_2 E_z}{\Lambda} \right) + \nabla_2 \times \left(\frac{k \nabla_2 H_z}{\Lambda \omega} \right) = -\varepsilon E_z \\ \nabla_2 \cdot \left(\frac{\mu \nabla_2 H_z}{\Lambda} \right) + \nabla_2 \times \left(\frac{k \nabla_2 E_z}{\Lambda \omega} \right) = -\mu H_z \end{cases}$$

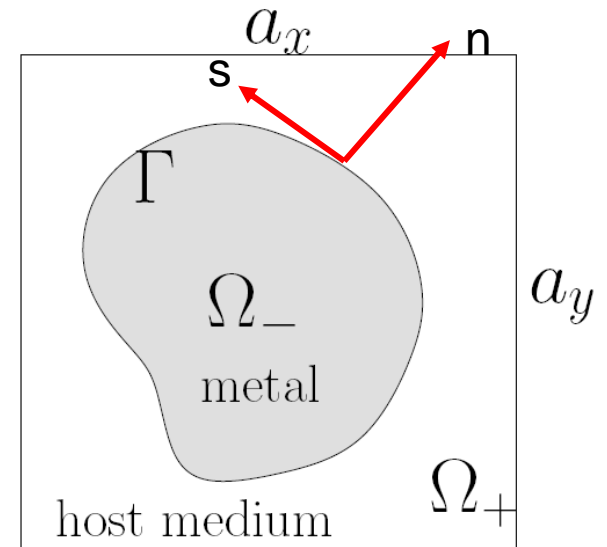
$$\nabla_2 = \left(\frac{\partial}{\partial x}, \frac{\partial}{\partial y} \right)$$

Interface Conditions

Continuous along the tangential direction

$$[E \cdot T] = 0, [H \cdot T] = 0$$

$$\Rightarrow \begin{cases} [E_z] = 0 \\ [H_z] = 0 \\ \omega \left[\frac{\epsilon}{\Lambda} \nabla E_z \cdot \mathbf{n} \right] = -k \left[\frac{1}{\Lambda} \nabla H_z \cdot \mathbf{s} \right] \\ \omega \left[\frac{\mu}{\Lambda} \nabla H_z \cdot \mathbf{n} \right] = k \left[\frac{1}{\Lambda} \nabla E_z \cdot \mathbf{s} \right] \end{cases}$$



Boundary Condition

Bloch Boundary Condition:

Suppose the domain is $[0, L] \times [0, L]$

$$\begin{cases} E_z(x + L, y + L) = E_z(x, y) e^{i(k_x L + k_y L)} \\ H_z(x + L, y + L) = H_z(x, y) e^{i(k_x L + k_y L)} \end{cases}$$

Quadratic Eigenvalue problem for k:

Interior:

$$\begin{cases} \nabla^2 E_z + \Lambda E_z = 0 \\ \nabla^2 H_z + \Lambda H_z = 0 \end{cases}$$

$$\Lambda = \omega^2 \varepsilon \mu - k^2$$

Boundary conditions:

$$\begin{cases} E_z(x+L, y+L) = E_z(x, y) e^{i(k_x L + k_y L)} \\ H_z(x+L, y+L) = H_z(x, y) e^{i(k_x L + k_y L)} \end{cases}$$

Interface conditions:

$$[E_z] = [H_z] = 0$$

$$\left[\frac{\varepsilon}{\Lambda} \nabla E_z \cdot \mathbf{n} \right] = - \left[\frac{k}{\Lambda \omega} \nabla H_z \cdot \mathbf{s} \right]$$

$$\left[\frac{\mu}{\Lambda} \nabla H_z \cdot \mathbf{n} \right] = \left[\frac{k}{\Lambda \omega} \nabla E_z \cdot \mathbf{s} \right]$$

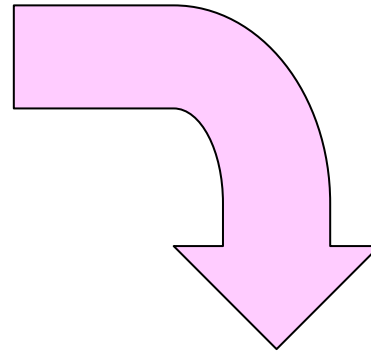
Ingredients of Numerical method

- Interfacial operator: to reduce interface condition to a quadratic eigenvalue problem
 - Augmented Coupling interface method: to discretize the equation under Cartesian grid and interface condition under uniform interfacial grids.
-

Interfacial operator:

To form a quadratic eigenvalue problem for k .

$$\begin{cases} \left[\frac{\varepsilon}{\Lambda} \nabla E_z \cdot \mathbf{n} \right] = - \left[\frac{k}{\Lambda \omega} \nabla H_z \cdot \mathbf{s} \right] \\ \left[\frac{\mu}{\Lambda} \nabla H_z \cdot \mathbf{n} \right] = \left[\frac{k}{\Lambda \omega} \nabla E_z \cdot \mathbf{s} \right] \end{cases}$$



$$\begin{cases} \omega^2 \varepsilon^+ \varepsilon^- \left(\mu^- \frac{\partial E^+}{\partial n} - \mu^+ \frac{\partial E^-}{\partial n} \right) = k^2 \left(\varepsilon^+ \frac{\partial E^+}{\partial n} - \varepsilon^- \frac{\partial E^-}{\partial n} \right) - k\omega \left(\varepsilon^- \mu^- \frac{\partial H^+}{\partial s} - \varepsilon^+ \mu^+ \frac{\partial H^-}{\partial s} \right) \\ \omega^2 \mu^+ \mu^- \left(\varepsilon^- \frac{\partial H^+}{\partial n} - \varepsilon^+ \frac{\partial H^-}{\partial n} \right) = k^2 \left(\mu^+ \frac{\partial H^+}{\partial n} - \mu^- \frac{\partial H^-}{\partial n} \right) + k\omega \left(\varepsilon^- \mu^- \frac{\partial E^+}{\partial s} - \varepsilon^+ \mu^+ \frac{\partial E^-}{\partial s} \right) \end{cases}$$

Interfacial operator

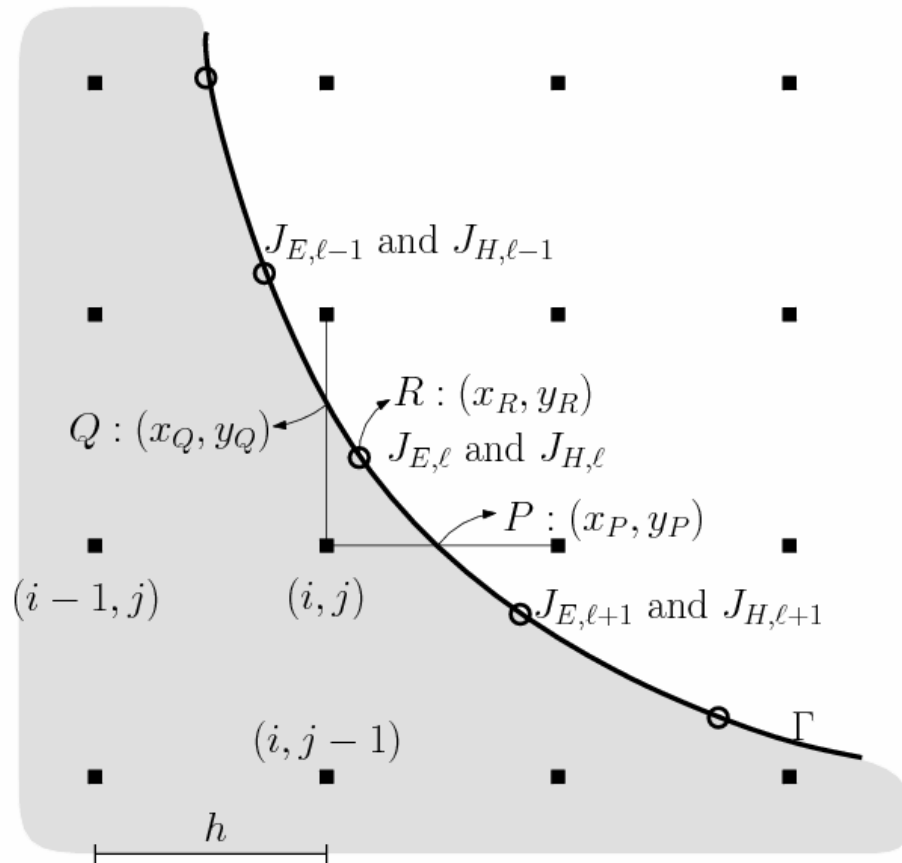
Interfacial Variables

C.C.Chang et.al. in 2005 (PRB 72, 205112)

Augmented CIM

- Auxiliary interfacial variables are distributed on the interface almost uniformly.
 - The jump information at the intersections of grid line and interface is expressed in terms of interfacial variables at nearby interfacial grid.
-

Variables setup



Apply 1-d method in x- and y-directions

$$\frac{\partial^2 E}{\partial x^2} \Big|_{i,j} = L_{i,j,x} (E_{i-1:i+2,j}, [\varepsilon u_x]_P)$$

$$\frac{\partial^2 E}{\partial y^2} \Big|_{i,j} = L_{i,j,y} (E_{i,j-1:j+2}, [\varepsilon u_y]_Q)$$

$$\left[\varepsilon \frac{\partial E}{\partial x} \right]_P = \left[\varepsilon \frac{\partial E}{\partial x} \right]_R + (x_P - x_R) \left[\varepsilon \frac{\partial^2 E}{\partial x^2} \right]_R + (y_P - y_R) \left[\varepsilon \frac{\partial^2 E}{\partial x \partial y} \right]_R$$

$$\left[\varepsilon \frac{\partial E}{\partial y} \right]_Q = \left[\varepsilon \frac{\partial E}{\partial x} \right]_R + (y_Q - y_R) \left[\varepsilon \frac{\partial^2 E}{\partial y^2} \right]_R + (x_P - x_R) \left[\varepsilon \frac{\partial^2 E}{\partial x \partial y} \right]_R$$

Resulting scheme

$$\frac{\partial^2 E}{\partial x^2} \Big|_{i,j} \approx \mathcal{L}'_{E_{xx}} (E_{i-1:i+2, j-1, j+2}, J_{E, \ell}),$$

$$\frac{\partial^2 E}{\partial y^2} \Big|_{i,j} \approx \mathcal{L}'_{E_{yy}} (E_{i-1:i+2, j-1, j+2}, J_{E, \ell}),$$

$$\nabla^2 E_{i,j} \approx (\mathcal{L}'_{E_{xx}} + \mathcal{L}'_{E_{yy}})(E_{i-1:i+2, j-1, j+2}, J_{E, \ell}).$$

Equations for interfacial variable

$$C \left(\left[\frac{1}{\mu} \frac{\partial E}{\partial n} \right]_{\Gamma} + \frac{k}{\omega \epsilon_0} \left[\frac{1}{\epsilon \mu} \frac{\partial H}{\partial s} \right]_{\Gamma} \right) = k^2 J_E,$$

$$C \left(\left[\frac{1}{\epsilon} \frac{\partial H}{\partial n} \right]_{\Gamma} - \frac{k}{\omega \mu_0} \left[\frac{1}{\epsilon \mu} \frac{\partial E}{\partial s} \right]_{\Gamma} \right) = k^2 J_H,$$

$$C = \left(\frac{\omega}{c} \right)^2 \epsilon_+ \epsilon_- \mu_+ \mu_-$$

Approximation

$$\left[\frac{1}{\mu} \frac{\partial E}{\partial n} \right]_R = \frac{1}{\varepsilon_+ \mu_+} J_{E,\ell} + \frac{\varepsilon_- \mu_- - \varepsilon_+ \mu_+}{\varepsilon_+ \mu_+ \mu_-} \left. \frac{\partial E^-}{\partial n} \right|_R,$$

$$\left[\frac{1}{\varepsilon \mu} \frac{\partial H}{\partial s} \right]_R = \frac{\varepsilon_- \mu_- - \varepsilon_+ \mu_+}{\varepsilon_+ \varepsilon_- \mu_+ \mu_-} \left. \frac{\partial H^-}{\partial s} \right|_R,$$

$$\left[\frac{1}{\varepsilon} \frac{\partial H}{\partial n} \right]_R = \frac{1}{\varepsilon_+ \mu_+} J_{H,\ell} + \frac{\varepsilon_- \mu_- - \varepsilon_+ \mu_+}{\mu_+ \varepsilon_+ \varepsilon_-} \left. \frac{\partial H^-}{\partial n} \right|_R,$$

$$\left[\frac{1}{\varepsilon \mu} \frac{\partial E}{\partial s} \right]_R = \frac{\varepsilon_- \mu_- - \varepsilon_+ \mu_+}{\varepsilon_+ \varepsilon_- \mu_+ \mu_-} \left. \frac{\partial E^-}{\partial s} \right|_R.$$

Approximation

$$\left[\frac{1}{\mu} \frac{\partial E}{\partial n} \right]_R = \frac{1}{\varepsilon_+ \mu_+} J_{E,\ell} + \frac{\varepsilon_- \mu_- - \varepsilon_+ \mu_+}{\varepsilon_+ \mu_+ \mu_-} \left. \frac{\partial E^-}{\partial n} \right|_R,$$

$$\left. \frac{\partial E^-}{\partial n} \right|_R = n_x \left. \frac{\partial E^-}{\partial x} \right|_R + n_y \left. \frac{\partial E^-}{\partial y} \right|_R,$$

$$\left. \frac{\partial E^-}{\partial x} \right|_R \approx \frac{1}{h} (E_{i,j} - E_{i-1,j}) + \left(\frac{1}{2} + \alpha_{R,x} \right) h \left. \frac{\partial^2 E}{\partial x^2} \right|_{i,j} + \alpha_{R,y} h \left. \frac{\partial^2 E}{\partial x \partial y} \right|_{i,j}$$

$$\left. \frac{\partial E^-}{\partial y} \right|_R \approx \frac{1}{h} (E_{i,j} - E_{i,j-1}) + \left(\frac{1}{2} + \alpha_{R,y} \right) h \left. \frac{\partial^2 E}{\partial y^2} \right|_{i,j} + \alpha_{R,x} h \left. \frac{\partial^2 E}{\partial x \partial y} \right|_{i,j}$$

$$\left. \frac{\partial^2 E}{\partial x^2} \right|_{i,j} \approx \mathcal{L}'_{E_{xx}} (E_{i-1:i+2, j-1, j+2}, J_{E,\ell}),$$

$$\left. \frac{\partial^2 E}{\partial y^2} \right|_{i,j} \approx \mathcal{L}'_{E_{yy}} (E_{i-1:i+2, j-1, j+2}, J_{E,\ell}),$$

Resulting linear combination

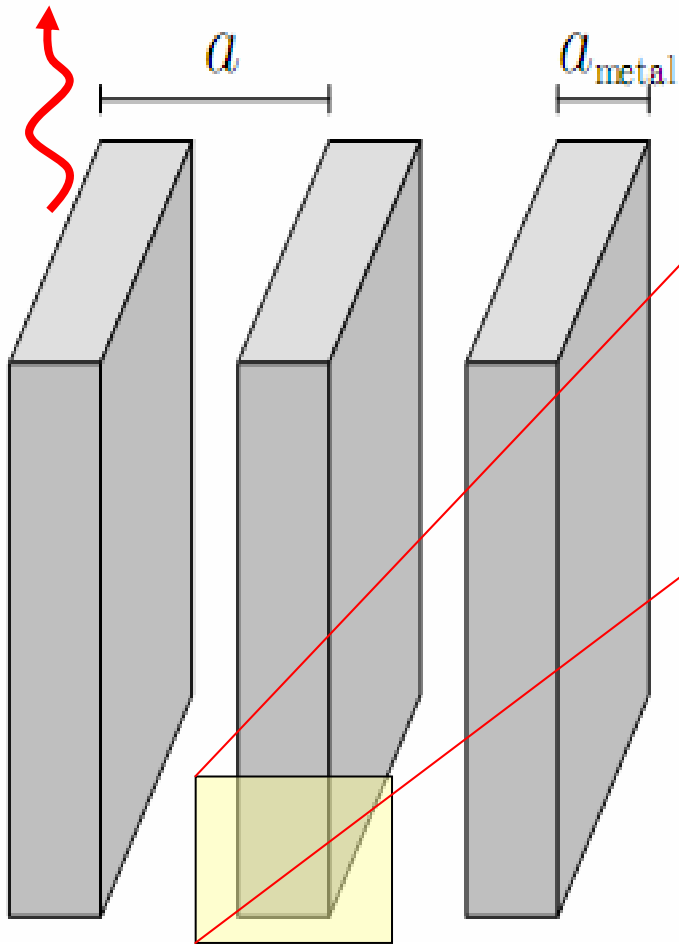
$$\Lambda \left[\frac{1}{\mu} \frac{\partial E}{\partial n} \right]_R \approx \mathcal{J}_{E_n} (E_{i-1:i+2, j-1, j+2}, J_{E, \ell}),$$

$$\frac{\Lambda}{\omega \epsilon_0} \left[\frac{1}{\epsilon \mu} \frac{\partial H}{\partial s} \right]_R \approx \mathcal{J}_{H_s} (H_{i-1:i+2, j-1, j+2}, J_{H, \ell}),$$

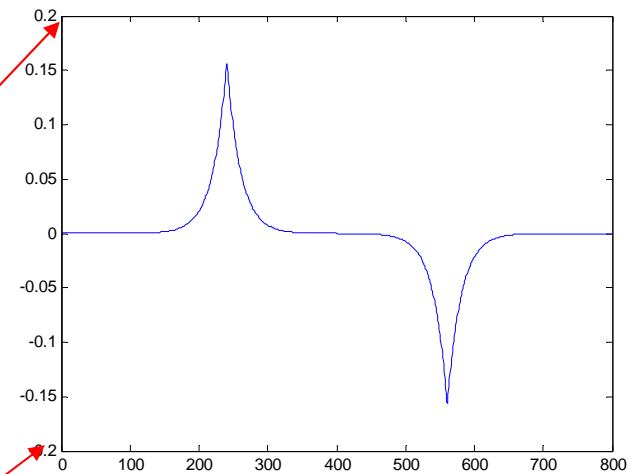
$$\Lambda \left[\frac{1}{\epsilon} \frac{\partial H}{\partial n} \right]_R \approx \mathcal{J}_{H_n} (H_{i-1:i+2, j-1, j+2}, J_{H, \ell}),$$

$$\frac{\Lambda}{\omega \mu_0} \left[\frac{1}{\epsilon \mu} \frac{\partial E}{\partial s} \right]_R \approx \mathcal{J}_{E_s} (E_{i-1:i+2, j-1, j+2}, J_{E, \ell}).$$

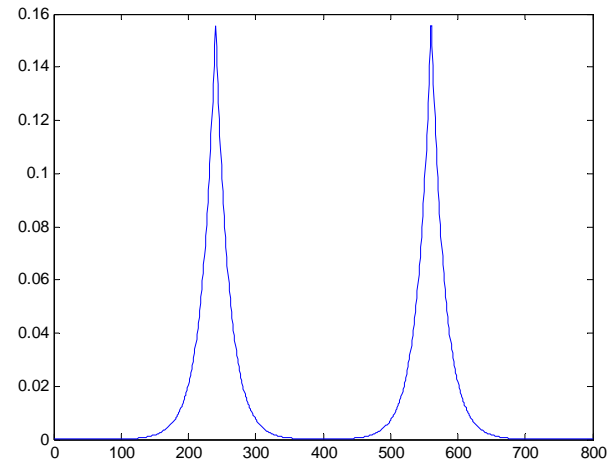
Numerical Validation: 1D test: parallel slab



E_z field



$k = 6.481958$



$k = 6.482042$

Convergence result-1: 1d method, 2nd order

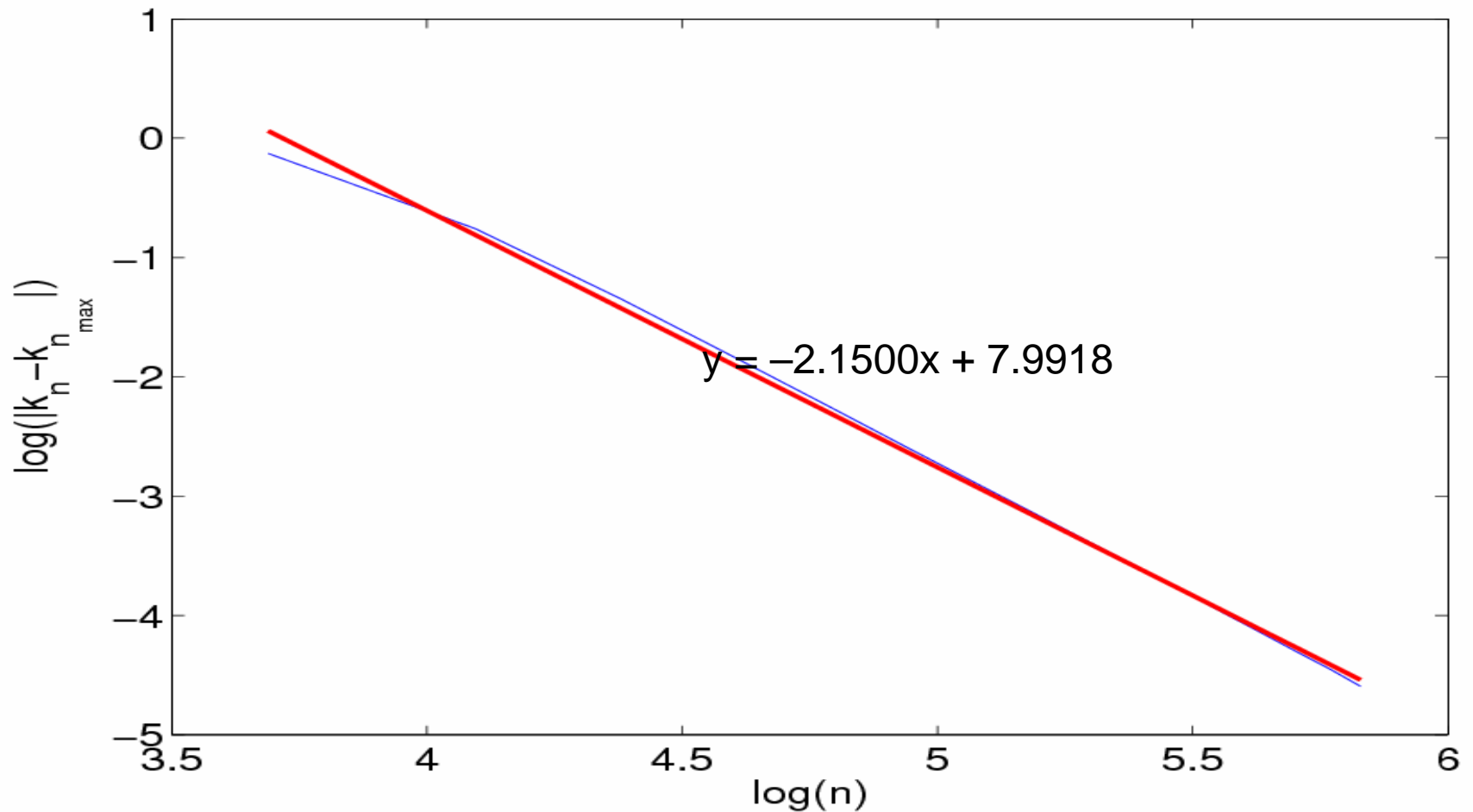
TM Mode. $\omega = 0.2$, $\omega_\tau = 0$

width of metal / width of unit cell = 0.5

| N | $\ \tilde{k} - \tilde{k}_{exact}\ $ | | |
|------|-------------------------------------|----------------------|----------------------|
| | IOA | CIM2, $\alpha = 0.2$ | CIM2, $\alpha = 0.5$ |
| 100 | 9.32222e-05 | 5.1570e-008 | 2.8789e-07 |
| 200 | 4.6903e-05 | 1.1416e-008 | 7.4446e-008 |
| 400 | 2.3524e-05 | 2.6622e-009 | 1.8928e-008 |
| 800 | 1.1780e-05 | 6.3402e-010 | 4.7793e-009 |
| 1600 | 5.8947e-06 | 1.4703e-010 | 1.2083e-009 |
| 3200 | 2.9485e-06 | 2.8160e-011 | 3.1120e-010 |
| 6400 | 1.4745e-06 | 1.6538e-012 | 8.6405e-011 |

Insensitive to the relative location α of the interface in a cell

Convergent order: 1d method, 2nd order



Least square fit for errors from $N \times N$ runs,
 $N=40,60,80,\dots,360$

Convergence Result-2:

1d method, 2nd order,

different width of metal with damping

TM Mode. $\omega = 0.2$, $\omega_\tau = 0.003$, $\alpha = 0.5$

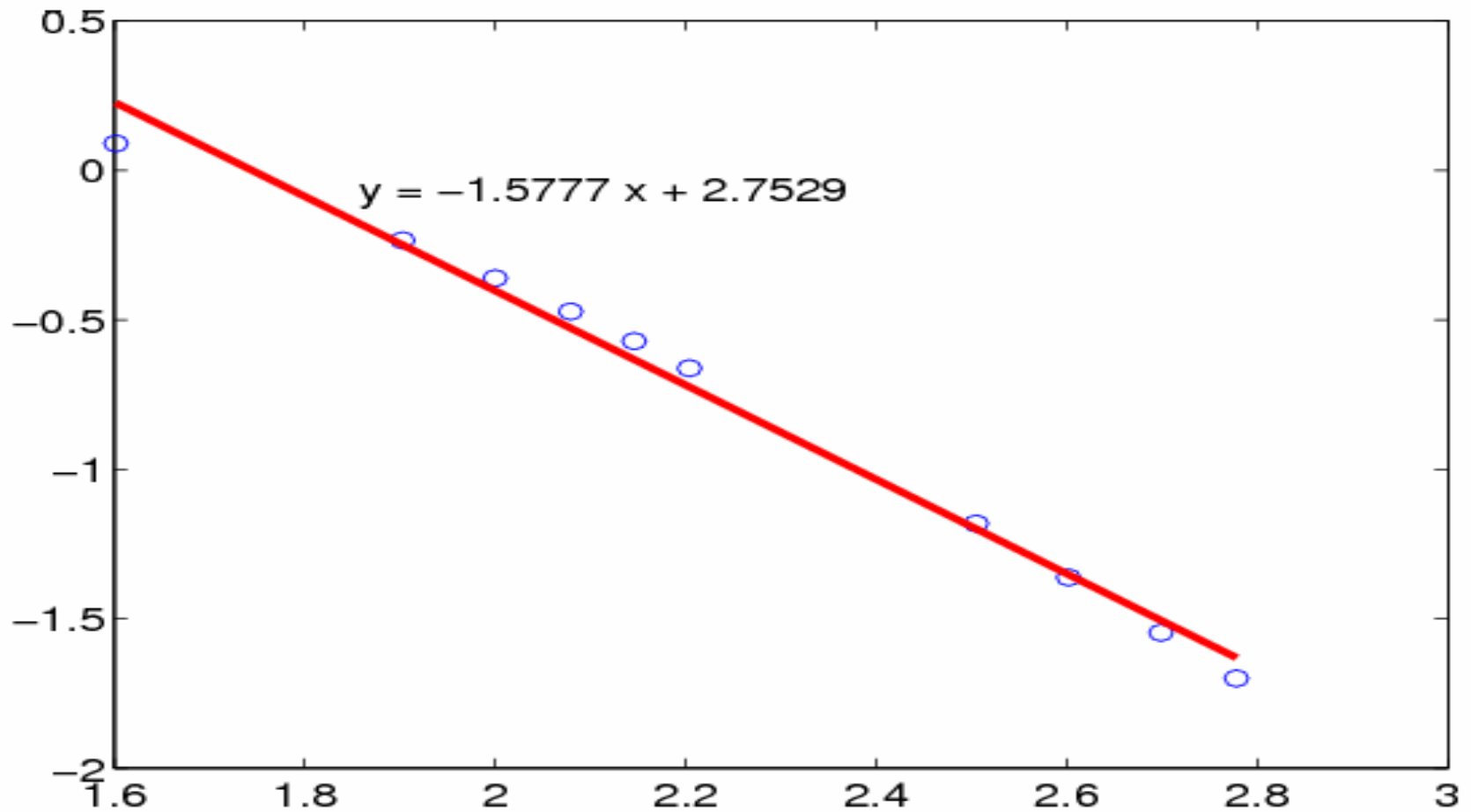
| N | $\alpha_L^+ = \alpha_L^- = 0.5$ | | $\alpha_L^+ = 0.2, \alpha_L^- = 0.8$ | |
|------|---------------------------------|----------------|--------------------------------------|----------------|
| | real part | imaginary part | real part | imaginary part |
| 100 | 5.1605e-08 | 8.5679e-10 | 2.1476e-07 | 3.3083e-09 |
| 200 | 1.1463e-08 | 1.9652e-10 | 5.2862e-08 | 7.9373e-10 |
| 400 | 2.7112e-09 | 4.7411e-11 | 1.3100e-08 | 1.9579e-10 |
| 800 | 6.8358e-10 | 1.2125e-11 | 3.2477e-09 | 5.0111e-11 |
| 1600 | 1.9732e-10 | 3.7323e-12 | 8.0094e-10 | 1.4140e-11 |
| 3200 | 8.1069e-11 | 1.8781e-12 | 2.0158e-10 | 4.7240e-12 |
| 6400 | 4.6360e-11 | 1.0169e-12 | 8.5888e-11 | 2.9376e-12 |

Numerical Validation:

2d test: layer structure

- Computational parameters of layer structure
 - The metal layer is located at the center of the unit cell and
 - the width of metal layer is $0.4a$.
 - Target frequency is 0.7. There is no damping effect.
 - Periodic boundary condition ($k_x = k_y = 0$) is applied at the cell boundary.
 - $N = 40, 80, 100, 120, 140, 160, 320, 400, 500, 600$.
 - The exact solution is $k = 1.888$.
-

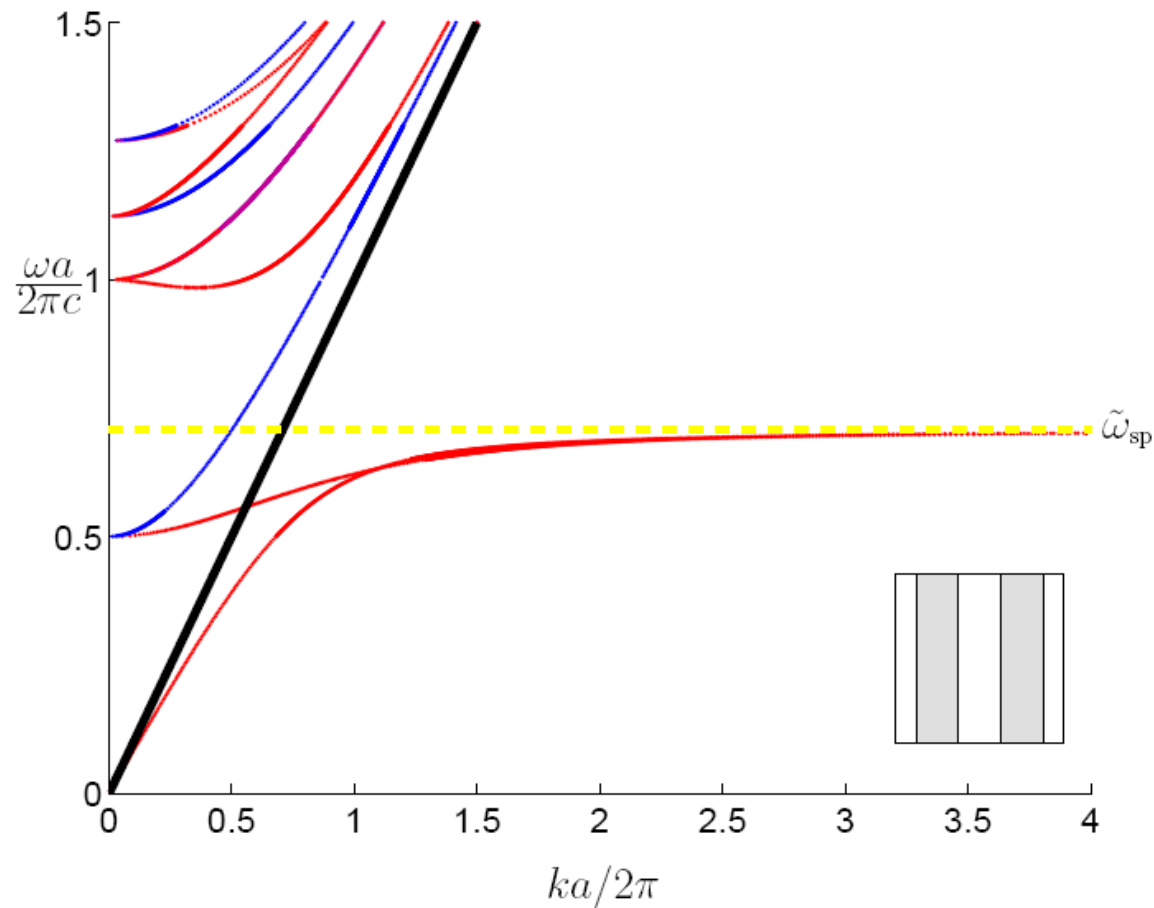
Converge result for layer structure using 2d method



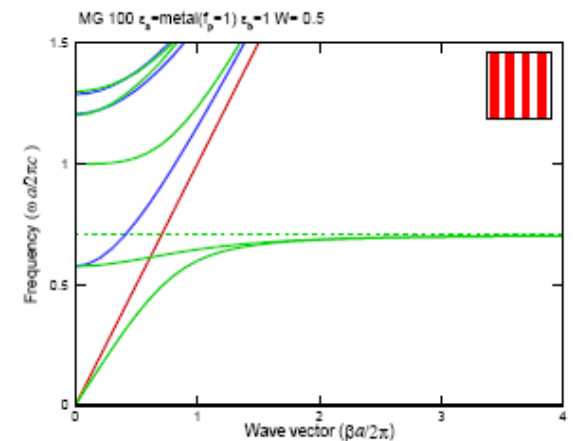
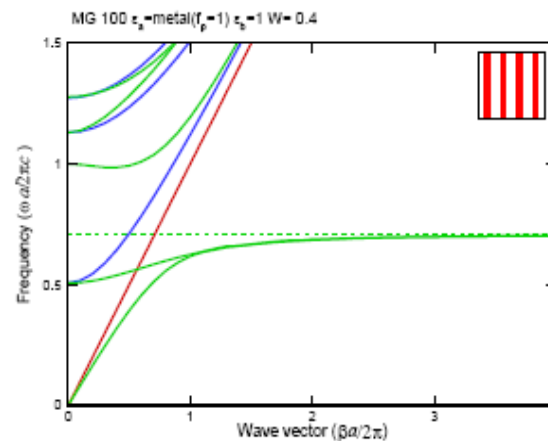
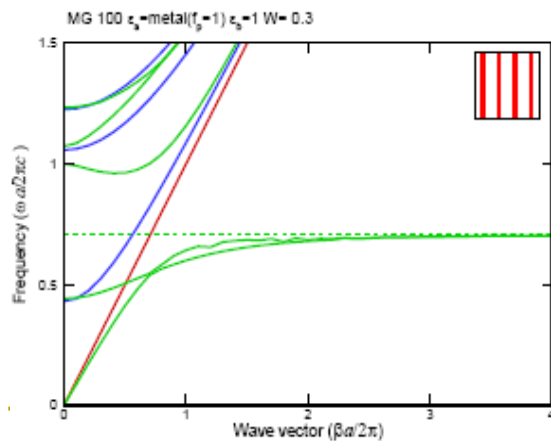
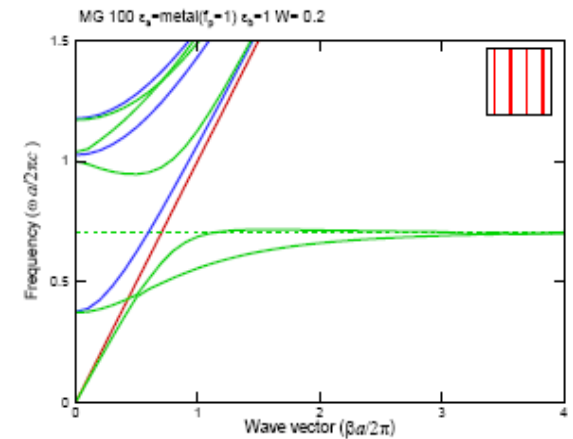
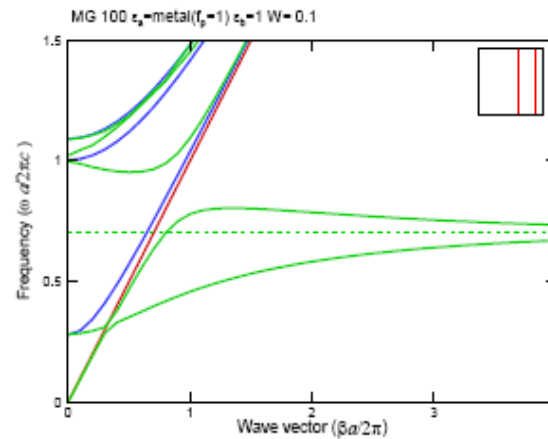
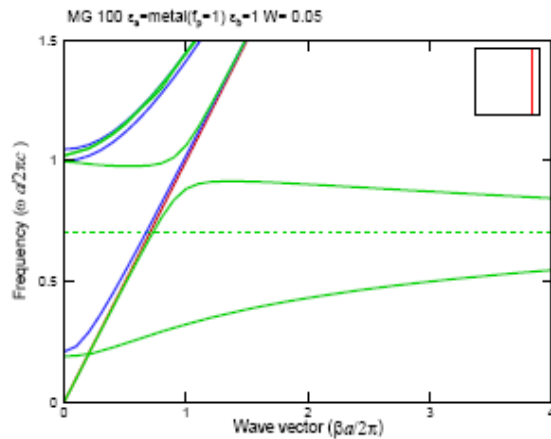
Study of frequency band

- Study signal propagation via plasmonic crystal wave guide
 - Energy absorbing problem via plasmonic crystal
-

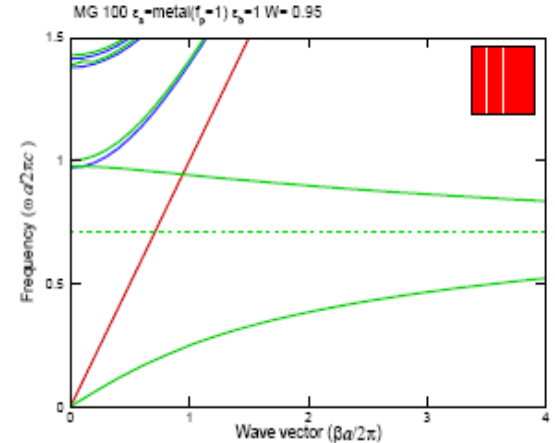
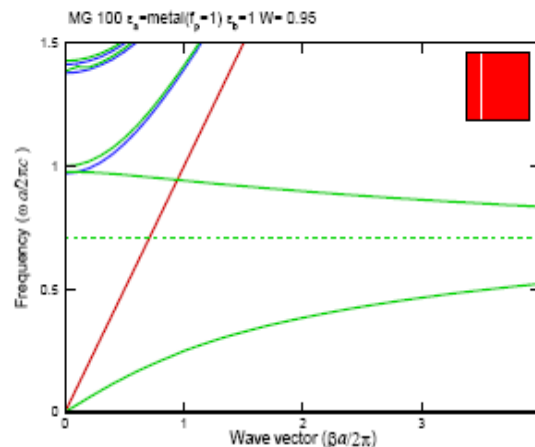
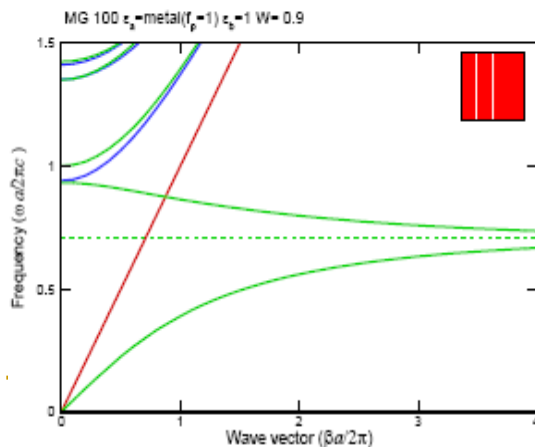
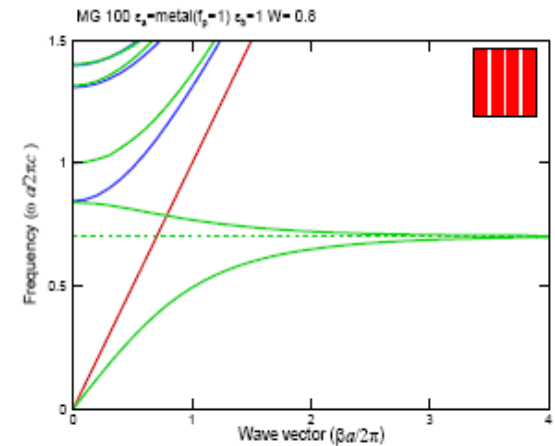
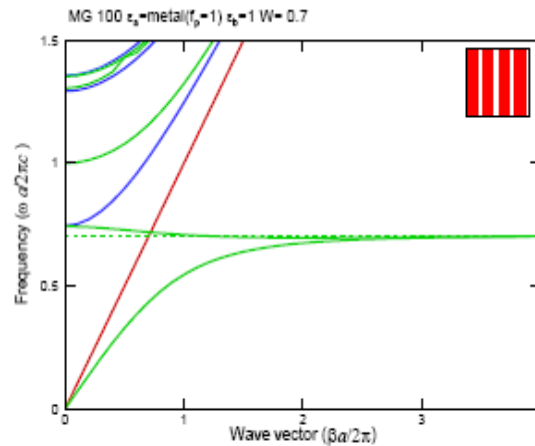
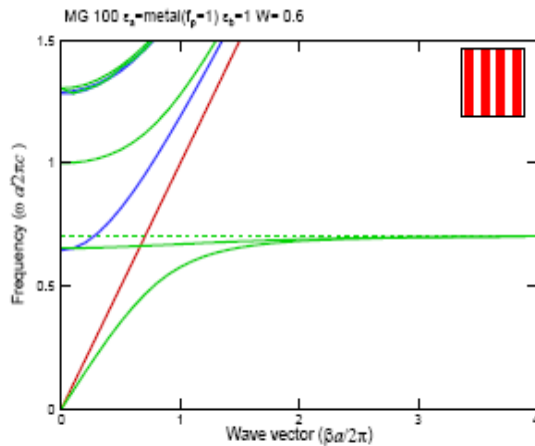
Study of frequency band: parallel slab



Dispersion relation with different metal ratio



Dispersion relation with different metal ratio



Negative group velocity

- For metal ratio > 0.5 , the dispersion relation has negative group velocity. This means that energy can propagate in reverse direction.



Skin depth: k larger, skin thinner

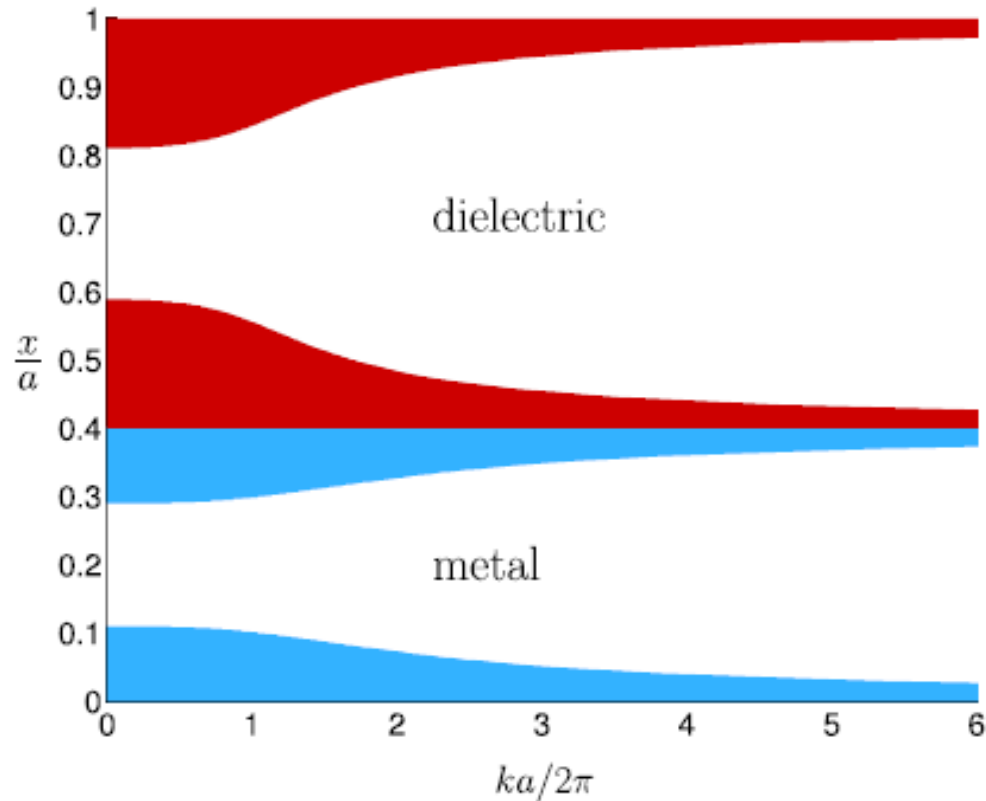
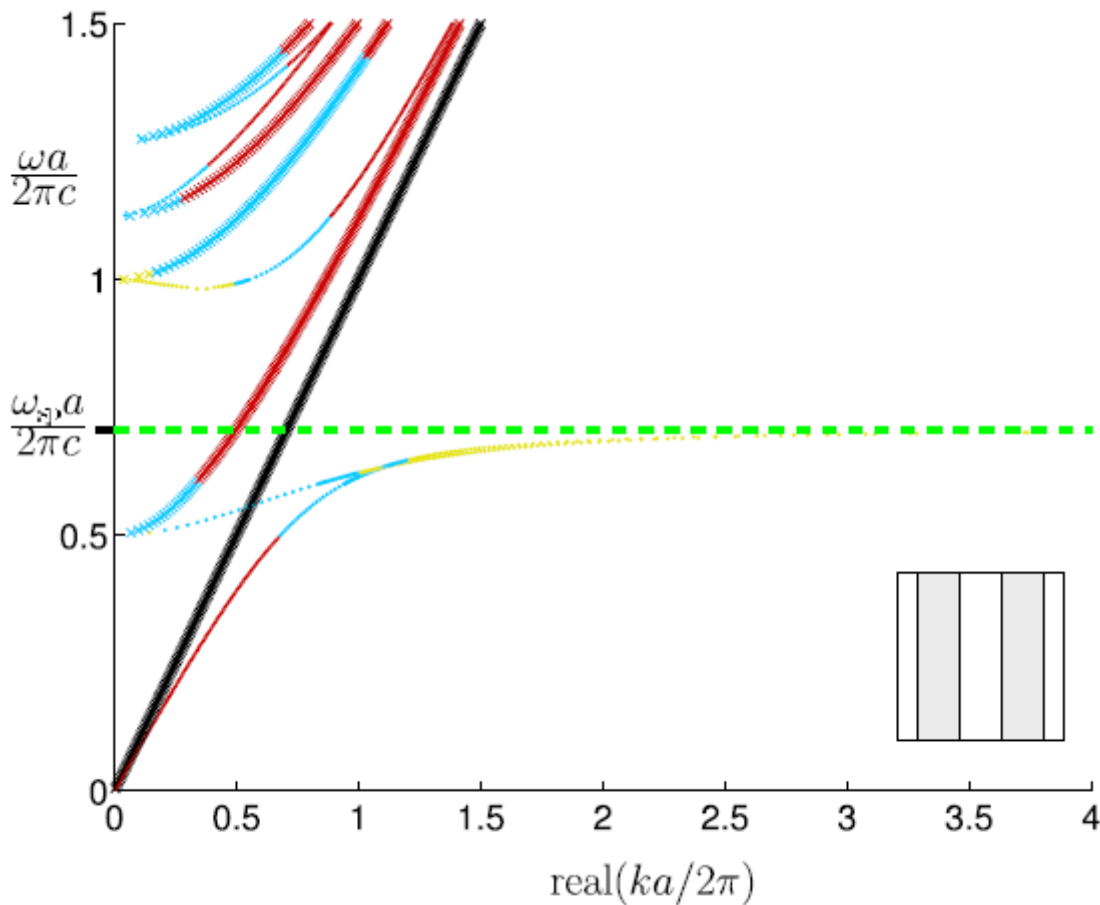


FIG. 5. (Color online) The skin depths versus the axial wave number k for the layer structure. The Bloch wave number is $k_x=0$. The skin depth is defined to be the distance from the peak of E to where E decays to E_{peak}/e . The red (dark gray) part is the skin depth in the dielectric part whereas the cyan (light gray) part is the metal part.

Damping effect for SPP

k larger, damp faster



$$\frac{\omega_{\tau} a}{2\pi c} = 0.00296$$

$$\text{Im}(ka / 2\pi c) \in$$

$$[0, 10^{-6}) : \textit{red}$$

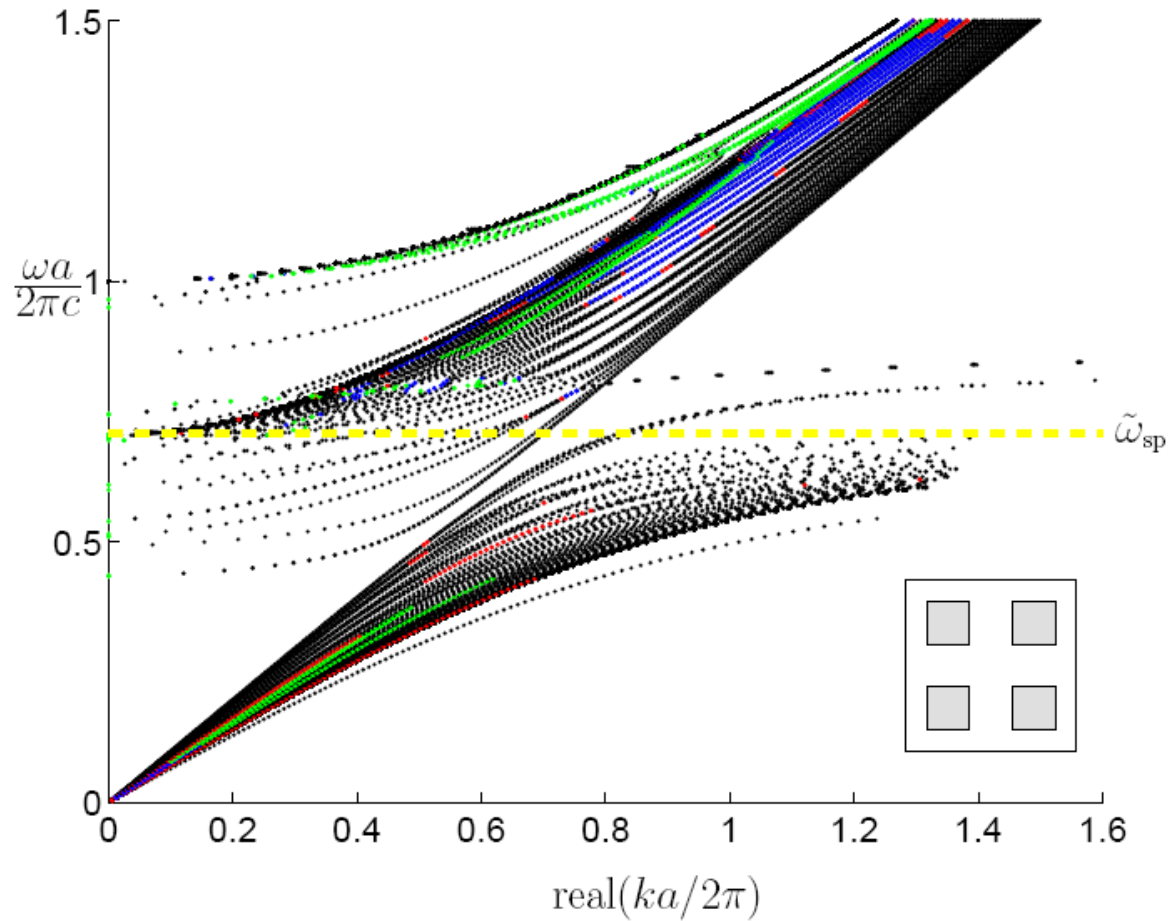
$$[10^{-6}, 10^{-3}) : \textit{cyan}$$

$$[10^{-3}, 10^{-2}) : \textit{yellow}$$

Damping effect

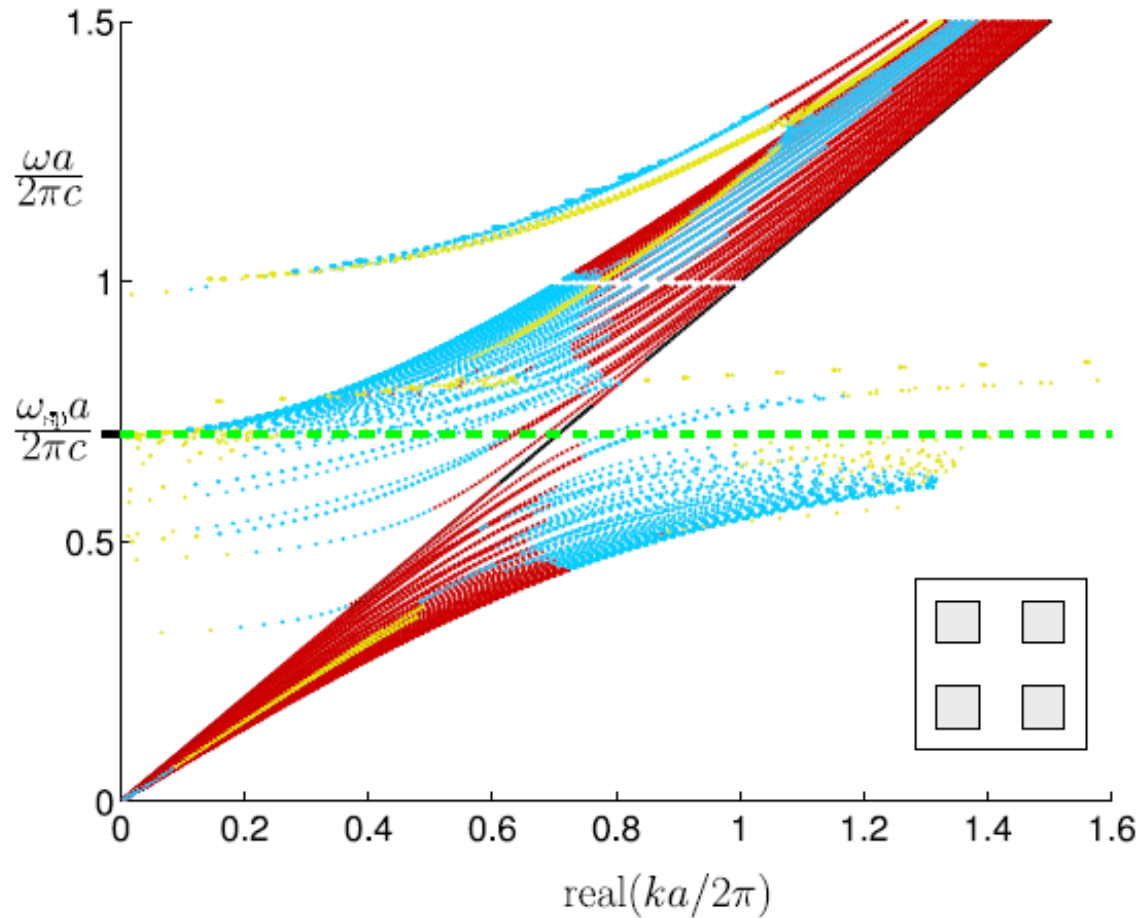
- The band lines closer to light line can travel longer
 - For surface plasmon, the larger k , the faster the waves decay
-

Study of frequency band: parallel square



More SPP bands

Damping effect

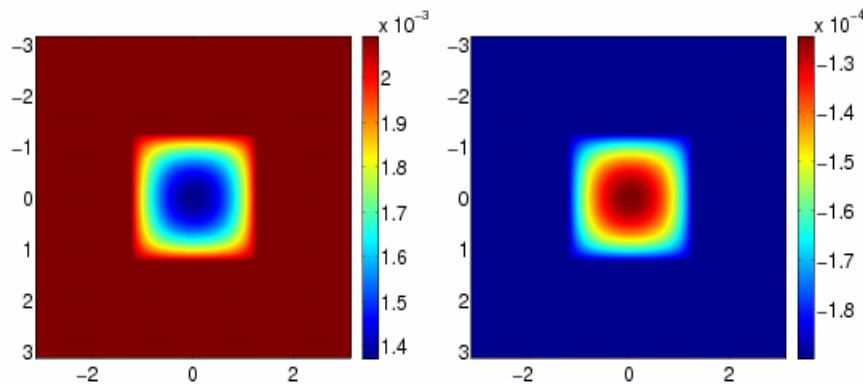


Waves corresponding to bands closer to light line survive longer.

Computational parameters of eigenmodes of box

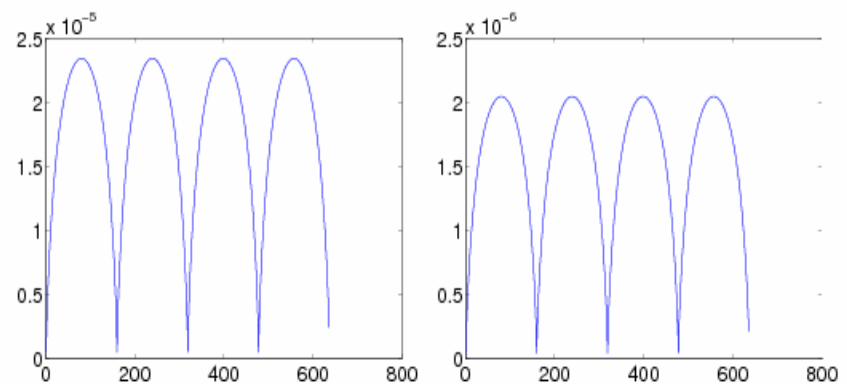
- The box is located at the center of the unit cell and the metal is inside the box. Length of box/length of unit cell = 0.4. Target frequency is 0.7. There is no damping effect. Periodic boundary condition ($k_x = k_y = 0$) is applied at the cell boundary. $N = 400$.
-

Upper($k=0.7000$), Lower($k=0.7001$), Eigenmodes of box



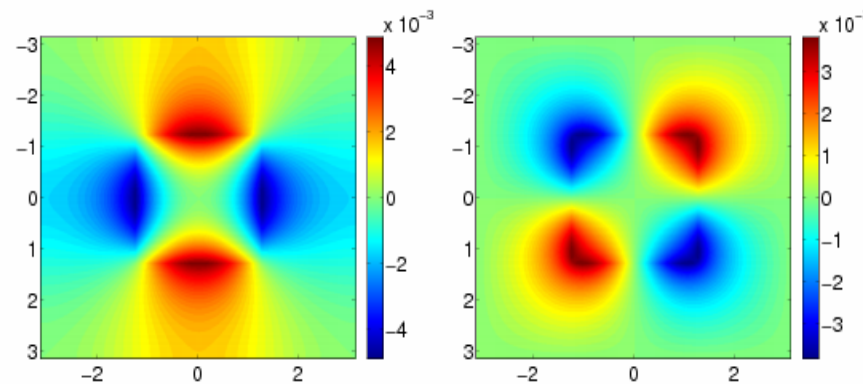
(a) E

(b) H



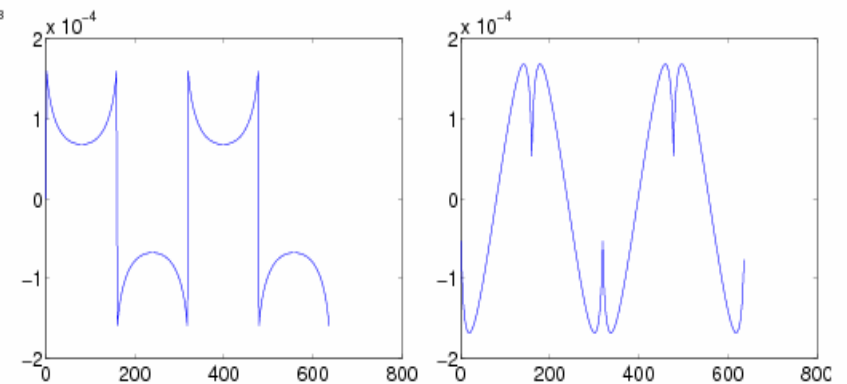
(c) J_E

(d) J_H



(e) E

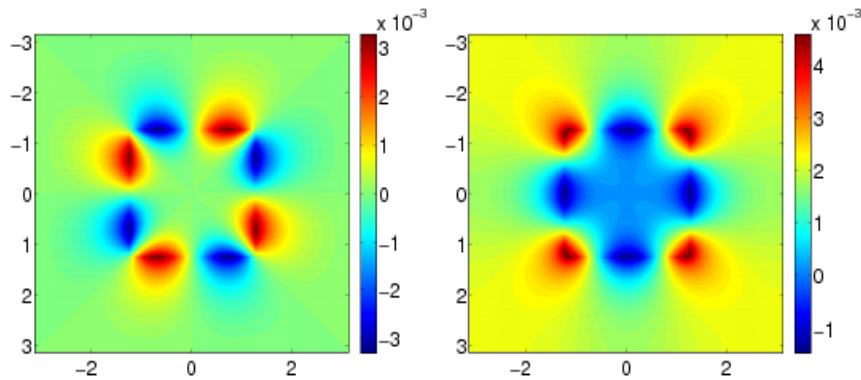
(f) H



(g) J_E

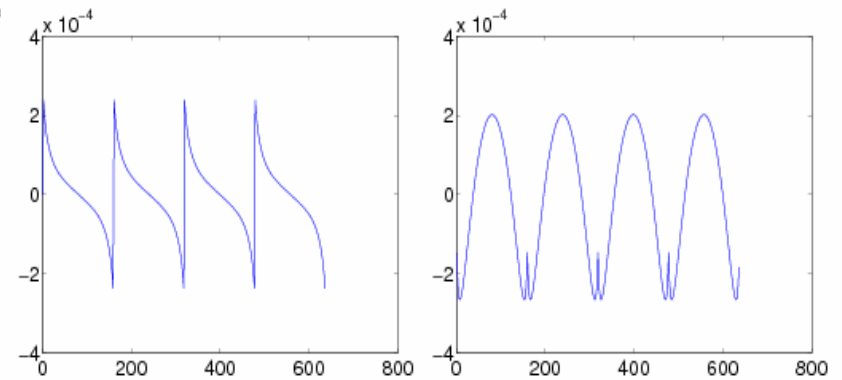
(h) J_H

Upper($k=0.7008$), Lower($k=0.7161$), Eigenmodes of box



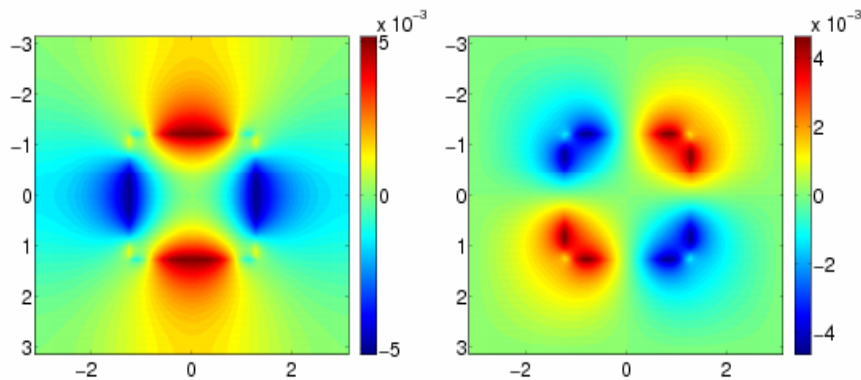
(i) E

(j) H



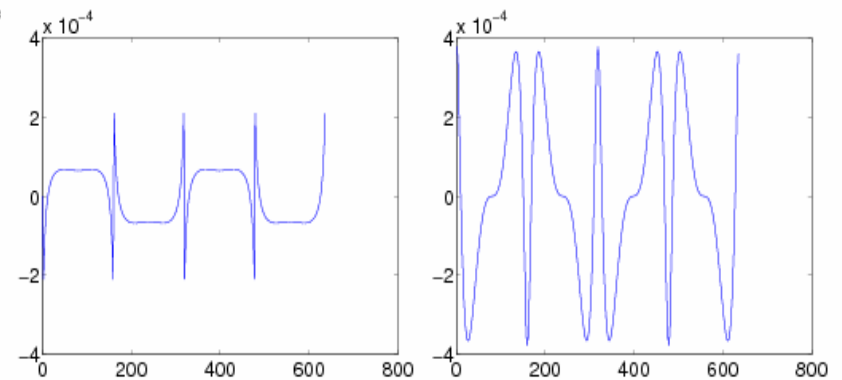
(k) J_E

(l) J_H



(m) E

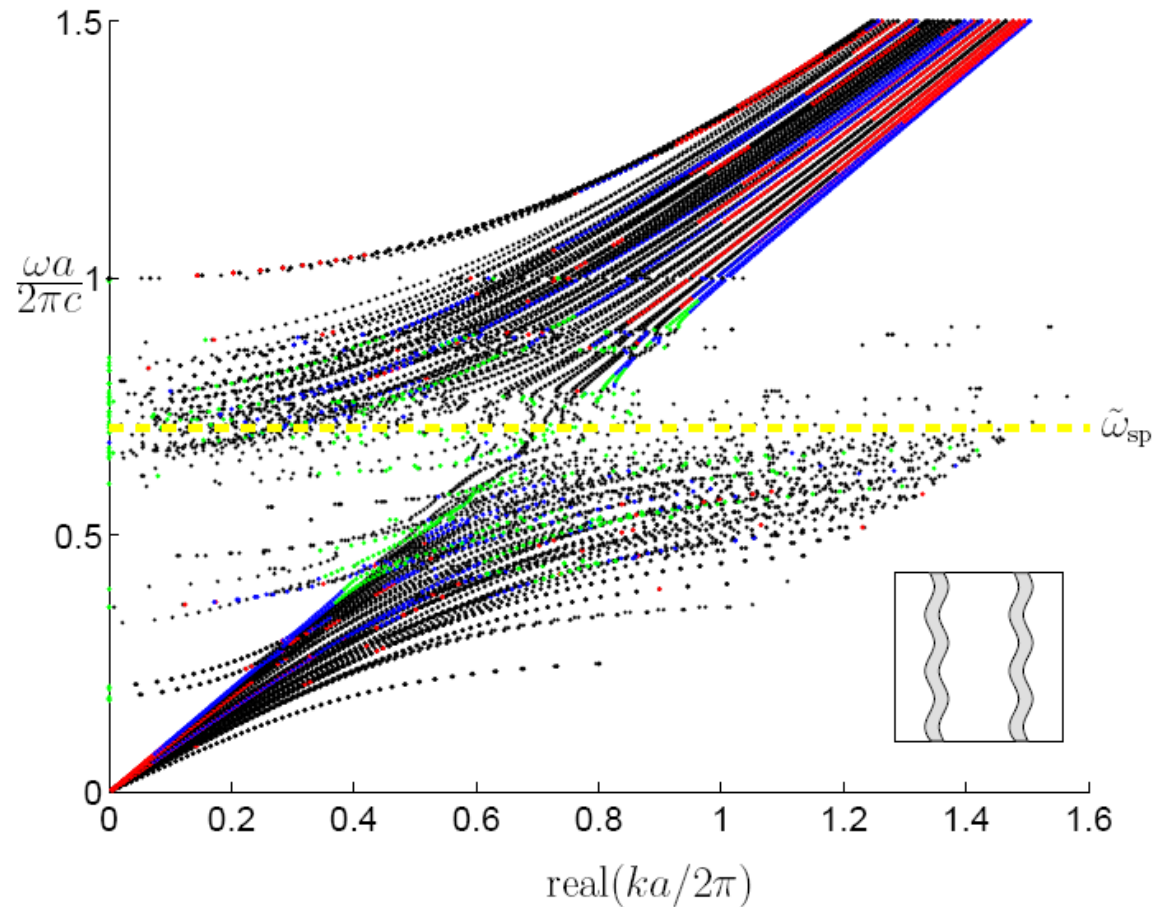
(n) H



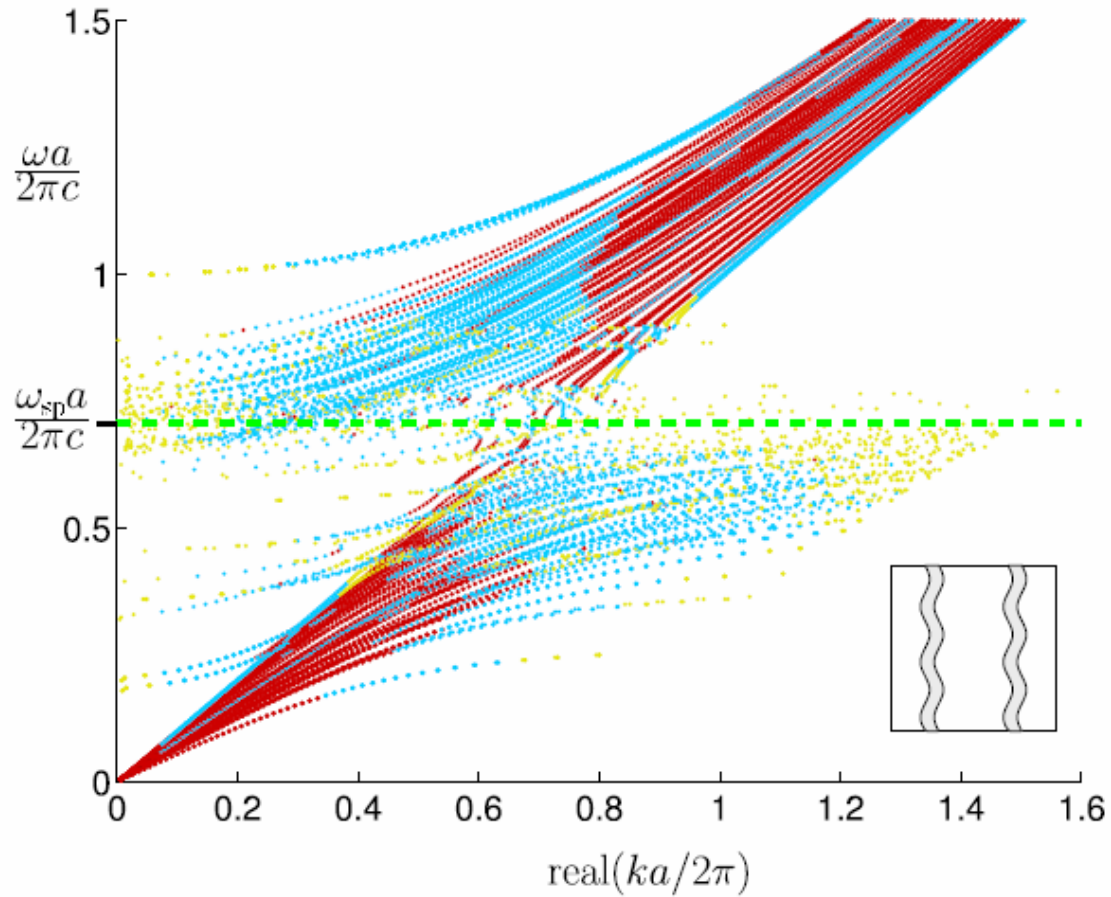
(o) J_E

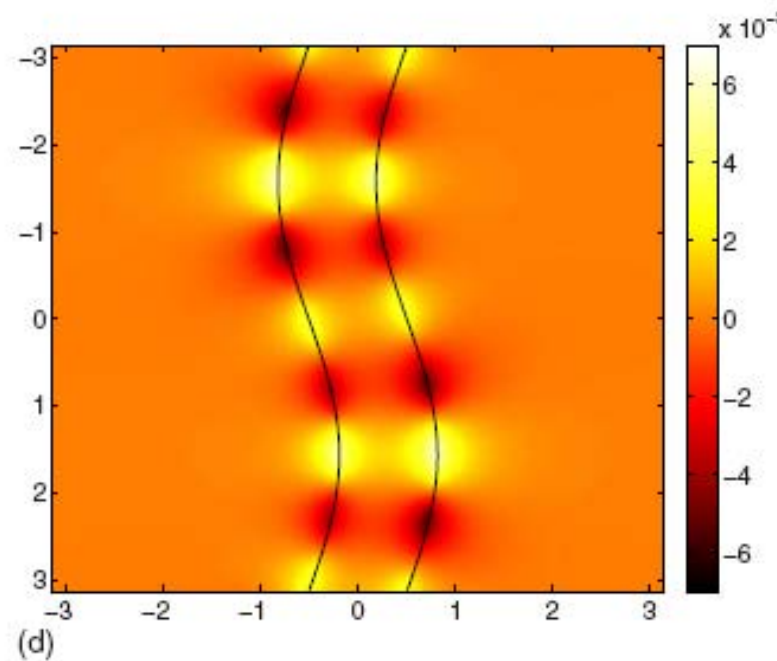
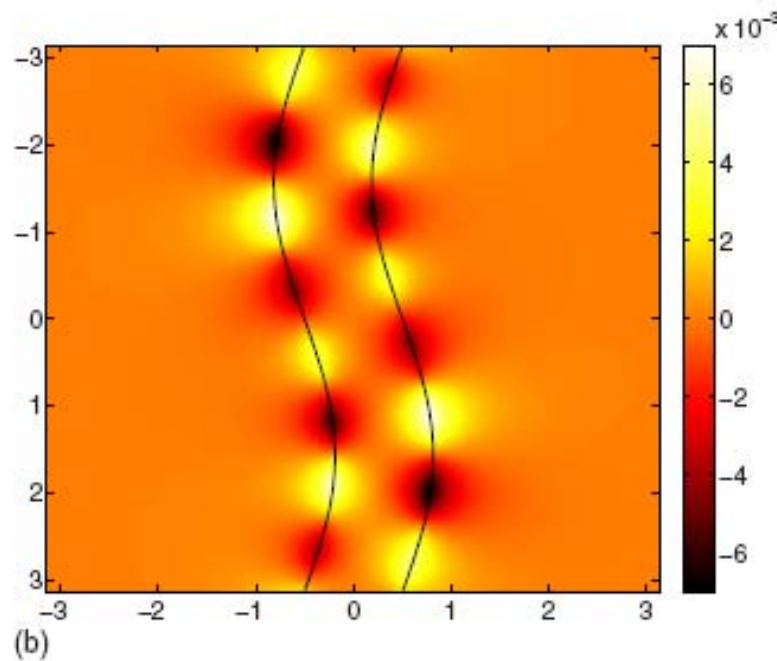
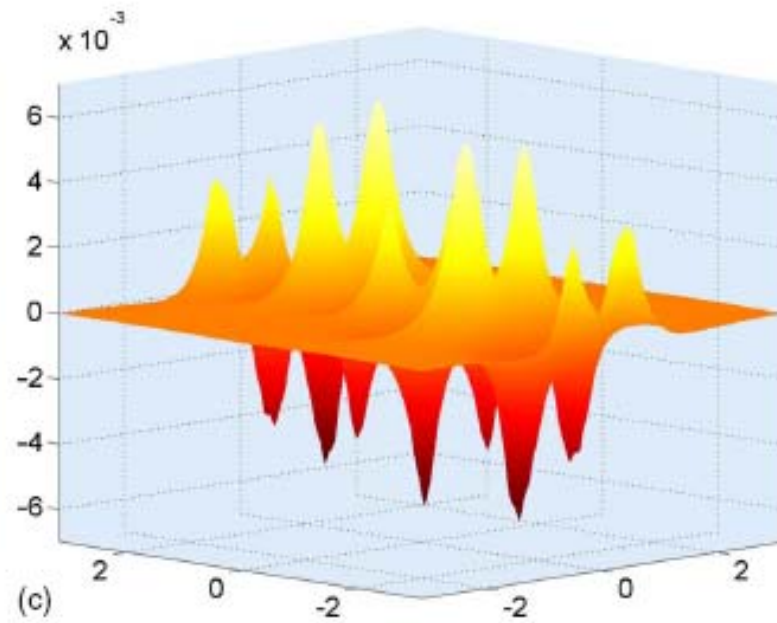
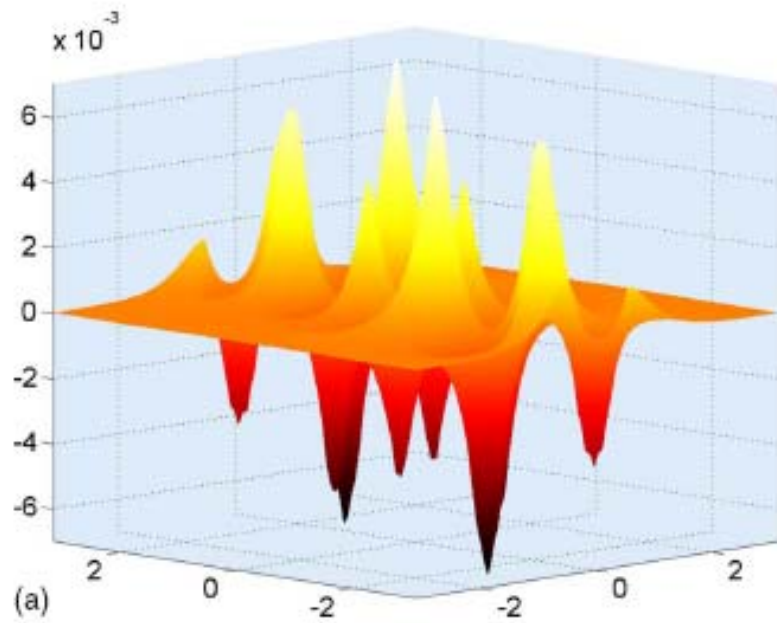
(p) J_H

Study of frequency band: wavy slab



Damping effect for wavy structure





Signal propagation via plasmonic wave

- As k increases, group velocity becomes slower, skin thickness becomes thinner, propagation length becomes shorter
 - Transmission of signal via plasmonic wave is a trade-off problem between thinner thickness, faster group velocity and longer propagation length
 - Wavy structure provides more frequency for signal propagation
-

Energy absorbing problem

- Standing waves are concerned
 - Curvature in wavy structure provides more frequency bands near $k = 0$
 - Wavy structure can absorb energy from wider range of frequency bands
-

Conclusions

- Augmented coupling interface method: 2nd order
 - Interfacial operator: reduce the problem to a standard quadratic eigenvalue problem
 - Coupling interface method:
 - Cartesian grid in interior region
 - Interfacial grid on interface
 - Dimension-by-dimension approach
 - Dimensional coupling through solving coupling equation for second order derivatives
 - Wavy structure provides more frequency bands for signal propagation and energy absorption
-

Summary

- Propose coupling interface method for solving elliptic interface problems
 - CIM1, CIM2
 - Augmented CIM
 - Applications
 - Macromolecule in solvent
 - Tumor growth simulation
 - Computing dispersion relation for surface plasmon at THz frequency ranges.
-

Thank you for your attention!
